Charles University in Prague
Faculty of Mathematics and Physics

MASTER THESIS

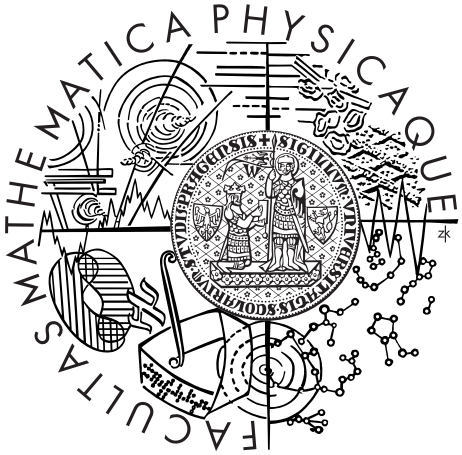

Bc. Petr Žáček

Numerical simulation of cerebrospinal fluid transport

Mathematical Institute, Charles University

Supervisor of the master thesis:	prof. Ing. František Maršík, DrSc.
Study programme:	Matemathics
Specialization:	Mathematical Modeling in Physics and Technology

Prague 2012

I would like to thank my supervisor prof. František Maršík for his patience and the encouragements he gave me, and to my family and Aneta for their support during my studies.

I declare that I carried out this master thesis independently, and only with the cited sources, literature and other professional sources.

I understand that my work relates to the rights and obligations under the Act No. 121/2000 Coll., the Copyright Act, as amended, in particular the fact that the Charles University in Prague has the right to conclude a license agreement on the use of this work as a school work pursuant to Section 60 paragraph 1 of the Copyright Act.

In Prague, 30th June, 2012 Petr Žáček

Název práce: Počítačové modelování transportu mozkomíšní tekutiny

Autor: Bc. Petr Žáček

Katedra: Matematický ústav UK

Vedoucí diplomové práce: prof. Ing. František Maršík, DrSc., Matematický ústav UK

Abstrakt: Modelování proudění mozkomíšního moku je důležité pro pochopení jeho vlivu na centrální nervovou soustavu, obzvlášť míchu. Jednou z motivací studia je nemoc zvaná syringomyelie, která pravděpodobně vzniká přerušením nervových drah bublinkami vznikajícími při průchodu tlakových (expanzních) poruch míchou a jejím okolím, a jejíž znakem jsou tekutinou naplněné dutinky v míše. V práci je navržen model tekutinou naplněných koaxiálních elastických trubic, pomocí kterého lze simulovat šíření tlakových poruch míchou včetně jejich vzájemné interakce a možného zvětšení v důsledku interferencí nebo odrazu. Odvodíme kvazilineární řídící rovnice ve tvaru nelineárního hyperbolického systému zákonů zachování, jejichž numerickým řešením pomocí dvoukrokové Lax-Wendroffovy metody s přidanou umělou viskozitou lze i kvantitativně odhadnout až dvojnásobný nárůst tlakové diference.

Klíčová slova: mozkomíšní mok, syringomyelie, proudění v koaxiálních elastických trubicích, nelineární hyperbolický systém, charakteristiky, Lax-Wendroffovo schéma

Title: Numerical simulation of cerebrospinal fluid transport

Author: Bc. Petr Žáček

Department: Mathematical Institute, Charles University

Supervisor: prof. Ing. František Maršík, DrSc., Mathematical Institute, Charles University

Abstract: Modelling of cerebrospinal fluid flow is important for understanding its influence on central nervous system, especially spinal cord. One of the reasons for its study is a disease called syringomyelia that probably develops as a result of severance of neural pathways by bubbles emerging during the propagation of pressure (expansion) disturbances through spinal cord and its surroundings. It is characterized by fluid-filled cavities in spinal cord. In this thesis, a model of fluid-filled co-axial elastic tubes is proposed that can help us simulate pressure disturbances propagation through spinal cord including its interactions and possible increase as the result of interferences or reflection. We derive quasi-one-dimensional governing equations in the form of nonlinear hyperbolic system of conservational laws and with its numerical solution by two-step Lax-Wendroff method with added artificial viscosity we can quantitatively estimate almost twofold increase of pressure difference.

Keywords: cerebrospinal fluid, syringomyelia, flow in co-axial elastic tubes, nonlinear hyperbolic system, characteristics, Lax-Wendroff scheme

Contents

Introduction **3**

1 Cerebrospinal fluid flow **4**
1.1 Cerebrospinal fluid 4
1.2 Syringomyelia 5
1.3 Anatomy of spinal cord 5
1.4 Mathematical representation 6
1.5 Viscosity effects 7

2 Describtion of fluid motion **9**
2.1 Material derivative 9
2.2 Localization theorem 10

3 Governing equations **11**
3.1 Balance laws 11
3.2 Balance of mass 11
3.3 Balance of linear momentum 13
3.4 Modified balance of mass 16
3.5 Final system of equations 16

4 Governing equations analysis **18**
4.1 Pressure wave speed 18
4.2 Characteristics 19
4.3 Characteristic speeds 21
4.4 Analysis of the weak nonlinearity 24
4.5 Hyperbolic system of PDR 28

5 Numerical solution **31**
5.1 Lax-Wendroff scheme 31
5.2 Stability of numerical scheme 31
5.3 Constants, initial and boundary conditions 37
5.4 Results 39

Conclusion **47**

Bibliography **48**

Notation **49**

List of abbreviations **50**

A One pulse without artificial viscosity **51**

B One pulse with bigger Courant number ν **55**

C One pulse **57**

D Two pulses **61**

E Reflection from the blockage **67**

F Sinusoidal wave **70**

G Source code for MATLAB (one pulse with artificial viscosity) **76**

Introduction

Cerebrospinal fluid flow is a problem solved by various authors, for example [11], [1], [4]. Since measurment can be highly invasive procedure, it is important to have methods for studying cerebrospinal fluid flow in the whole central nervous system. One of the reasons for studying it is a disease known as syringomyelia that is related to damage of spinal cord, it is characterized by fluid-filled cavities in spinal cord called syrinxes that can affect nervous system. Although we know what symptoms syringomyelia causes, there is still the question of its origin and what causes its ultimate development.

One of the approach is considering pressure waves propagating through the spinal cord because of, for example, cough related shocks[1]. There's the question of interfering waves or possible reflection from blockage or the end of the spinal cord. These can contribute to the rise of high transmural pressure differences that could possibly damage the spinal cord and lead to the creation of fluid-filled cavity.

In this work, we will make some basic assumptions of the considered model, derive governing equations and solve them numerically to observe the formation of pressure differences almost twice as large as the initial pressure difference.

1. Cerebrospinal fluid flow

1.1 Cerebrospinal fluid

Cerebrospinal fluid (*liquor cerebrospinalis*, CSF) is colourless bodily fluid that is created primarily in choroid plexus (see 1.1). It is also produced by secretion on the surface of the brain and maybe even ultrafiltration of plasma. Percentage of extrachoroidal production is a subject of discussion and it is possible it can go as high as 60% of the whole CSF production[10]. Its daily production is around $500ml$.

Importance of CSF lies mainly in its protective function of central nervous system (CNS). It occupies the subarachnoid space and also fill outs the space around and inside brain and spinal cord. Therefore it acts as a cushion against various shocks that could mechanically damage CNS. Another functions of CSF varies from homeostatic function (it maintains suitable environment for CNS cells) to information transfer (neurotransmitters and its metabolites can be transported via CSF), so it's an essential bodily fluid.

CSF have density of $1003 - 1008kg/m^3$[10] and approximately the same viscosity as water. Unlike blood it contains minumum of proteins or cells. In fact, higher counts of proteins or cells in CSF are a sign of infection or another problem.

The velocity of CSF is very small, in the order of mm/min. Since our main goal would be to examine behaviour of pressure pulse entering the system and pulse speed would be much bigger than normal flow velocities, we would consider them to be initially equal to zero, thus examining propagation of pressure pulse into undisturbed flow.

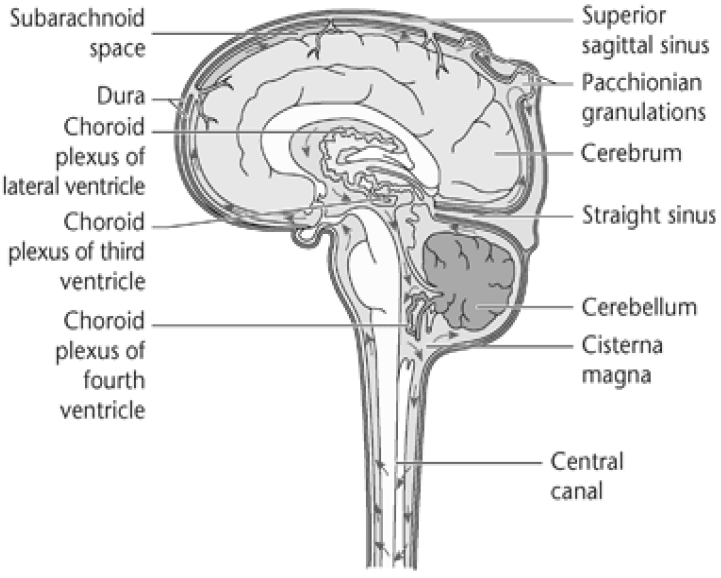

Figure 1.1: Brain and spinal cord[12]

1.2 Syringomyelia

Syringomyelia is a serious disease characterized by the longitudinal cavities within the spinal cord [1]. These cavities, called syrinxes, can be very large and damage the spinal cord. That may cause variety of symptoms, for example loss of sensation and loss of ability to feel extremes of cold and hot in hands, muscle atrophies in upper limbs, etc. It is comparatively rare with 8.4 cases per 100,000 in the United States[1]. Majority of these are associated with Arnold-Chiari malformation, brain deformation consisting of a downward displacement of the cerebellar tonsils. However, syringomyelia can also be aquired through some trauma, for example car accident, or as a complication of a disease, e.g. an arachnoiditis (disease caused by the inflammation of the arachnoid). Complicating factor in determining the exact causes is that it takes long time to develop syringomyelia so the symptoms are noticeable. Therefore we are interested if there exists mechanism that can cause formation of syrinxes in a long period of time. We will be mainly interested in mechanism proposed by Berkouk[1] that considered cough related pressure waves propagating in spinal cord.

We will investigate how transmural pressure difference behaves during its propagation. If there would be point where the pressure difference rises, it can be seen as potentially harmful for the spinal cord. If the spinal cord would be damaged or penetrated, CSF flow could make fluid filled cavity, syrinx.

1.3 Anatomy of spinal cord

We will be interested mainly in CSF flow in and around spinal cord. It occupies subarachnoidal space and central canal (1.2).

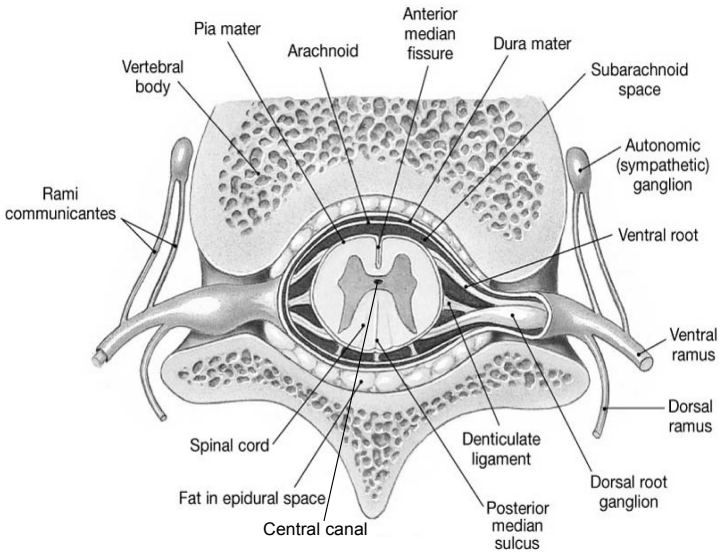

Figure 1.2: Spine and spinal cord[13]

Sagital and transverse diameter of spinal cord and results of measurments differ, for example [6],[4]. For our model, we will use results of Elliot[4] used in his upgraded model based on Berkouk[1]. Those will be specified later.

1.4 Mathematical representation

Our model will follow the work of Berkouk et al and their fluid-filled co-axial elastic tubes model [1]. It comprises of outer rigid tube and inner elastic tube as depicted in (1.3).

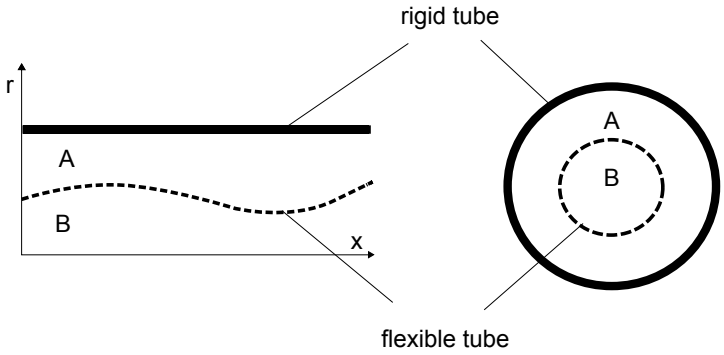

Figure 1.3: Co-axial tubes

There are two possible interpretations of this system. Space A denotes spinal subarachnoid space between dura mater and pia mater, rigid tube denotes dura mater (that is restricted by spinal canal) and either space B represents central canal and flexible tube represents the spinal cord[1], or space B represents spinal cord[4]. In this approach, the elastic tube is merely a boundary of spinal cord. Elliot[4] argued that in this approach, it is possible to consider spinal cord as a fluid like with approximately the same density as the CSF flowing in the spinal subarachnoid space, since it is filled with CSF. So even though we will be following approach of Berkouk[1], we can use some Elliot's results.

We define cross-sectional areas A_A and A_B, where subscripts A and B denotes the outer rigid and inner elastic tubes respectively. But A_A isn't cross-sectional area of the whole rigid tube A, because we are only interested in the space between inner elastic and outer rigid wall. Thus $A_A + A_B = A_T$, where A_T is total cross-sectional area of both tubes.

First important simplification of this model is that we consider changes in only one spatial dimension represented by streamwise coordinate x. That means we neglect radial or transverse variations in flow variables and we focus only on changes along the x axis. As will be seen during deriving governing equations, this approach have its own advantages and since spinal cord has small cross-sectional area and cerebrospinal fluid flows very slowly, it's not unreasonable simplification. That way we get quasi-one-dimensional model.

Another sipmlifications will be that the flow is uncompressible, isothermic and non-viscous. Legitimacy of the first two assumptions follows immediately from properties of CSF and spinal cord envirnoment. Neglecting viscosity will be further discussed in chapter (1.5.)

We introduce cross-sectional area ratio α as follows

$$\begin{aligned} \alpha &= \frac{A_A}{A_T} \\ 1-\alpha &= \frac{A_B}{A_T}. \end{aligned} \tag{1.1}$$

Elasticity of inner tube can be expressed either as

$$\alpha = \alpha_0 - D\Delta p, \tag{1.2}$$

where D is known as distensibility[1] and $\Delta p = p_B - p_A$ is transmural pressure difference, or following[11] as

$$p(t) - p_0 = \frac{V(t) - V_0}{C},$$

where spinal cord is divided into several compartments, $V(t)$ is the volume of certain compartment at time t, V_0 is initial volume of that compartment for pressure $p(t) = p_0$ and $C\,[m^3/Pa]$ is so-called compliance. For maximum value of compliance C_{max}, C_0 if $p(t) = p_0$ and coefficient θ holds

$$C(t) = C_{max} + (C_0 - C_{max})\, e^{\left[\theta\left(\frac{V(t)}{V_0} - 1\right)\right]}.$$

If we consider $C = 10^{-10} m^3 Pa^{-1}$ constant as some mean value of $C(t)$ and

$$\begin{aligned}
\alpha - \alpha_0 &= -D\Delta p \\
\frac{A_A}{A_T} - \frac{A_{A0}}{A_T} &= -D\Delta p \\
\frac{A_A \Delta x}{A_T \Delta x} - \frac{A_{A0}\Delta x}{A_T \Delta x} &= -D\Delta p \\
\frac{A_A \Delta x - A_{A0}\Delta x}{A_T \Delta x D} &= -\Delta p \\
\frac{dV(t) - dV_0}{A_T \Delta x D} &= -\Delta p,
\end{aligned}$$

where Δx is small streamwise interval. We can see that it's possible to find a relation between those two properties of spinal cord, but since $p(t) - p_0 \neq -\Delta p$ and ambiguous Δx, it would be better for our case to follow [4] and take constant $D = 10^{-5} Pa^{-1}$ (even though computing from constant C would yield similar result). It can be computed from (4.9) and known pulse wave speed (that have yet to be defined) and we will apply it as a given parameter of our model.

Following [1], (1.2) neglects effects of tube inertia and change in cross-sectional area depends purely on change in transmural pressure.

As a diameter of flexible tube and diameter of rigid tube, we will take $r_B = 4mm$ and $r_T = 7,5mm$ respectively[4]. This will give us cross-sectional area ratio $\alpha_0 \doteq 0,7$. We will consider tubes of length $50cm$, such length roughly corresponds with length of spinal cord.

1.5 Viscosity effects

According to Berkouk[1], if we try to evaluate shear stress from equations (3.12) and (3.13), we obtain

$$\tau_A = \frac{\rho u_A}{\sqrt{\pi}}\sqrt{\frac{\nu}{h}},$$
$$\tau_B = \frac{\rho u_B}{\sqrt{\pi}}\sqrt{\frac{\nu}{h}},$$

where ν is the kinematic viscosity of the fluid, h is thickness of the wall, u_A and u_B are flow speeds in corresponding tubes. An estimate of the ratio of viscous to the inertial term takes the form of non-dimensional characteristic (relaxation) time

$$\left|\frac{\tau_A \pi d_A}{\rho A_A \partial u_A/\partial h}\right| = O(T_A); T_A = \sqrt{\frac{\nu\tau_A}{d_A^2}}$$
$$\left|\frac{\tau_B \pi d_B}{\rho A_B \partial u_B/\partial h}\right| = O(T_B); T_B = \sqrt{\frac{\nu\tau_B}{d_B^2}},$$

where $d_B = r_B$ is diameter of elastic tube B and $d_A = 0.5(r_T - r_B)$. For the assumption of non-viscous flow to be reasonable, non-dimensional characteristic times must be $T_{A,B} \ll 1$ and both terms can be roughly estimated as follows

$$T_{A,B} \doteq \sqrt{\frac{10^{-6}\cdot 10^{-4}}{(10^{-3})^2}} = 10^{-8} \ll 1.$$

2. Describtion of fluid motion

2.1 Material derivative

There are two basic descriptions of continuum: *Lagrangian* and *Eulerian* description. *Lagrangian* description focuses on specific particle and its trajectory. Let E be Euclidean space $\mathbb{R}^3$. Position $x \in E$ of this particle in time $t \in (0,T)$ is determined by its referential position $X \in E$ in time t_0 (usually $t_0 = 0$) and mapping $\xi(.,.) : E \times (0,T) \to E$:

$$x = \xi(X,t),$$

where position of referential point X in time t_0 is

$$x = \xi(X,t_0) = X.$$

Velocity and acceleration can then be expressed as

$$\begin{aligned} u_L(X,t) &= \frac{d\xi(X,t)}{dt} = \frac{\partial \xi(X,t)}{\partial t}, \\ a_L(X,t) &= \frac{d^2\xi(X,t)}{dt^2} = \frac{\partial^2 \xi(X,t)}{\partial t^2}. \end{aligned}$$

On the other hand, in *Eulerian* description we focus on specific point x in space and we are interested in velocity and acceleration of specific particle that go through that point in time t. This is better suited for our model, because we can examine certain spots in our fluid-filled tubes and we don't need to know how certain particle enter and exit whole system.

Velocity of a particle must be the same in both desriptions, so

$$u(x,t) = u_E(x,t) = u_L(X,t) = \frac{\xi(X,t)}{\partial t},$$

but for determining the acceleration we need to derive as follows:

$$\begin{aligned} a_E(x,t) &= \frac{du_E(x,t)}{dt} = \frac{du_E(\xi(X,t),t)}{dt} \\ &= \frac{\partial}{\partial t} u_E(x,t) + \frac{\partial u_E(\xi(X,t),t)}{\partial \xi} \frac{\partial \xi(X,t)}{\partial t} \\ &= \frac{\partial u_E(x,t)}{\partial t} + (u_E(x,t).\nabla)\, u_E(x,t). \end{aligned} \tag{2.1}$$

As you can see, acceleration in *Eulerian* and *Lagrangian* description differ in convective derivative - the last term in (2.1). Now we can define material derivative

$$\frac{d}{dt} = \frac{\partial}{\partial t} + (u.\nabla)\,. \tag{2.2}$$

That generally holds for $u(x,t) = (u_1(x,t), u_2(x,t), u_3(x,t)) : E \times (0,T) \to E$, where $x = (x_1, x_2, x_3) \in E$, but since our model is quasi-one-dimensional, we can modify (2.2) to obtain

$$\frac{d}{dt} = \frac{\partial}{\partial t} + u(x,t)\frac{\partial}{\partial x}, \tag{2.3}$$

where $u(x,t)$ is velocity of a particle in (x,t).
Material derivative is often denoted $\dot{()}$, for example:

$$\dot{u} = \frac{\partial}{\partial t}u + u\frac{\partial}{\partial x}u.$$

Last equation we need to prepare is

$$\begin{aligned} x &= \xi(X,t) \\ \frac{dx}{dX} &= \frac{\xi(X,t)}{dX} \\ dx &= \frac{\partial \xi(X,t)}{\partial X} dX, \end{aligned} \tag{2.4}$$

which will be very useful afterwards.

2.2 Localization theorem

Result from this theorem will help us when deriving governing equations from balance laws in the next chapter. Let ψ be a continuous vector or scalar field on an open set $\Omega \subset E$. Then given any $x_0 \in \Omega$

$$\psi(x_0) = \lim_{\delta \to 0} \frac{1}{vol B_\delta(x_0)} \int\limits_{B_\delta(x_0)} \psi dV,$$

where $B_\delta(x_0)$ is closed ball of radius $\delta > 0$ centered at a point x_0. Proof of this theorem can be found in [5]. Important is that if

$$\int\limits_B \psi dV = 0$$

for every closed ball $B \in \Omega$, then

$$\psi = 0. \tag{2.5}$$

3. Governing equations

3.1 Balance laws

Now we need to derive governing equations for our model. In order to achieve that, we generally need to use four basic conservation laws:

- *balance of mass*
- *balance of linear momentum*
- *balance of angular momentum*
- *balance of energy.*

However, in our simplified model we only need to consider the balance laws of mass and linear momentum. The balance of angular momentum holds due to our one dimensional approach and the balance of energy is of no significance for us, because of our isothermal approach.

3.2 Balance of mass

Let ρ and V_t be a density of cerebrospinal fluid and a control volume in time t, respectively. Then mass $m(V_t)$ of this control volume can be expressed as

$$m(V_t) = \int_{V_t} \rho dV.$$

Balance of mass states that mass remains the same in control volume with respect to time differences, that means

$$\overline{\int_{V_t} \rho dV}^{\cdot} = 0. \tag{3.1}$$

Now we substitute volume element dV with product Adx, where A denotes cross-sectional area of elastic tube and dx is element of streamwise axis. As you can see, this is a good way of representing volume element in quasi-one-dimensional model such is ours, because even though we consider only changes in streamwise axis, we are still taking the whole volume of the tube into account. Moreover, we can interchange derivation and integration

$$\begin{aligned} \overline{\int_{V_t} \rho dV}^{\cdot} &= \int_{V_t} \overline{\rho A dx}^{\cdot} \\ &= \int_{V_t} \overline{\rho A}^{\cdot} dx + \int_{V_t} \rho A \overline{dx}^{\cdot} \end{aligned} \tag{3.2}$$

Using (2.3) on the first term in (3.2) we obtain

$$\dot{\overline{\rho A}} = \frac{\partial}{\partial t}(\rho A) + u\frac{\partial}{\partial x}(\rho A)$$

and using (2.3) and (2.4) on the second term in (3.2) we obtain

$$\dot{\overline{dx}} = \dot{\overline{\frac{\partial \xi(X,t)}{\partial X}dX}} = \frac{\partial u(X,t)}{\partial X}dX = \frac{\partial u(x,t)}{\partial x}dx$$

and (3.2) can be written as follows:

$$\begin{aligned}\dot{\overline{\int_{V_t} \rho dV}} &= \int_{V_t}\left(\frac{\partial}{\partial t}(\rho A) + u\frac{\partial}{\partial x}(\rho A)\right)dx + \int_{V_t}\rho A\frac{\partial u}{\partial x}dx \\ &= \int_{V_t}\left(\frac{\partial}{\partial t}(\rho A) + \frac{\partial}{\partial x}(\rho A u)\right)dx = 0. \end{aligned} \tag{3.3}$$

Now using the localization theorem (2.5), we can write 3.3 in local form

$$\frac{\partial}{\partial t}(\rho A) + \frac{\partial}{\partial x}(\rho A u) = 0. \tag{3.4}$$

We divide equation (3.4) by ρ and replace variables A and u with their counterparts in both tubes A and B. This way we obtain two equations representing the balance of mass.

$$\begin{aligned}\frac{\partial}{\partial t}A_A + \frac{\partial}{\partial x}(A_A u_A) = 0 \\ \frac{\partial}{\partial t}A_B + \frac{\partial}{\partial x}(A_B u_B) = 0\end{aligned}$$

Furthemore, we can divide both equations with total cross-sectional area A_T and using (1.1) we obtain balance of mass equations in this form

$$\frac{\partial}{\partial t}\alpha + \frac{\partial}{\partial x}(\alpha u_A) = 0 \tag{3.5}$$

$$-\frac{\partial}{\partial t}\alpha + \frac{\partial}{\partial x}((1-\alpha)u_B) = 0. \tag{3.6}$$

With (1.2) we can eliminate α from equations and get balance of mass equations for variables Δp, u_A and u_B. For equation (3.5) we get

$$\begin{aligned}-D\frac{\partial}{\partial t}\Delta p + \alpha_0\frac{\partial u_A}{\partial x} - D\Delta p\frac{\partial u_A}{\partial x} - Du_A\frac{\partial \Delta p}{\partial x} = 0 \\ \frac{\partial}{\partial t}\Delta p + \left(\Delta p - \frac{\alpha_0}{D}\right)\frac{\partial u_A}{\partial x} + u_A\frac{\partial \Delta p}{\partial x} = 0\end{aligned} \tag{3.7}$$

and for equation (3.6) we get

$$D\frac{\partial}{\partial t}\Delta p + (1-\alpha_0)\frac{\partial u_B}{\partial x} + D\Delta p\frac{\partial u_B}{\partial x} + Du_B\frac{\partial \Delta p}{\partial x} = 0$$
$$\frac{\partial}{\partial t}\Delta p + \left(\Delta p + \frac{1-\alpha_0}{D}\right)\frac{\partial u_B}{\partial x} + u_B\frac{\partial \Delta p}{\partial x} = 0. \tag{3.8}$$

Finally, (3.7) and (3.8) are balance of mass equations for tubes A and B.

3.3 Balance of linear momentum

Linear momentum $l(V_t)$ of control volume V_t at time t can be expressed as

$$l(V_t) = \int_{V_t} \rho u(x,t) dV.$$

In contrast to balance of mass, linear momentum doesn't stay the same with respect to time differences, but we need to describe how exactly it will change. We can write that

$$\overline{\int_{V_t} \rho u(x,t) dV}^{\cdot} = \int_{\partial V_t} s(n,x,t) dA + \int_{V_t} \rho b(x,t) dV,$$

where the two terms on the right side of equation denotes surface forces s and volume forces b respectively. Volume forces have effect on every point in control volume V_t, an example would be gravity. We won't consider any volume forces in our model.

Surface forces affects only surface of control volume V_t. $s(n,x,t)$ is a surface force on every point on the boundary of V_t, where n is unit outer normal at point (x,t). For Cauchy stress tensor $T(x,t)$ holds that $T(x,t)\cdot n = s(n,x,t)$, so we can write our balance of linar momentum as follows[5]

$$\overline{\int_{V_t} \rho u(x,t) dV}^{\cdot} = \int_{\partial V_t} T(x,t)\cdot n dA.$$

and using the divergence theorem we can write

$$\overline{\int_{V_t} \rho u(x,t) dV}^{\cdot} = \int_{V_t} \nabla T(x,t) dV. \tag{3.9}$$

We can divide stress tensor T into two parts $T = T_{el} + T_{dis}$, where T_{el} is the elastic part and T_{dis} is dissipative part. Since we don't consider any dissipative effects, neither viscosity nor tube inertia effects, we can concentrate only on elastic part, which we can for our one-dimensional case write as $T_{el} = -pI$[8], where p is static (hydrodynamic) pressure and I unit tensor.

By substituting volume element $dV = Adx$ we obtain

$$\dot{\overline{\int_{V_t} \rho u(x,t) A dx}} = \int_{V_t} \nabla p(x,t) A dx$$

and using (2.3) and (2.4) on the first term we can write

$$\begin{aligned}
\dot{\overline{\int_{V_t} \rho u(x,t) dV}} &= \int_{V_t} \dot{\overline{\rho u A dx}} \\
&= \int_{V_t} \dot{\overline{\rho u A}} dx + \int_{V_t} \rho u A \dot{\overline{dx}} \\
&= \int_{V_t} \left(\frac{\partial}{\partial t}(\rho A u) + \frac{\partial}{\partial x}(\rho A u^2) \right) dx.
\end{aligned}$$

Using this and localization theorem (2.5) as with the mass balance law, we can rewrite (3.9) as

$$\begin{aligned}
\frac{\partial}{\partial t}\rho A u + \frac{\partial}{\partial x}\rho A u^2 &= -A\frac{\partial p}{\partial x} \\
u\frac{\partial}{\partial t}A + A\frac{\partial}{\partial t}u + 2Au\frac{\partial}{\partial x}u + u^2\frac{\partial}{\partial x}A &= -\frac{A}{\rho}\frac{\partial p}{\partial x} \\
u\left(\frac{\partial}{\partial t}A + A\frac{\partial}{\partial x}u + u\frac{\partial}{\partial x}A\right) + A\frac{\partial}{\partial t}u + Au\frac{\partial}{\partial x}u &= -\frac{A}{\rho}\frac{\partial p}{\partial x} \qquad (3.10)
\end{aligned}$$

Using (3.4) we see, that the first term on the left side in (3.10) is equal to 0 and we obtain

$$A\frac{\partial}{\partial t}u + Au\frac{\partial}{\partial x}u = -\frac{A}{\rho}\frac{\partial p}{\partial x}$$

By dividing this equation by A we come to our final form of balance of linear momentum in local form:

$$\frac{\partial}{\partial t}u + u\frac{\partial}{\partial x}u = -\frac{1}{\rho}\frac{\partial p}{\partial x} \qquad (3.11)$$

Now we need to distinguish between compartments A and B as we did in the case of balance of mass.

$$\frac{\partial u_A}{\partial t} + u_A\frac{\partial u_A}{\partial x} = -\frac{1}{\rho}\frac{\partial p_A}{\partial x} \qquad (3.12)$$

$$\frac{\partial u_B}{\partial t} + u_B\frac{\partial u_B}{\partial x} = -\frac{1}{\rho}\frac{\partial p_B}{\partial x} \qquad (3.13)$$

As we can see, there is an increase in number of variables. We now have two more, p_A and p_B and we need to find a way how to express them in our three main variables Δp, u_A and u_B. According to [4] we can relate p_A and p_B as follows:

$$p_A = -\frac{1-\alpha_0}{\alpha_0} p_B \tag{3.14}$$

This will be discussed further in section 4.4. Now it's easy to find a way how we can express the terms p_A and p_B with Δp. For p_A holds

$$\begin{aligned} p_A &= -\frac{1-\alpha_0}{\alpha_0} p_B \\ \Delta p &= p_B - p_A \\ p_A &= -\frac{1-\alpha_0}{\alpha_0} \left(\Delta p + p_A\right) \\ \frac{1}{\alpha_0} p_A &= -\frac{1-\alpha_0}{\alpha_0} \Delta p \\ p_A &= -\left(1-\alpha_0\right) \Delta p \end{aligned}$$

and for p_B holds

$$\begin{aligned} p_B &= -\frac{\alpha_0}{1-\alpha_0} p_A \\ p_B &= \alpha_0 \Delta p. \end{aligned}$$

Right sides of equations (3.12) and (3.13) can be written as

$$\frac{1}{\rho}\frac{\partial p_A}{\partial x} = -\frac{\partial}{\partial x}\left(\frac{1-\alpha_0}{\rho}\Delta p\right) \tag{3.15}$$

$$\frac{1}{\rho}\frac{\partial p_B}{\partial x} = \frac{\partial}{\partial x}\left(\frac{\alpha_0}{\rho}\Delta p\right) \tag{3.16}$$

and therefore our final balance of linear momentum laws for both tubes are as following

$$\begin{aligned} \frac{\partial u_A}{\partial t} + \frac{\partial}{\partial x}\left(\frac{{u_A}^2}{2} - \frac{1-\alpha_0}{\rho}\Delta p\right) &= 0 \\ \frac{\partial u_B}{\partial t} + \frac{\partial}{\partial x}\left(\frac{{u_B}^2}{2} + \frac{\alpha_0}{\rho}\Delta p\right) &= 0. \end{aligned}$$

There's no need for special balance of angular momentum law. It is satisfied by tensor T being symmetrical[5] and since we substitued $T = -pI$, it clearly holds.

3.4 Modified balance of mass

Both (3.7) and (3.8) describe time evolution of transmural pressure difference Δp with help of variables u_A and u_B, every other element is a constant. Since Δp is exactly the same in these two equations, we would prefer to merge them in only one equation describing Δp changes in relation to changes of flow speeds u_A and u_B.

If we make a sum of equation (3.7) multiplied by α_0 and equation (3.8) multiplied by $(1-\alpha_0)$, we will obtain combined balance of mass in the form very well suited for finding characteristic speeds in the next chapter.

$$\begin{aligned}\alpha_0\frac{\partial}{\partial t}\Delta p + (1-\alpha_0)\frac{\partial}{\partial t}\Delta p + \left(\alpha_0\Delta p - \frac{{\alpha_0}^2}{D}\right)\frac{\partial u_A}{\partial x} + \\ + \left((1-\alpha_0)\Delta p + \frac{(1-\alpha_0)^2}{D}\right)\frac{\partial u_B}{\partial x} + \\ + \alpha_0 u_A\frac{\partial \Delta p}{\partial x} + (1-\alpha_0)u_B\frac{\partial \Delta p}{\partial x} = 0\end{aligned}$$

We can see that any unnecessary time derivatives of Δp will disappear. With little adjustments we obtain

$$\begin{aligned}\frac{\partial}{\partial t}\Delta p + (\alpha_0 u_A + (1-\alpha_0)u_B)\frac{\partial \Delta p}{\partial x} + \Delta p\frac{\partial}{\partial x}\alpha_0 u_A + (1-\alpha_0)u_B) + \\ + \frac{(1-\alpha_0)^2}{D}\frac{\partial u_B}{\partial x} - \frac{{\alpha_0}^2}{D}\frac{\partial u_A}{\partial x} = 0\end{aligned}$$

and finally we get to our combined balance of mass equation:

$$\frac{\partial}{\partial t}\Delta p + \frac{\partial}{\partial x}\left(\Delta p(\alpha_0 u_A + (1-\alpha_0)u_B) - u_A\frac{{\alpha_0}^2}{D} + u_B\frac{(1-\alpha_0)^2}{D}\right) = 0$$

3.5 Final system of equations

In this chapter, we derived governing equations describing our model.

$$\begin{aligned}\frac{\partial}{\partial t}\Delta p + \frac{\partial}{\partial x}\left(\Delta p(\alpha_0 u_A + (1-\alpha_0)u_B) - u_A\frac{{\alpha_0}^2}{D} + u_B\frac{(1-\alpha_0)^2}{D}\right) = 0 \\ \frac{\partial u_A}{\partial t} + \frac{\partial}{\partial x}\left(\frac{{u_A}^2}{2} - \frac{1-\alpha_0}{\rho}\Delta p\right) = 0 \\ \frac{\partial u_B}{\partial t} + \frac{\partial}{\partial x}\left(\frac{{u_B}^2}{2} + \frac{\alpha_0}{\rho}\Delta p\right) = 0\end{aligned}$$

We can see those are already in conservation form and so we can easily rewrite them as a vector equation in conservation form

$$\frac{\partial}{\partial t}W + \frac{\partial}{\partial x}F(W) = 0,$$

where $W = (u_A, u_B, \Delta p)^\top$ is a vector of conserved quantities and

$$
\begin{aligned}
F(W) &= (F_1(W), F_2(W), F_3(W))^\top \\
F_1(W) &= \frac{{u_A}^2}{2} - \frac{1-\alpha_0}{\rho}\Delta p \\
F_2(W) &= \frac{{u_B}^2}{2} + \frac{\alpha_0}{\rho}\Delta p \\
F_3(W) &= \Delta p(\alpha_0 u_A + (1-\alpha_0)u_B) - u_A\frac{{\alpha_0}^2}{D} + u_B\frac{(1-\alpha_0)^2}{D}
\end{aligned}
$$

is a vector of so-called fluxes.

This is our final system of governing equations for co-axial fluid-filled elastic tubes that we want to solve with consideration to problem of cerebrospinal fluid flow.

4. Governing equations analysis

Before we proceed to numerical solution, we need to further examine our system of equations. We assume it's a hyperbolic system, but we need to confirm that. Furthemore we need to introduce new variables that will help us better understand our model.

4.1 Pressure wave speed

We will follow the approach of Berkouk et al [1] and substract equation (3.12) from equation (3.13) to obtain

$$\begin{aligned}
&\frac{\partial u_B}{\partial t} - \frac{\partial u_A}{\partial t} + u_B\frac{\partial u_B}{\partial x} - u_A\frac{\partial u_A}{\partial x} = -\frac{1}{\rho}\frac{\partial p_B}{\partial x} + \frac{1}{\rho}\frac{\partial p_A}{\partial x} \\
&\frac{\partial u_B}{\partial t} - \frac{\partial u_A}{\partial t} + u_B\frac{\partial u_B}{\partial x} - u_A\frac{\partial u_A}{\partial x} = -\frac{1}{\rho}\frac{\partial \Delta p}{\partial x}
\end{aligned} \tag{4.1}$$

If we consider small-amplitude waves propagating into an initially undisturbed state where the flow is stationary, we can neglect third and fourth term on the left side of (4.1). If we now differentiate this equation with respect to x, we obtain

$$\frac{\partial^2 u_B}{\partial t \partial x} - \frac{\partial^2 u_A}{\partial t \partial x} + \frac{1}{\rho}\frac{\partial^2 \Delta p}{\partial x^2} = 0 \tag{4.2}$$

First and second term can be expressed by equations (3.5) and (3.6). We differentiate them with respect to t, so from (3.5) we obtain

$$\begin{aligned}
&\frac{\partial^2}{\partial t^2}\alpha + \frac{\partial^2}{\partial x \partial t}\left(\alpha u_A\right) = 0 \\
&\frac{\partial^2}{\partial t^2}\alpha + \alpha\frac{\partial^2}{\partial x \partial t}u_A + u_A\frac{\partial^2}{\partial x \partial t}\alpha + \frac{\partial}{\partial x}\alpha\frac{\partial}{\partial t}u_A + \frac{\partial}{\partial x}u_A\frac{\partial}{\partial t}\alpha = 0 \\
&\frac{\partial^2}{\partial t^2}\alpha + u_A\frac{\partial^2}{\partial x \partial t}\alpha + \frac{\partial}{\partial x}\alpha\frac{\partial}{\partial t}u_A + \frac{\partial}{\partial x}u_A\frac{\partial}{\partial t}\alpha = -\alpha\frac{\partial^2}{\partial x \partial t}u_A
\end{aligned} \tag{4.3}$$

and from (3.6) we obtain

$$\begin{aligned}
&-\frac{\partial^2}{\partial t^2}\alpha + \frac{\partial^2}{\partial x \partial t}\left(\left(1-\alpha\right)u_B\right) = 0 \\
&-\frac{\partial^2}{\partial t^2}\alpha + (1-\alpha)\frac{\partial^2}{\partial x \partial t}u_B + u_B\frac{\partial^2}{\partial x \partial t}(1-\alpha) + \\
&\qquad + \frac{\partial}{\partial x}(1-\alpha)\frac{\partial}{\partial t}u_B + \frac{\partial}{\partial x}u_B\frac{\partial}{\partial t}(1-\alpha) = 0 \\
&\frac{\partial^2}{\partial t^2}\alpha - u_B\frac{\partial^2}{\partial x \partial t}(1-\alpha) - \frac{\partial}{\partial x}(1-\alpha)\frac{\partial}{\partial t}u_B - \\
&\qquad - \frac{\partial}{\partial x}u_B\frac{\partial}{\partial t}(1-\alpha) = (1-\alpha)\frac{\partial^2}{\partial x \partial t}u_B
\end{aligned} \tag{4.4}$$

Again, we are considering only small-amplitude waves so we can neglect most of terms in both equations and end with

$$\frac{\partial^2}{\partial t^2}\alpha = -\alpha\frac{\partial^2}{\partial x \partial t}u_A \tag{4.5}$$

$$\frac{\partial^2}{\partial t^2}\alpha = (1-\alpha)\frac{\partial^2}{\partial x \partial t}u_B \tag{4.6}$$

So when we replace matching terms in (4.2) with (4.5) and (4.6) and if we use (1.1) and (1.2), we obtain

$$\begin{aligned}
\frac{1}{1-\alpha}\frac{\partial^2}{\partial t^2}\alpha + \frac{1}{\alpha}\frac{\partial^2}{\partial t^2}\alpha + \frac{1}{\rho}\frac{\partial^2 \Delta p}{\partial x^2} &= 0 \\
\left(\frac{1}{1-\alpha} + \frac{1}{\alpha}\right)\frac{\partial^2}{\partial t^2}\alpha + \frac{1}{\rho}\frac{\partial^2 \Delta p}{\partial x^2} &= 0 \\
\frac{\partial^2 \Delta p}{\partial x^2} - \left(\frac{D\rho}{\alpha(1-\alpha)}\right)\frac{\partial^2 \Delta p}{\partial t^2} &= 0
\end{aligned} \tag{4.7}$$

Equation 4.7 is a wave equation with wave speed

$$c^2 = \frac{\alpha(1-\alpha)}{D\rho}. \tag{4.8}$$

We can also define

$${c_0}^2 = \frac{\alpha_0(1-\alpha_0)}{D\rho}, \tag{4.9}$$

for chosen value of distensibility $c_0 \doteq 4,5mm/s$, which is in measured range[1].

4.2 Characteristics

For further study of our system of equations, we need to find its *characteristics* and especially relevant *characteristic speeds*. Whether they will be real, imaginary, positive or negative, will help us in numerical solution and further analysis of system.

Characteristics of system of partial differential equations

$$A(W,x,t)\frac{\partial W}{\partial t} + B(W,x,t)\frac{\partial W}{\partial x} = 0$$

with solution $W(x,t) = (W_1, W_2, W_3)$ are curves $\phi_i(x,t) = x - at = const$, $i = 1,2,3$, where the solution W is constant along those curves and a is *characteristic speed*. If we parametrize them with variable s, $\phi_i(s) = \phi_i(x(s), t(s)) = const$ we can find characteristic curves by solving ordinary differential equations

$$\frac{\partial t}{\partial s} = A(W,x,t),$$

$$\frac{\partial x}{\partial s} = B(W, x, t).$$

We can see that

$$\frac{dW}{ds} = \frac{\partial t}{\partial s}\frac{\partial W}{\partial t} + \frac{\partial x}{\partial s}\frac{\partial W}{\partial x} = 0$$

and therefore solution W is constant along $\phi_i(s)$, $i = 1, 2, 3$. And if I will denote unit matrix 3×3, we can write that

$$\begin{aligned} \frac{dW}{ds} = \frac{\partial W}{\partial t}\frac{dt}{ds} + \frac{\partial W}{\partial x}\frac{dx}{ds} = 0 \\ dW = \frac{\partial W}{\partial t}dt + \frac{\partial W}{\partial x}dx = 0 \\ \frac{\partial W}{\partial t}Idt + \frac{\partial W}{\partial x}Idx = 0 \end{aligned} \tag{4.10}$$

holds along characteristic curves.

Characteristic speed a satisfies $\phi_i(x, t) = x - at = const$, therefore along the characteristic curve holds

$$\begin{aligned} x + dx - a(t + dt) &= x - at \\ dx - adt &= 0 \\ dx &= dta \end{aligned}$$

and we can see that $a = \frac{dx}{dt}$.

Now if we look at our system of equations

$$\frac{\partial}{\partial t}W + \frac{\partial}{\partial x}F(W) = 0,$$

we can see that it also needs to hold along the characteristic curves. So we have two matrix equations that needs to be satisfied

$$\begin{aligned} \frac{\partial}{\partial t}W + \frac{\partial}{\partial x}F(W) = 0, \\ \frac{\partial W}{\partial t}Idt + \frac{\partial W}{\partial x}Idx = 0, \end{aligned}$$

and if we slightly rewrite the first equation

$$\begin{aligned} I\frac{\partial W}{\partial t} + F'(W)\frac{\partial W}{\partial x} = 0, \\ Idt\frac{\partial W}{\partial t} + Idx\frac{\partial W}{\partial x} = 0, \end{aligned} \tag{4.11}$$

where $F'(W)$ is a 3×3 Jacobian matrix that satisfies

$$\left(\frac{\partial F_1}{\partial x}, \frac{\partial F_2}{\partial x}, \frac{\partial F_3}{\partial x}\right)^\top = F'(W)\left(\frac{\partial W}{\partial x}, \frac{\partial W}{\partial x}, \frac{\partial W}{\partial x}\right)^\top,$$

we can see, that it can be considered system of linear equations for variables $\frac{\partial W}{\partial t}$ and $\frac{\partial W}{\partial x}$. Since our concern is that those equations hold, we are not interested in exact solution, but only in existence of non-trivial solution, i.e. $\frac{\partial W}{\partial t} \neq 0$ and $\frac{\partial W}{\partial x} \neq 0$.

Let us rewrite (4.11) in the following form

$$\begin{pmatrix} I & F'(W) \\ Idt & Idx \end{pmatrix} \begin{pmatrix} \frac{\partial W}{\partial t} \\ \frac{\partial W}{\partial x} \end{pmatrix} = \begin{pmatrix} 0 \\ 0 \end{pmatrix}.$$

Since the right side of this system is equal to null vector, it has non-trivial solution if and only if it's described by singular matrix. That means

$$\begin{vmatrix} I & F'(W) \\ Idt & Idx \end{vmatrix} = 0.$$

With a few adjustments we obtain

$$\begin{vmatrix} I & F'(W) \\ Idt & Idx \end{vmatrix} = dt^3 \begin{vmatrix} I & F'(W) \\ I & I\frac{dx}{dt} \end{vmatrix} = dt^3 \begin{vmatrix} 0 & F'(W) - I\frac{dx}{dt} \\ I & I\frac{dx}{dt} \end{vmatrix} = 0.$$

Now if we set $\lambda = \frac{dx}{dt}$ we see, that the whole problem is reduced to

$$det(F'(W) - I\lambda) = 0$$

and finding λ that satisfies this equation is equivalent to finding eigenvalues of matrix $F'(W)$ and those eigenvalues equals to characteristic speeds.

The reason we are interested in characteristic speeds is that since the solution is constant along the characteristic curve, we can use an intial condition $u_0(x) = u(x, 0)$ to determine solution $u(x, t)$ in time t. We can write $\phi_i(x, t) = x - at = const = \phi_i(x - at, 0)$, so

$$u(x, t) = u_0(x - at).$$

Initial condition at point $x - at$ determines solution at (x, t). This is important for boundary conditions as we can see that characteristic speed a determines if we can calculate solution from the inside of the computational domain (i.e. we can't set the boundary condition) or from the outside (i.e. we must set the boundary condition).

4.3 Characteristic speeds

First we need to rewrite our system of governing equations so it corresponds with aforementioned method. With a little adjustments we can write

$$\begin{aligned} \frac{\partial}{\partial t}\Delta p + \frac{\partial}{\partial x}\left(\Delta p(\alpha_0 u_A + (1-\alpha_0)u_B) - u_A {\alpha_0}^2/D + u_B(1-\alpha_0)^2/D\right) &= 0 \\ \frac{\partial u_A}{\partial t} + \frac{\partial}{\partial x}\left(\frac{{u_A}^2}{2} - \frac{1-\alpha}{\rho}\Delta p\right) &= 0 \\ \frac{\partial u_B}{\partial t} + \frac{\partial}{\partial x}\left(\frac{{u_B}^2}{2} + \frac{\alpha}{\rho}\Delta p\right) &= 0 \end{aligned}$$

We can see that

$$F'(W) = \begin{pmatrix} u_A & 0 & \alpha_0\Delta p - {\alpha_0}^2/D \\ 0 & u_B & (1-\alpha_0)\Delta p + (1-\alpha_0)^2/D \\ -(1-\alpha_0)/\rho & \alpha_0/\rho & \alpha_0 u_A + (1-\alpha_0)u_B \end{pmatrix},$$

so to find characteristic speed we need to find λ such that it satisfies

$$\begin{vmatrix} u_A - \lambda & 0 & \alpha_0\Delta p - {\alpha_0}^2/D \\ 0 & u_B - \lambda & (1-\alpha_0)\Delta p + (1-\alpha_0)^2/D \\ -(1-\alpha_0)/\rho & \alpha_0/\rho & \alpha_0 u_A + (1-\alpha_0)u_B - \lambda \end{vmatrix} = 0$$

Since we are trying to find determinant of 3×3 matrix, after using Sarrus' scheme we obtain

$$(u_A - \lambda)(u_B - \lambda)((1-\alpha_0)u_A + \alpha_0 u_B - \lambda) - \tag{4.12}$$

$$-(u_B - \lambda)(-\frac{(1-\alpha_0)}{\rho})(\alpha_0\Delta p - {\alpha_0}^2/D) - \tag{4.13}$$

$$-(u_A - \lambda)\frac{\alpha_0}{\rho}((1-\alpha_0)\Delta p + (1-\alpha_0)^2/D) = 0 \tag{4.14}$$

For easier computing we establish notation

$$\bar{u} = u_A + u_B$$

$$\acute{u_0} = \alpha_0 u_A + (1-\alpha_0)u_B$$

and we start with expanding (4.12):

$$\begin{aligned} &(u_A - \lambda)(u_B - \lambda)(\acute{u_0} - \lambda) = \\ &= u_A u_B \acute{u_0} - \lambda(u_A u_B + u_A \acute{u_0} + u_B \acute{u_0}) + \\ &+ \lambda^2(\bar{u} + \acute{u_0}) - \lambda^3. \end{aligned}$$

From (4.13) we obtain

$$\begin{aligned} &- (u_B - \lambda)(-\frac{\alpha_0(1-\alpha_0)}{\rho}\Delta p + \frac{{\alpha_0}^2(1-\alpha_0)}{D\rho}) = \\ &- (u_B - \lambda)(-{c_0}^2\Delta p D + \alpha_0 {c_0}^2) \end{aligned} \tag{4.15}$$

and from (4.14) we obtain

$$\begin{aligned} &- (u_A - \lambda)(\frac{\alpha_0(1-\alpha_0)}{\rho}\Delta p + \frac{\alpha_0(1-\alpha_0)^2}{D\rho} = \\ &- (u_A - \lambda)({c_0}^2\Delta p D + (1-\alpha_0){c_0}^2). \end{aligned} \tag{4.16}$$

Now if we add (4.15) and (4.16) we can write

$$\lambda\left(-{c_0}^2\Delta p D + \alpha_0 {c_0}^2 + {c_0}^2\Delta p D + (1-\alpha_0){c_0}^2\right) +$$

$$+u_B {c_0}^2 \Delta pD - u_B \alpha_0 {c_0}^2 - u_A {c_0}^2 \Delta pD - u_A(1-\alpha_0){c_0}^2 =$$

$$= \lambda {c_0}^2 + (u_B - u_A)\, {c_0}^2 \Delta pD - ((1-\alpha_0)u_A + \alpha_0 u_B)\, {c_0}^2 =$$

$$= \lambda {c_0}^2 + (u_B \Delta pD - u_A \Delta pD - u_A + \alpha_0 u_A - \alpha_0 u_B)\, {c_0}^2 =$$

$$= \lambda {c_0}^2 + ((\alpha_0 - \Delta pD - 1)u_A + (\Delta pD - \alpha_0)u_B)\, {c_0}^2 =$$

$$= \lambda {c_0}^2 - ((1-\alpha)u_A + \alpha u_B)\, {c_0}^2 =$$

$$= \lambda {c_0}^2 - (\bar{u} - \acute{u})\, {c_0}^2$$

Where we introduced, similarly to $\acute{u_0}$,

$$\acute{u} = \alpha u_A + (1-\alpha)u_B,$$
$$\bar{u} - \acute{u} = (1-\alpha)u_A + \alpha u_B.$$

Adding (4.12), (4.15) and (4.16) we obtain equation for characteristic polynomial $\chi(\lambda)$ of matrix $F'(W)$

$$\chi(\lambda) = \lambda^3 - \lambda^2(\bar{u} + \acute{u_0}) + \lambda(u_A u_B + u_A \acute{u_0} + u_B \acute{u_0} - {c_0}^2) + {c_0}^2(\bar{u} - \acute{u}) - u_A u_B \acute{u_0}.$$

Since ${c_0}^2 \gg u^2$, where $u \approx u_A,\ u_B,\ \acute{u_0}$, we can neglect several terms and end up with

$$\lambda^3 - \lambda^2(\bar{u} + \acute{u_0}) - \lambda({c_0}^2) + {c_0}^2(\bar{u} - \acute{u}) =$$
$$\lambda^2(\lambda - (\bar{u} + \acute{u_0})) - {c_0}^2(\lambda - (\bar{u} - \acute{u})).$$

We need λ to satisfy $\chi(\lambda) = 0$ and we can already guess that two roots of characteristic polynomial will relate to pressure-wave speed c_0:

$$\lambda_1 \approx -c_0$$
$$\lambda_2 \approx +c_0,$$

Suppose we rewrite polynomial $\chi(\lambda)$ as following

$$\chi(\lambda) = \lambda^2(\lambda - (\bar{u} + \acute{u_0})) - {c_0}^2(\lambda - (\bar{u} + \acute{u_0})) - {c_0}^2(\acute{u_0} - \acute{u}) =$$

$$= (\lambda^2 - {c_0}^2)(\lambda - (\bar{u} + \acute{u_0})) - {c_0}^2(\acute{u_0} - \acute{u}) =$$

$$= (\lambda^2 - {c_0}^2)(\lambda - (\bar{u} + \acute{u_0})) - {c_0}^2(\alpha_0 u_A + (1-\alpha_0)u_B - \alpha u_A - (1-\alpha)u_B) =$$

$$= (\lambda^2 - {c_0}^2)(\lambda - (\bar{u} + \acute{u_0})) - {c_0}^2((\alpha_0 - \alpha)u_A - (\alpha_0 - \alpha)u_B) =$$

$$= \overline{\chi(\lambda)} - {c_0}^2 D\Delta p(u_A - u_B)$$

Now we can see, that polynomials $\overline{\chi(\lambda)}$ and $\chi(\lambda)$ differ only in the last term. This term is very small, in fact we can write that

$${c_0}^2 D\Delta p(u_A - u_B) \approx 10^1 \cdot 10^{-5} \cdot 10^3 \cdot 10^{-1} = 10^{-2},$$

so polynomial $\overline{\chi(\lambda)}$ is, for our purposes, a good approximation of polynomial $\chi(\lambda)$. It's eigenvalues are

$$\bar{\lambda}_1 = \bar{u} + \acute{u_0}$$
$$\bar{\lambda}_2 = -c_0$$
$$\bar{\lambda}_3 = +c_0$$

and we can express eigenvalues of polynomial $\chi(\lambda)$ as

$$\lambda_1 \approx \bar{u} + \acute{u_0},$$
$$\lambda_2 \approx -c_0,$$
$$\lambda_3 \approx +c_0,$$

so we can see we have three real-valued eigenvalues. Evidently $\lambda_2 < 0$, $\lambda_3 > 0$, but we need to further investigate λ_1 to find out if corresponding characteristic speed is negative or positive.

4.4 Analysis of the weak nonlinearity

According to Berkouk et al [1] we can develop weakly nonlinear theory based on small parameter $\epsilon = D\Delta p \ll 1$ and expand variables in powers of ϵ as follows:

$$\alpha = \alpha_0 - \epsilon \tag{4.17}$$
$$u_A = \epsilon u_{A1} + O(\epsilon^2) \tag{4.18}$$
$$u_B = \epsilon u_{B1} + O(\epsilon^2). \tag{4.19}$$

Let us consider elastic jump that forms as the leading edge of the pressure wave steepens and let us denote variables after an elastic jump as $U_{A'}$, $U_{B'}$, $P_{A'}$, $P_{B'}$, $\Delta P'$, $\alpha' = A_{A'}/A_T$ and variables before elasitc jump as U_{A_0}, U_{B_0}, P_{A_0}, P_{B_0}, ΔP_0, $\alpha_0 = A_{A_0}/A_T$ and V as speed of pressure pulse (See fig. 4.1). Since we are considering propagation into undisturbed flow, we can take $U_{A_0} = U_{B_0} = P_{A_0} = P_{B_0} = \Delta P_0 = 0$. Assumption for P_{A_0} and P_{B_0} is justifiable since we are never interested in actual values of those variables, only their difference.

If we consider volume marked by dashed lines, we see that flow-rate through the boundary 0 equals $\rho A_{A_0} C$, while through the $'$ boundary it's equal to $A_{A'}(C - U_{A'})$. Moreover, we won't be interested in change in time, because our control volume travels along the elastic jump with the same speed and its value can be considered equal to its value in next time step.

Therefore we take the mass balance equation (3.3) in the form

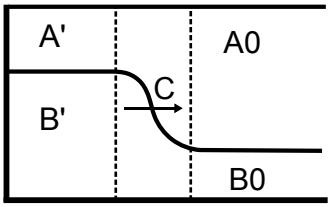

Figure 4.1: Propagating of pulse pressure wave into undisturbed flow

$$\int_0^{'} \frac{\partial}{\partial x} \rho A u dx = 0$$

and for compartment A we obtain

$$\begin{aligned} \int_0^{'} \frac{\partial}{\partial x} \rho A_A u dx &= 0 \\ \rho A_{A'}(V - U_{A'}) - \rho A_{A_0}(V - U_{A_0}) &= 0 \\ \rho A_{A'}(V - U_{A'}) &= \rho A_{A_0}. \end{aligned}$$

Doing the same in compartment B and little dividing the equations by ρA_T gives us

$$\alpha_0 C = \alpha' (C - U_{A'}) \tag{4.20}$$

$$(1 - \alpha_0) C = (1 - \alpha') (C - U_{B'}) . \tag{4.21}$$

Using the same approach on balance of linear momentum

$$\int_{V_t} \left(\frac{\partial}{\partial t}(\rho A u) + \frac{\partial}{\partial x}(\rho A u^2) \right) dx = \int_{V_t} \nabla p A dx$$

we obtain for compartment A following:

$$\int_0^{'} \frac{\partial}{\partial x}(\rho A_A u_A^2) dx = \int_0^{'} \nabla p_A A_A dx$$

$$\rho A_{A'}(C - u_{A'})^2 - \rho A_{A_0} u_{A_0}^2 = P_{A'} A_{A'} - P_{A_0} A_{A_0} - \int_0^{'} p_A \frac{\partial}{\partial x} A_A dx$$

$$\rho \left[A_{A'}(C - u_{A'}) \right] (C - u_{A'}) = P_{A'} A_{A'} - \int_{A_{A_0}}^{A_{A'}} p_A dA_A$$

using (4.20) and dividing by A_T gives us

$$\rho\alpha_0 C(C - u_{A'}) = p_{A'}A_{A'} - \int_{\alpha_0}^{\alpha'} p_A d\alpha.$$

For both compartmens we obtain equations

$$P_{A'}\alpha' - \int_{\alpha_0}^{\alpha'} p_A d\alpha = \rho\alpha_0 C U_{A'} \tag{4.22}$$

$$P_{B'}(1-\alpha') + \int_{\alpha_0}^{\alpha'} p_B d\alpha = \rho(1-\alpha_0) C U_{B'}. \tag{4.23}$$

Adding equations (4.22) and (4.23) gives us

$$P_{A'} + \Delta P'(1-\alpha') + \int_{\alpha_0}^{\alpha'} \Delta p d\alpha = \rho C\left[\alpha_0 U_{A'} + (1-\alpha_0)U_{B'}\right] \tag{4.24}$$

and substracting equation (4.22) divided by α' from equatin (4.23) divided by $(1-\alpha')$ gives us

$$\Delta P' + \frac{1}{1-\alpha'}\int_{\alpha_0}^{\alpha'} \Delta p d\alpha + \left(\frac{1}{\alpha'} + \frac{1}{1-\alpha'}\right)\int_{\alpha_0}^{\alpha'} p_A d\alpha = \rho C\left(\frac{1-\alpha_0}{1-\alpha'}U_{B'} - \frac{\alpha_0}{\alpha'}U_{A'}\right). \tag{4.25}$$

We would like to evaluate integrals in both equations. Substituting $d\alpha = d(-D\Delta p) = -Dd\Delta p$ we can write

$$\int_{\alpha_0}^{\alpha'} \Delta p d\alpha = -D\int_0^{\Delta P'} \Delta p d\Delta p = -\frac{D(\Delta P')^2}{2}$$

For evaluating integral containing p_A we will use following estimation[1]:

$$\int_{\alpha_0}^{\alpha'} p_A d\alpha \simeq -\frac{DP_{A'}\Delta P'}{2}.$$

Substituting in equations gives us

$$P_{A'} + \Delta P'(1-\alpha') - \frac{D(\Delta P')^2}{2} = \rho V\left[\alpha_0 U_{A'} + (1-\alpha_0)U_{B'}\right] \tag{4.26}$$

$$\Delta P' - \frac{D}{1-\alpha'}\frac{(\Delta P')^2}{2} - DP_{A'}\frac{\Delta P'}{2}\left(\frac{1}{\alpha'} + \frac{1}{1-\alpha'}\right) = \rho V\left(\frac{1-\alpha_0}{1-\alpha'}U_{B'} - \frac{\alpha_0}{\alpha'}U_{A'}\right). \tag{4.27}$$

Now using the expansion of main variables in powers of small parameter ϵ:

$$\begin{aligned} U_{A'} &= \epsilon U_{A'1} + O(\epsilon^2) \\ U_{B'} &= \epsilon U_{B'1} + O(\epsilon^2) \\ C &= c_0 + \epsilon C_1 + O(\epsilon^2) \\ P'_A &= \epsilon P_{A'1} + O(\epsilon^2) \end{aligned}$$

gives us from equations (4.20) and (4.21):

$$\begin{aligned} U_{A'1} &= -\frac{c_0}{\alpha_0} \\ U_{B'1} &= \frac{c_0}{1-\alpha_0} \end{aligned}$$

from equation (4.26):

$$P_{A'1} = -\frac{1-\alpha_0}{D}$$

and from equation (4.27):

$$\begin{aligned} C_0 &= c_0 \\ C_1 &= \frac{3}{4}\left(\frac{1}{1-\alpha_0} - \frac{1}{\alpha_0}\right) c_0. \end{aligned}$$

We can see, that when $\epsilon > 0$, more precisely $p_B > p_A$, then $u_A < 0$ and $u_B > 0$. Also, considering eigenvalues $F'W$

$$\begin{aligned} \bar{u} + \acute{u_0} &= (1+\alpha_0)u_A + (2-\alpha_0)u_B = \\ &= -c_0\frac{1+\alpha_0}{\alpha_0}\epsilon + c_0\frac{2-\alpha_0}{1-\alpha_0}\epsilon \\ &= \left(\frac{2-\alpha_0}{1-\alpha_0}\right) - \frac{1+\alpha_0}{\alpha_0}c_0\epsilon \\ &= \left(\frac{2\alpha_0 - \alpha_0^2 - 1 + \alpha_0^2}{\alpha_0(1-\alpha_0)}\right) c_0\epsilon \\ &= \left(\frac{2\alpha_0 - 1}{\alpha_0(1-\alpha_0)}\right) c_0\epsilon. \end{aligned}$$

So when $\alpha_0 > 0.5$ and $\Delta p > 0$, $\lambda_1 = \bar{u} + \acute{u_0} > 0$. We can also see, that

$$\begin{aligned} P_{B'} - P_{A'} &= \Delta P' \\ P_{B'} &= \Delta P' - \frac{1-\alpha_0}{D}\epsilon \\ P_{B'} &= \Delta P' - \Delta P'(1-\alpha_0) \\ \epsilon P_{B'1} &= \Delta P'\alpha_0 \\ P_{B'1} &= \frac{\alpha_0}{D} \end{aligned}$$

and from this we can obtain previously used (3.14).

4.5 Hyperbolic system of PDR

Let us consider our system of partial differential equations in the form

$$\frac{\partial}{\partial t}W + F'(W)\frac{\partial}{\partial x}W = 0.$$

This system is called **strictly hypebolic**[2], if each matrix $F'(W)$ has 3 real distinc eigenvalues $\lambda_i \neq \lambda_j$, for $i \neq j$, $i, j = 1 \dots 3$, which is our case.

Classical solution to system

$$\begin{aligned} \frac{\partial}{\partial t}W + \frac{\partial}{\partial x}F(W) &= 0 \\ W_t + F(W)_x &= 0, \\ W(x,0) = W_0(x) &= (0,0,0)^\top \end{aligned} \tag{4.28}$$

on domain $\Omega \times (0,T) \subset \mathbb{R} \times \mathbb{R}$, T is maximum time, satisfies equations (4.28) in every point of $\Omega \times (0,T)$ and $W \in C^1(\Omega \times (0,T))$, $W_0 \in C^1(\Omega)$. If this solution exists, it is unique.

Problem with non-linear hyperbolic systems such as ours is that classical solution can very easily collapse in very small times. This can be shown on Burgers' equation

$$\begin{aligned} u_t + uu_x &= 0, \\ u(x,0) &= u_0(x), \end{aligned} \tag{4.29}$$

where $u_t = \frac{\partial u}{\partial t}$ and $u_x = \frac{\partial u}{\partial x}$.

The characteristic curves are straight lines and we can show that even for initial data from C^∞, those characteristic curves crosses.

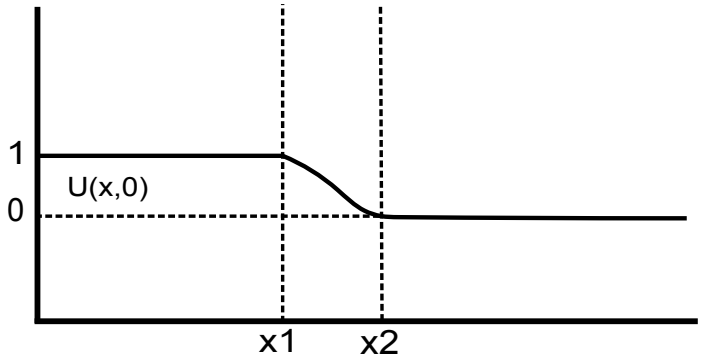

Figure 4.2: Initial condition for equation 4.29

For equation (4.29) with initial data similar to (4.2), the slope of characteristic curves equals

$$\frac{dt}{dx} = \frac{1}{u(x,t)} = \frac{1}{u_0(\bar{x})},$$

where $\bar{x}$ are corresponding coordinates along the straight line characteristic. Figure 4.3 shows what happens with characteristic curves and how classical solution can't be used for determining actual solution of equation for $t \geq T$.

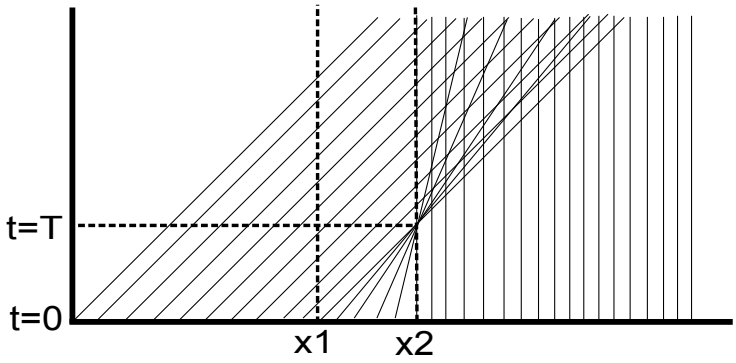

Figure 4.3: Slopes of characteristics for given initial condition

We need to consider another solution, so-called weak solution that allows discontinuous solutions and initial conditions. Let us take our system of equations (4.28), multiply it by some differentiable function with compact support $\phi \in C_0^1(\Omega \times [0,T])$, integrate it with respect to $x \in \Omega$ and $t \in (0,T)$ and use the divergence theorem, we see that

$$\int_0^T \int_\Omega W_t \phi dx dt + \int_0^\infty \int_\Omega F(W)_x \phi dx dt = 0$$
$$\int_0^T \int_\Omega \{W\phi_t + F(W)\phi_x\} dx dt = 0$$

Therefore according to[2], we will call locally integrable function $W = W(t,x)$ a weak solution of (4.28) if $t \to u(t,\cdot)$ is continuous as a map with values in L^1_{loc} and

$$\int_0^T \int_\Omega \{W\phi_t + F(W)\phi_x\} dx dt = 0$$

for every differentiable function with compact support $\phi \in C_0^1(\Omega \times (0,T))$.

Weak solution always exists, but in contrast with classical solution, it is generally not unique. We can find many weak solutions and since any real problem modelled by hyperbolic system has unique real world solution, it is evident that not all of those weak solutions make physical sense and should be used. So we need to find restrictive condition that selects only acceptable weak solution.

Let $\eta \in C^1(\mathbb{R}^3)$, $\eta : \mathbb{R}^3 \to \mathbb{R}$ be called entropy and $q \in C^1(\mathbb{R}^3)$ that satisfies

$$\sum_k^3 \frac{\partial F_k}{\partial W_l} \frac{\partial \eta}{\partial W_k} = \frac{\partial q}{\partial W_l}$$

be called entropy flux, then C^1 solution $W(x,t)$ of (4.28) satisfies[2]

$$\eta(W)_t + q(W)_x = 0.$$

This is in a sense an additional conservation law for our hyperbolic system (4.28) and we will call a weak solution $W(x,t)$ entropy-admissable[2], if

$$\eta(W)_t + q(W)_x \geq 0$$

holds in distribution sense, i.e.

$$\int_0^T \int_\Omega \{\eta(W)\phi_t + q(W)\phi_x\} dxdt \geq 0,$$

for every $\phi \geq 0$, $\phi \in C_0^1(\Omega \times (0,T))$[2].

Now, let us consider the Cauchy problem for modified hyperbolic system with viscosity

$$\begin{aligned} W_t^\epsilon + F(W^\epsilon)_x &= \epsilon W_{xx}^\epsilon, \\ W^\epsilon(x,0) &= W_0(x), \end{aligned} \tag{4.30}$$

where ϵ is a small parameter $\epsilon > 0$, then if

$$\begin{aligned} V(W_0,\Omega) &< \delta, \\ \|W_0\|_{L^\infty} &< \delta, \end{aligned}$$

where $V(W_0,\Omega) = sup\left[\int_\Omega W_0 \cdot div(\phi)dx : \phi \in C_0^1(\Omega,\mathbb{R}), \|\phi\|_{L^\infty(\Omega)} \leq 1\right]$ is total variation of W_0 and $\delta > 0$, then (4.30) has unique solution for all ϵ[2]. If those solutions converges for $\epsilon \to 0$ to some $W(x,t)$ boundedly almost everywhere (i.e. in L^1 norm), then W would be admissable solution to problem (4.28)(satisfying the entropy condition)[3].

We will further adress the problem of correct weak solution in section 5.1.

5. Numerical solution

5.1 Lax-Wendroff scheme

For computing approximate solution to our system of equations we will use Richtmyer two-step Lax-Wendroff scheme as described in [9]. Let $\tau > 0$ be a length of time step, $n \in \mathbb{N}$ be a number of time step and let h be a length of minimal spatial interval, $j \in \mathbb{N}$ be a number of spatial interval. When we denote the count of all spatial intervals J then $J \cdot h$ is the whole spatial interval, where we want to compute solution. Then the scheme looks like this

$$\begin{aligned} U_j^{n+1} &= U_j^n - \frac{\tau}{h}\left[F\left(U_{j+\frac{1}{2}}^{n+\frac{1}{2}}\right) - F\left(U_{j-\frac{1}{2}}^{n+\frac{1}{2}}\right)\right] \\ U_{j+\frac{1}{2}}^{n+\frac{1}{2}} &= \frac{1}{2}\left(U_j^n + U_{j+1}^n\right) - \frac{\tau}{2h}\left[F\left(U_{j+1}^n\right) - F\left(U_j^n\right)\right] \end{aligned} \tag{5.1}$$

According to[7] we will add so called artificial viscosity to (5.1) to help us damp oscillations that would appear in our solution.

$$\begin{aligned} U_j^{n+1} &= U_j^n - \frac{\tau}{h}\left[F\left(U_{j+\frac{1}{2}}^{n+\frac{1}{2}}\right) - F\left(U_{j-\frac{1}{2}}^{n+\frac{1}{2}}\right)\right] \\ U_{j+\frac{1}{2}}^{n+\frac{1}{2}} &= \frac{1}{2}\left(U_j^n + U_{j+1}^n\right) - \frac{\tau}{2h}\left[F\left(U_{j+1}^n\right) - F\left(U_j^n\right)\right] + \gamma\left(U_{j+1}^n - 2U_j^n + U_{j-1}^n\right), \end{aligned} \tag{5.2}$$

where $\gamma = \tau Q$, Q is a constant. By comparing appendices A and C we can see the effect of added term. Furthermore, scheme in this form imitates vanishing viscosity solution of our hyperbolic system. For $\tau \to 0$ it converges to numerical solution to our original problem.

Scheme (5.2) is suitable for nonlinear problems such as ours and we need to further examine its properties, namely its stability and phase error (dispersion) and order of dissipation. Since it is in conservative form, we can expect it to be convergent, if it is stable.

5.2 Stability of numerical scheme

We would want to use von Neumann stability analysis (also known as Fourier stability analysis), so we need to consider linear scheme

$$\begin{aligned} U_j^{n+1} &= U_j^n - \frac{\tau}{h}\left[aU_{j+\frac{1}{2}}^{n+\frac{1}{2}} - aU_{j-\frac{1}{2}}^{n+\frac{1}{2}}\right] + \gamma\left(U_{j+1}^n - 2U_j^n + U_{j-1}^n\right) \\ U_{j+\frac{1}{2}}^{n+\frac{1}{2}} &= \frac{1}{2}\left(U_j^n + U_{j+1}^n\right) - \frac{\tau}{2h}\left[aU_{j+1}^n - aU_j^n\right] \\ U_j^{n+1} &= U_j^n - a\frac{\tau}{2h}\left[U_{j+1}^n - U_{j-1}^n - a\frac{\tau}{h}\left(U_{j+1}^n - 2U_j^n + U_{j-1}^n\right)\right] + \\ &\quad + \gamma\left(U_{j+1}^n - 2U_j^n + U_{j-1}^n\right), \end{aligned} \tag{5.3}$$

where a is characteristic speed and is constant. This can be a problem, but if we take our system

$$\begin{aligned}\frac{\partial}{\partial t}W + \frac{\partial}{\partial x}F(W) = 0\\ \frac{\partial W}{\partial t}I + F'(W)^\top \frac{\partial W}{\partial x} = 0,\end{aligned}$$

and consider matrix of left eigenvectors S and diagonal matrix of eigenvalues Λ,

$$SF'(W)^\top = \Lambda S,$$

we can see that

$$\begin{aligned}\frac{\partial}{\partial t}W + \frac{\partial}{\partial x}F(W) = 0\\ S\frac{\partial W}{\partial t}I + SF'(W)^\top \frac{\partial W}{\partial x} = 0\\ S\frac{\partial W}{\partial t}I + \Lambda S\frac{\partial W}{\partial x} = 0\\ \frac{\partial R}{\partial t}I + \Lambda \frac{\partial R}{\partial x} = 0,\end{aligned}$$

where $R_x = SW_x$ and $R_t = SW_t$. Since our characteristic speeds are bounded and don't change that much with respect to time and spatial coordinates, stability analysis for a linear version of Lax-Wendroff scheme with $a = max(\lambda_1, \lambda_2, \lambda_3)$ can be applied to our case.

Using approximation of solution

$$W(x,t) = \sum_{m=-\infty}^{\infty} e^{im\pi x - (m\pi)^2 t},$$

where $x = jh$, $t = n\tau$ and $m\pi = k$ we can write our approximate solution in the form

$$U_j^n = \lambda^n e^{ijkh},$$

where λ is an amplification factor that we want to examine. Introducing the parameter

$$\tilde{\nu} = a\frac{\tau}{2h}, \tag{5.4}$$

we can expand our scheme using (5.4)

$$
\begin{aligned}
U_j^{n+1} &= U_j^n - \tilde{\nu}\left(U_{j+1}^n - U_{j-1}^n\right) + \\
&+ 2\tilde{\nu}^2\left(U_{j+1}^n - 2U_j^n + U_{j-1}^n\right) + \gamma\left(U_{j+1}^n - 2U_j^n + U_{j-1}^n\right) \\
\lambda^{n+1}e^{ijkh} &= \lambda^n e^{ijkh} - \tilde{\nu}\left(\lambda^n e^{i(j+1)kh} - \lambda^n e^{i(j-1)kh}\right) + \\
&+ 2\tilde{\nu}^2\left(\lambda^n e^{i(j+1)kh} - 2\lambda^n e^{ijkh} + \lambda^n e^{i(j-1)kh}\right) + \\
&+ \gamma\left(\lambda^n e^{i(j+1)kh} - 2\lambda^n e^{ijkh} + \lambda^n e^{i(j-1)kh}\right) \\
\lambda &= 1 - \tilde{\nu}\left(e^{ikh} - e^{-ikh}\right) + 2\tilde{\nu}^2\left(e^{ikh} - 2 + e^{-ikh}\right) + \gamma\left(e^{ikh} - 2 + e^{-ikh}\right)
\end{aligned}
\tag{5.5}
$$

Using Euler's formula we can write

$$
\begin{aligned}
e^{ikh} + e^{-ikh} &= 2\cos(kh) \\
e^{ikh} - e^{-ikh} &= 2i\sin(kh).
\end{aligned}
$$

and we can also rewrite

$$
\nu = a\frac{\tau}{h} = 2\tilde{\nu}, \tag{5.6}
$$

where ν is so-called Courant number. Now let us further adjust

$$
\begin{aligned}
\lambda &= 1 - 2i\tilde{\nu}\sin(kh) + 2\tilde{\nu}^2\left(2\cos(kh) - 2\right) + \gamma\left(2\cos(kh) - 2\right) \\
\lambda &= 1 - i\nu\sin(kh) + \nu^2\left(\cos(kh) - 1\right) + 2\gamma\left(\cos(kh) - 1\right).
\end{aligned}
\tag{5.7}
$$

To obtain amplification factor only in terms of sin, we can use

$$
\begin{aligned}
\cos(kh) &= \cos\left(2\frac{kh}{2}\right) = \cos^2\left(\frac{kh}{2}\right) - \sin^2\left(\frac{kh}{2}\right) \\
\cos(kh) - 1 &= \cos^2\left(\frac{kh}{2}\right) - \sin^2\left(\frac{kh}{2}\right) - \left[\cos^2\left(\frac{kh}{2}\right) + \sin^2\left(\frac{kh}{2}\right)\right] \\
&= -2\sin^2\left(\frac{kh}{2}\right)
\end{aligned}
$$

and finally get from (5.7) equation for amplification factor λ.

$$
\begin{aligned}
\lambda &= 1 - i\nu\sin(kh) - 2\nu^2\sin^2\left(\frac{kh}{2}\right) - 4\gamma\sin^2\left(\frac{kh}{2}\right) \\
\lambda &= 1 - i\nu\sin(kh) - (2\nu^2 + 4\gamma)\sin^2\left(\frac{kh}{2}\right)
\end{aligned}
\tag{5.8}
$$

We are interested in magnitude of λ, if we would find out that $\|\lambda\| > 1$ then the error would be amplified and the scheme wouldn't be stable. Therefore we want to know when $\|\lambda\| < 1$ and it's easier to examine the case of $\|\lambda\|^2 < 1$.

$$
\begin{aligned}
&\|\lambda(k)\|^2 = \\
&= \left(1 - (2\nu^2 + 4\gamma)\sin^2\left(\frac{kh}{2}\right)\right)^2 + \nu^2\sin^2(kh) \\
&= 1 - 2(2\nu^2 + 4\gamma)\sin^2\left(\frac{kh}{2}\right) + \left((2\nu^2 + 4\gamma)\sin^2\left(\frac{kh}{2}\right)\right)^2 + \nu^2\sin^2(kh) \\
&= 1 - 4(\nu^2 + 2\gamma)\sin^2\left(\frac{kh}{2}\right) + 4\left(\nu^2 + 2\gamma\right)^2\sin^4\left(\frac{kh}{2}\right) + \\
&+ 4\nu^2\sin^2\left(\frac{kh}{2}\right)\cos^2\left(\frac{kh}{2}\right) \\
&= 1 - 4(\nu^2 + 2\gamma)\sin^2\left(\frac{kh}{2}\right)\left(1 - \cos^2\left(\frac{kh}{2}\right)\right) + \\
&+ 4\left(\nu^2 + 2\gamma\right)^2\sin^4\left(\frac{kh}{2}\right) - 8\gamma\sin^2\left(\frac{kh}{2}\right)\cos^2\left(\frac{kh}{2}\right) \\
&= 1 - 4(\nu^2 + 2\gamma)(1 - (\nu^2 + 2\gamma))\sin^4\left(\frac{kh}{2}\right) - 2\gamma\sin^2(kh)
\end{aligned} \tag{5.9}
$$

Now, since we set $\gamma > 0$, it's only the second term in (5.9) that interests us. We can see that

$$
\begin{aligned}
\|\lambda(k)\| < 1 &\iff 1 - (\nu^2 + 2\gamma) > 0 \\
&\iff 1 - 2\gamma > \nu^2 \\
&\iff \sqrt{1 - 2\gamma} > \|\nu\|
\end{aligned} \tag{5.10}
$$

and 5.10 is our main condition of stability, so-called CFL condition for our numerical scheme (5.2).

For investigating dissipation of our scheme, we are interested in inequality

$$
\|\lambda(k)\| \leq 1 - C(\sin\frac{kh}{2})^{2r}. \tag{5.11}
$$

If we can find such an inequality for constant C independent on τ and h, the scheme will be dissipative of order r. Let us write

$$
\begin{aligned}
\|\lambda(k)\|^2 = 1 &- 4\nu^2(1 - \nu^2 - 4\gamma)\sin^4\left(\frac{kh}{2}\right) - 4(2\gamma - 4\gamma^2)\sin^4\left(\frac{kh}{2}\right) - \\
&- 8\gamma\sin^2\left(\frac{kh}{2}\right)\cos^2\left(\frac{kh}{2}\right) \\
&= 1 - 4\nu^2(1 - \nu^2 - 4\gamma)\sin^4\left(\frac{kh}{2}\right) - \\
&- 8\gamma\sin^2\left(\frac{kh}{2}\right) + 16\gamma^2\sin^4\left(\frac{kh}{2}\right)
\end{aligned}
$$

and with little adjustment we can write

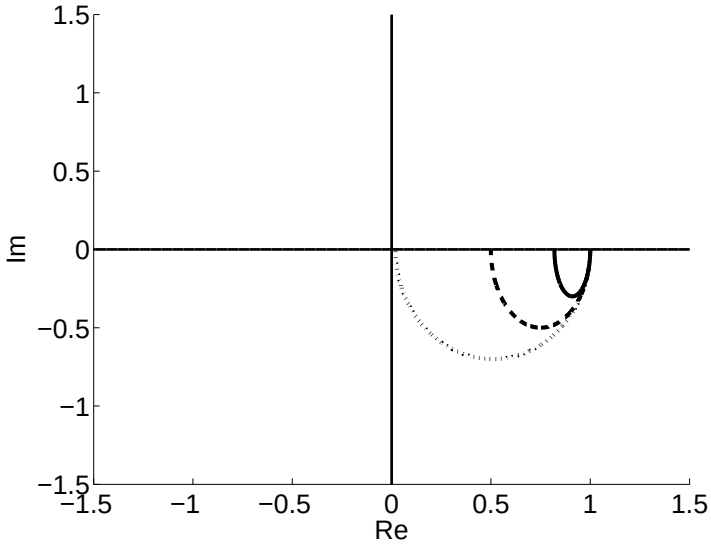

Figure 5.1: Amplification factor $\lambda(k)$ in complex plane (Re = real part of λ, Im = imaginary part of λ), $kh = (0, \pi)$ for $\nu = 0.3$(solid line), $\nu = 0.5$(dashed line) and $\nu = 0.7$(dotted line).

$$\begin{aligned}
\|\lambda(k)\|^2 &\leq 1 - 8\gamma \sin^2\left(\frac{kh}{2}\right) + 16\gamma^2 \sin^4\left(\frac{kh}{2}\right) \\
\|\lambda(k)\|^2 &\leq 1 - 2\left[4\gamma \sin^2\left(\frac{kh}{2}\right)\right] + \left[4\gamma^2 \sin^2\left(\frac{kh}{2}\right)\right]^2 \\
\|\lambda(k)\| &\leq 1 - 4\gamma \sin^2\left(\frac{kh}{2}\right).
\end{aligned}$$

However, $\gamma = \tau Q$ is dependent on τ, so we can see that our scheme (5.2) is not dissipative. Furthemore we can investigate dispersion of used scheme. Phase error can be written as

$$a - \beta(k)$$

and we would like that to be as small as possible. Dependence of the phase speed $\beta(k)$ on apmlification factor $\lambda(kh)$ can be written as

$$\begin{aligned}
\tan(k\beta(k)\tau) &= -\frac{Im(\lambda(k))}{Re(\lambda(k))} \\
&= \frac{\nu \sin(kh)}{1 - (2\nu^2 + 4\gamma)\sin^2\left(\frac{kh}{2}\right)}.
\end{aligned} \tag{5.12}$$

Now, if we prepare following Taylor series

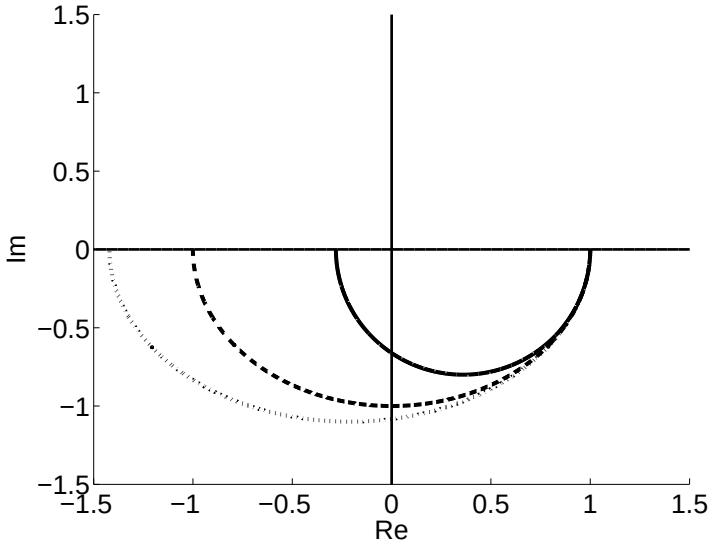

Figure 5.2: Amplification factor $\lambda(k)$ in complex plane (Re = real part of λ, Im = imaginary part of λ), $kh = (0, \pi)$ for $\nu = 0.8$(solid line), $\nu = 1$(dashed line) and $\nu = 1.1$(dotted line).

$$\sin x = x(1 - \frac{x^2}{6} + O(x^4))$$
$$\cos x = 1 - \frac{x^2}{2} + O(x^4)$$
$$\frac{1}{1-x} = 1 + x + O(x^2)$$
$$\arctan(x) = x(1 - \frac{x^2}{3} + O(x^4))$$

and relation

$$\sin^2\left(\frac{kh}{2}\right) = \frac{1 - \cos(kh)}{2} \tag{5.13}$$

we can easily rewrite (5.12) as follows

$$\begin{aligned}
&\tan(k\beta(k)\tau) = \\
&= \frac{\nu \sin(kh)}{1 - (2\nu^2 + 4\gamma)\sin^2\left(\frac{kh}{2}\right)} = \frac{\nu \sin(kh)}{1 - (\nu^2 + 2\gamma)(1 - \cos(kh))} \\
&= \frac{\nu kh\left(1 - \frac{(kh)^2}{6} + O((kh)^4)\right)}{1 - (\nu^2 + 2\gamma)\left(\frac{(kh)^2}{2} + O((kh)^4)\right)} \\
&= \nu kh\left(1 - \frac{(kh)^2}{6} + O((kh)^4)\right)\left(1 + (\nu^2 + 2\gamma)\frac{(kh)^2}{2} + O((kh)^4)\right) \\
&= \nu kh\left(1 + (\frac{3\nu^2}{2} + 3\gamma - \frac{1}{2})\frac{(kh)^2}{3} + O((kh)^4)\right)
\end{aligned} \tag{5.14}$$

Now, let us consider variable $z = \tan(k\beta(k)\tau)$. We can find Taylor series of $\arctan(z)$

$$\begin{aligned} z &= \nu kh\left(1 + (\nu^2 + 2\gamma - \frac{1}{3})\frac{(kh)^2}{2} + O((kh)^4)\right) \\ z^2 &= \nu^2(kh)^2\left(1 + 2(\nu^2 + 2\gamma - \frac{1}{3})\frac{(kh)^2}{2} + O((kh)^4)\right) \\ &= \nu^2(kh)^2 + O((kh)^4) \end{aligned}$$

$$\begin{aligned} &z(1 - \frac{z^2}{3}) = \\ &= \nu kh\left(1 + (\nu^2 + 2\gamma - \frac{1}{3})\frac{(kh)^2}{2} + O((kh)^4)\right)\left(1 - (\frac{\nu^2(kh)^2}{3} + O((kh)^4))\right) \\ &= \nu kh\left(1 + (3\nu^2 + 6\gamma - 1)\frac{(kh)^2}{6} + O((kh)^4)\right)\left(1 - 2\nu^2(\frac{(kh)^2}{6} + O((kh)^4))\right) \\ &= \nu kh\left(1 + (3\nu^2 + 6\gamma - 1)\frac{(kh)^2}{6} - 2\nu^2(\frac{(kh)^2}{6} + O((kh)^4))\right) \\ &= \nu kh\left(1 + (\nu^2 + 6\gamma - 1)\frac{(kh)^2}{6} + O((kh)^4))\right) \end{aligned}$$

and use that and (5.6) to find phase speed $\beta(k)$

$$\begin{aligned} k\beta(k)\tau &= \nu kh\left(1 + (\nu^2 + 6\gamma - 1)\frac{(kh)^2}{6} + O((kh)^4))\right) \\ \beta(k) &= \nu\frac{h}{\tau}\left(1 + (\nu^2 + 6\gamma - 1)\frac{(kh)^2}{6} + O((kh)^4))\right) \\ &= a\left(1 + (\nu^2 + 6\gamma - 1)\frac{(kh)^2}{6} + O((kh)^4))\right) \end{aligned}$$

We can see that our scheme has phase error of the order $(kh)^2$ and that we would ideally want

$$\begin{aligned} 0 &\approx \nu^2 + 6\gamma - 1 \\ 1 &\approx \nu^2 + 6\gamma. \end{aligned}$$

However since we can't chose specific ν (we don't have a specific a), it is better to have smaller ν, as can be seen in figure 5.3.

5.3 Constants, initial and boundary conditions

We will use our scheme (5.2) with following parameters:

τ	...	10^{-7}	time step
h	...	5×10^{-4}	interval length
γ	...	10^{-4}	artificial viscosity coefficient
J	...	1000	number of spatial intervals
D	...	10^{-5}	distensibility
α_0	...	0.7	initial cross-sectional area ratio

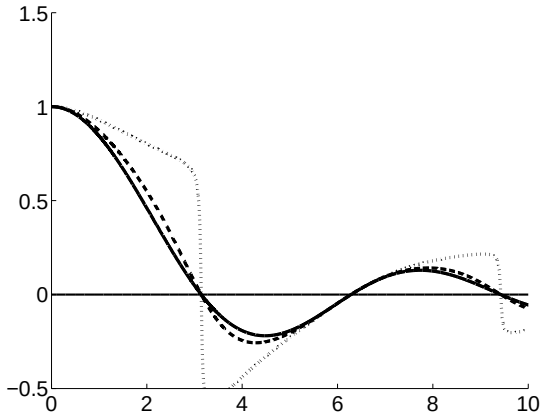

Figure 5.3: Relative phase error for $\nu = 0.1$(solid line), $\nu = 0.4$(dashed line) and $\nu = 0.7$(dotted line) plotted against kh.

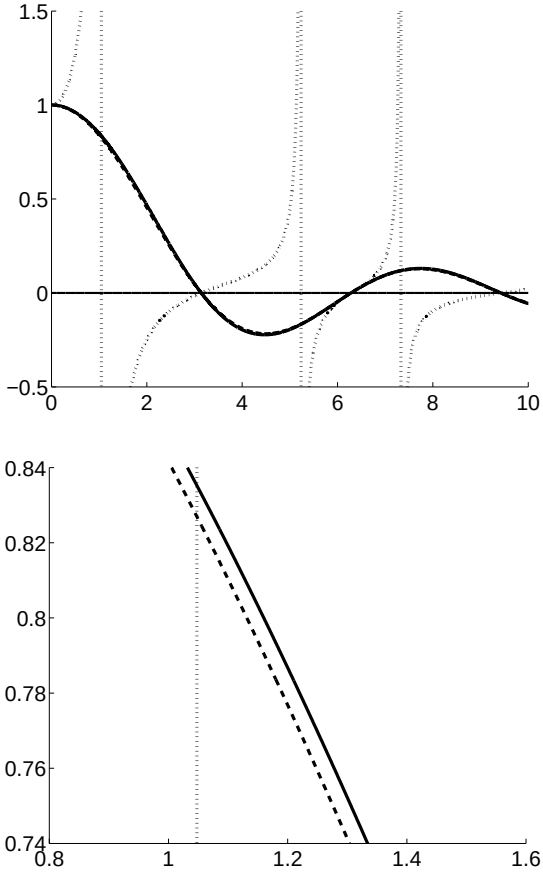

Figure 5.4: Relative phase error for $\nu = 0.001$ and $\gamma = 0.01$(solid line), $\gamma = 0.0001$(dashed line) and $\gamma = 1$(dotted line) plotted against kh.

We will use initial condition

$$W = (u_A, u_B, \Delta p)^\top = (0, 0, 0)^\top.$$

Boundary conditions can be entered for each variable only on one side of the

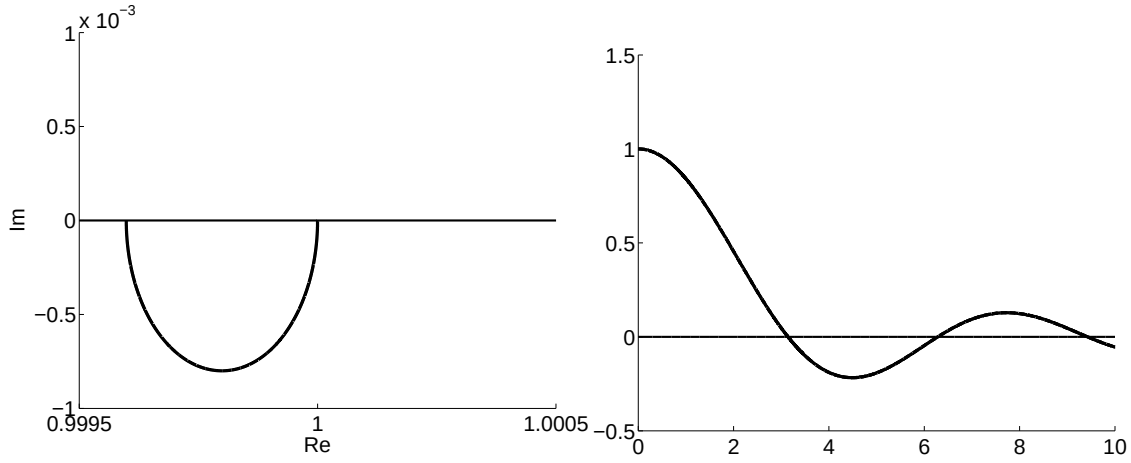

Figure 5.5: Amplification factor (left) and relative phase error (right) for given parameters.

boundary. Since we have two positive characteristics and one negative characteristic we know that two boundary conditions will be entered on left side $x = 0$, and one on the right side $x = J \cdot h$. We want to simulate propagation of a pressure pulse from one boundary to the other, so let us choose left side $x = 0$ as the beginning of this pressure pulse. We will let in pulse of total size $3kPa$ over a small amount of time $(0.01s)$ simulating a cough[4]. If this pressure pulse will be positive, i.e. $\Delta p = p_B - p_A > 0$, then in the near vicinity of pulse will hold $u_A < 0$ and $u_B > 0$, so we will set boundary condition for u_A on $x = J \cdot h$ and for u_B on $x = 0$. The rest values on boundaries will be computed in each step.

Our ν may seem too small $\nu \approx \left(\frac{5 \cdot 10^{-7}}{5 \cdot 0^{-4}}\right) = 10^{-3}$ considering our stability analysis. But this value guarantees stability and moreover gives solutions without unwanted oscilations. For comparison see appendix B.

5.4 Results

Now let us see some results of numerical method (5.2). More pictures with smaller time steps are in the appendices A - E.

Figure 5.6: Without artificial viscosity scheme (5.1) is too dispersive and can't be used.

Figure 5.7: Pressure wave travels through the spinal cord to its end where it reflects back. We can see that during the reflection, transmural pressure difference rises up to twice the size the pressure difference initially was. This can be seen as dangerous effect, that can potentially damage the spinal cord. Computed flow velocities in both tubes (figure: 5.8) match are approximations from section 4.4.

Figure 5.9: If we consider two similar pulses in a row, we can see that not only does pressure difference rises at the end of our tubes, but also when first reflected and second pulse meet. That way the spinal cord could be damaged along its whole length.

Figure 5.10: If there would be a blockage in outer tube A, then pressure pulse can again produce great pressure difference. That can be especially dangerous,

since the blockage itself may have damaged the spinal cord already and thus weakened the tissue.

Figure 5.11: Last case is one pulse consisting of positive and negative pressure difference. That can be interpreted as a result of for example an impact to the head, where head moves quickly one way, hits something and moves back. Since we are considering $\Delta P < 0$, we need to be cautious on the boundary and always check, if characteristic speed $\lambda_1(W)$ is positive or negative. If it's positive, there's no change, however if it's negative, we need to switch boundary conditions for u_A and u_B (we can see that in this case $u_A > 0$ and $u_B < 0$).

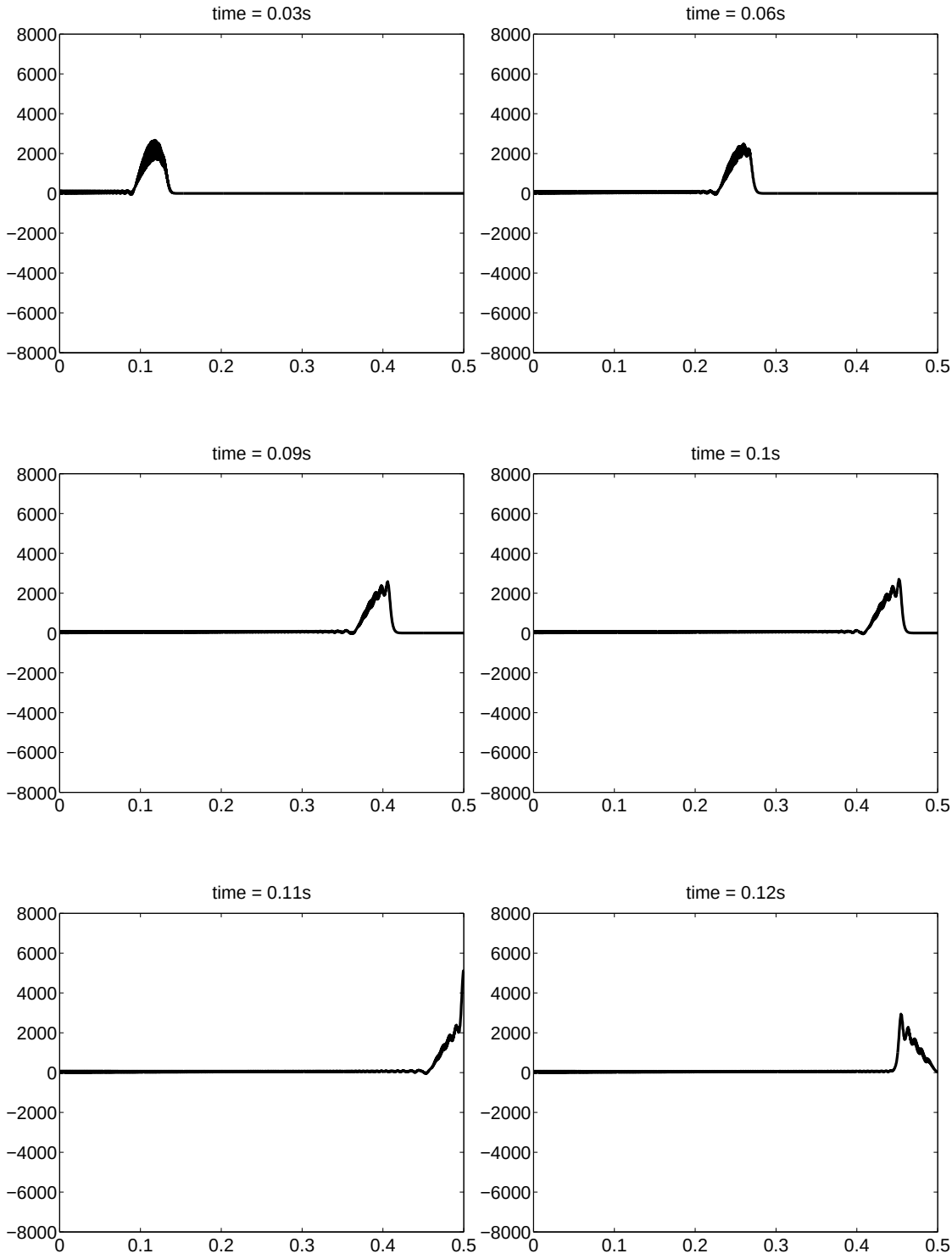

Figure 5.6: One pulse without artificial dampening (more in appendix A). Pressure difference Δp in every point of mesh.

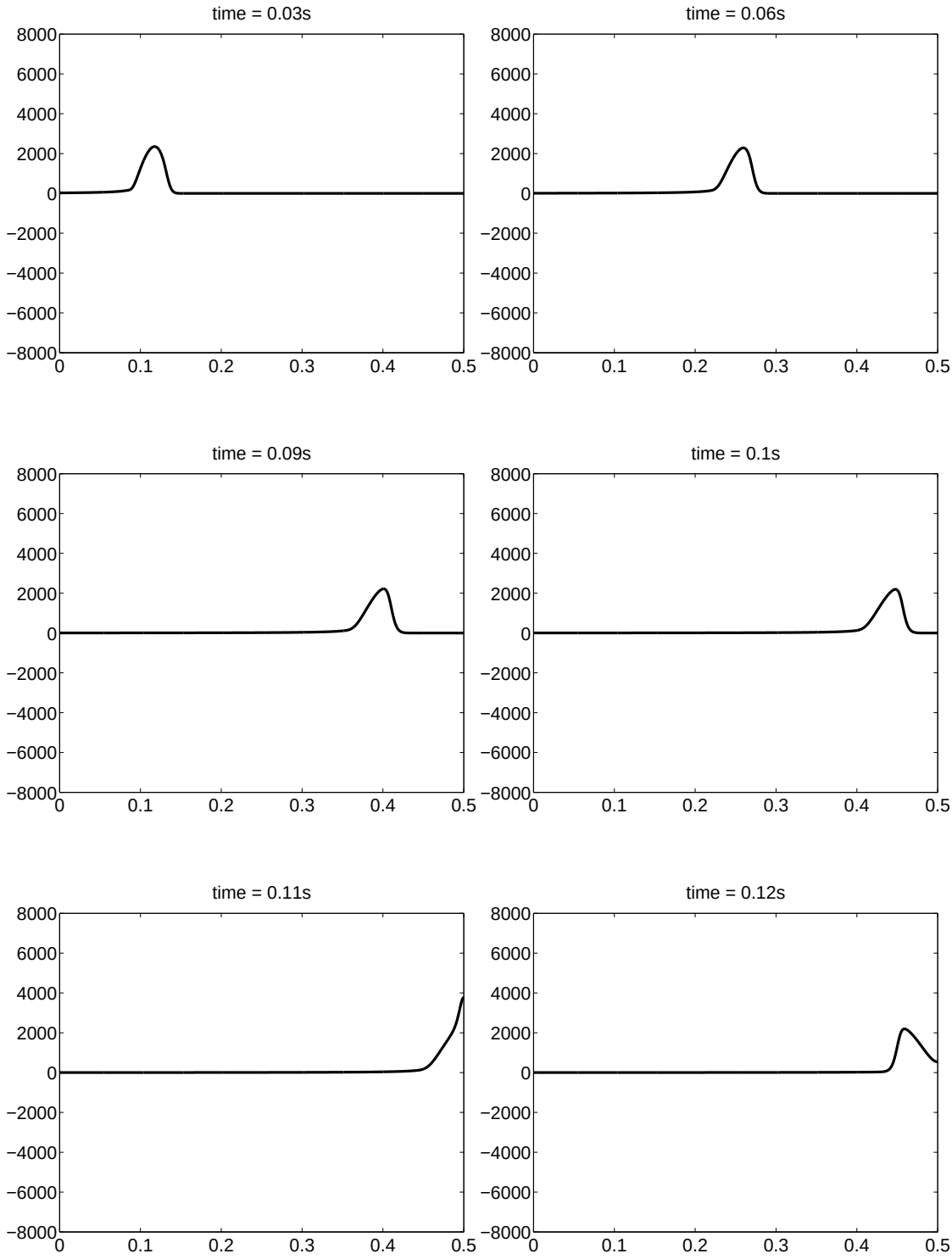

Figure 5.7: One pulse with artificial dampening (more in appendix B). Pressure difference Δp in every point of mesh.

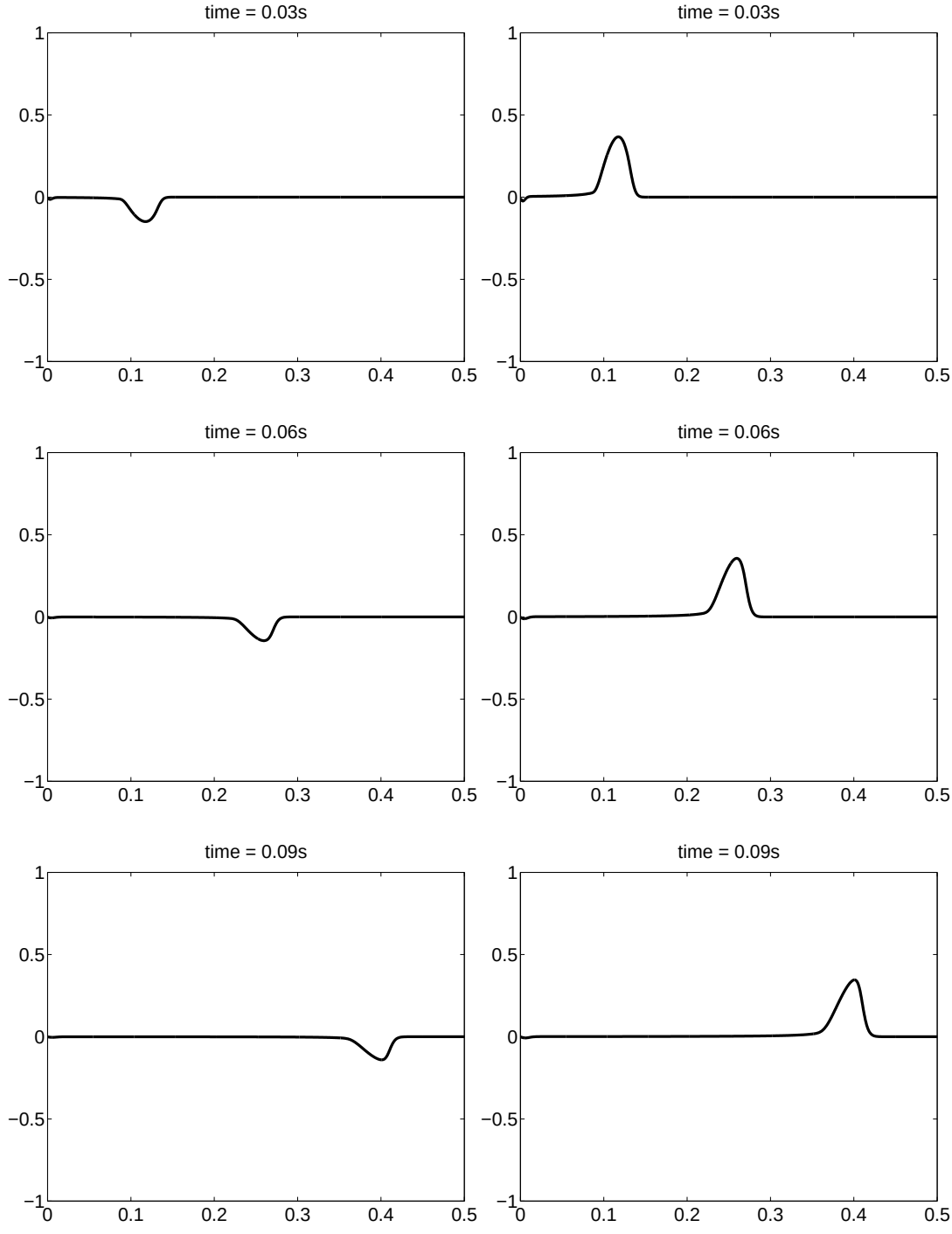

Figure 5.8: Two pulses - flow velocities u_A (left) and u_B (right) in every point of mesh.

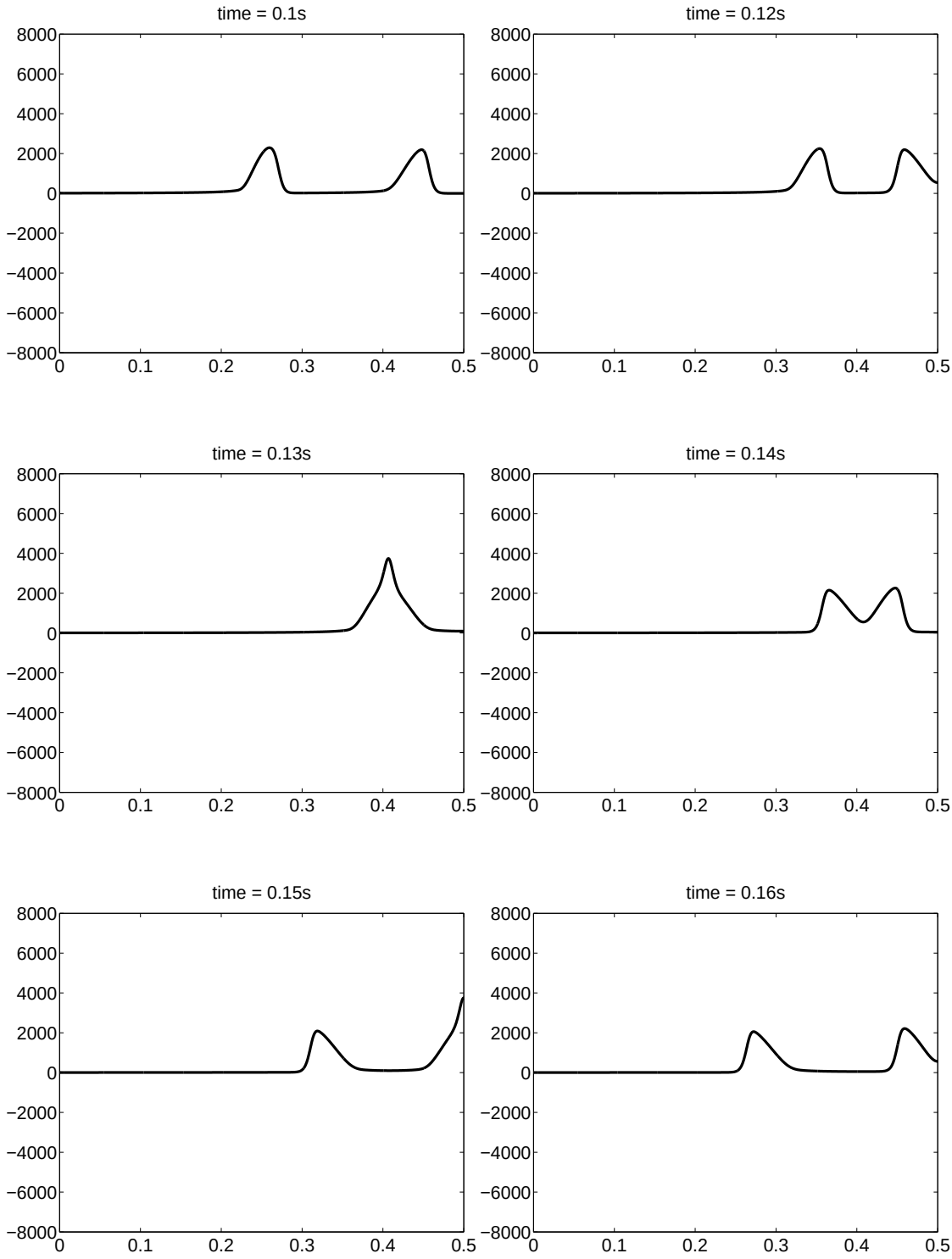

Figure 5.9: Two pulses (more in appendix C). Pressure difference Δp in every point of mesh.

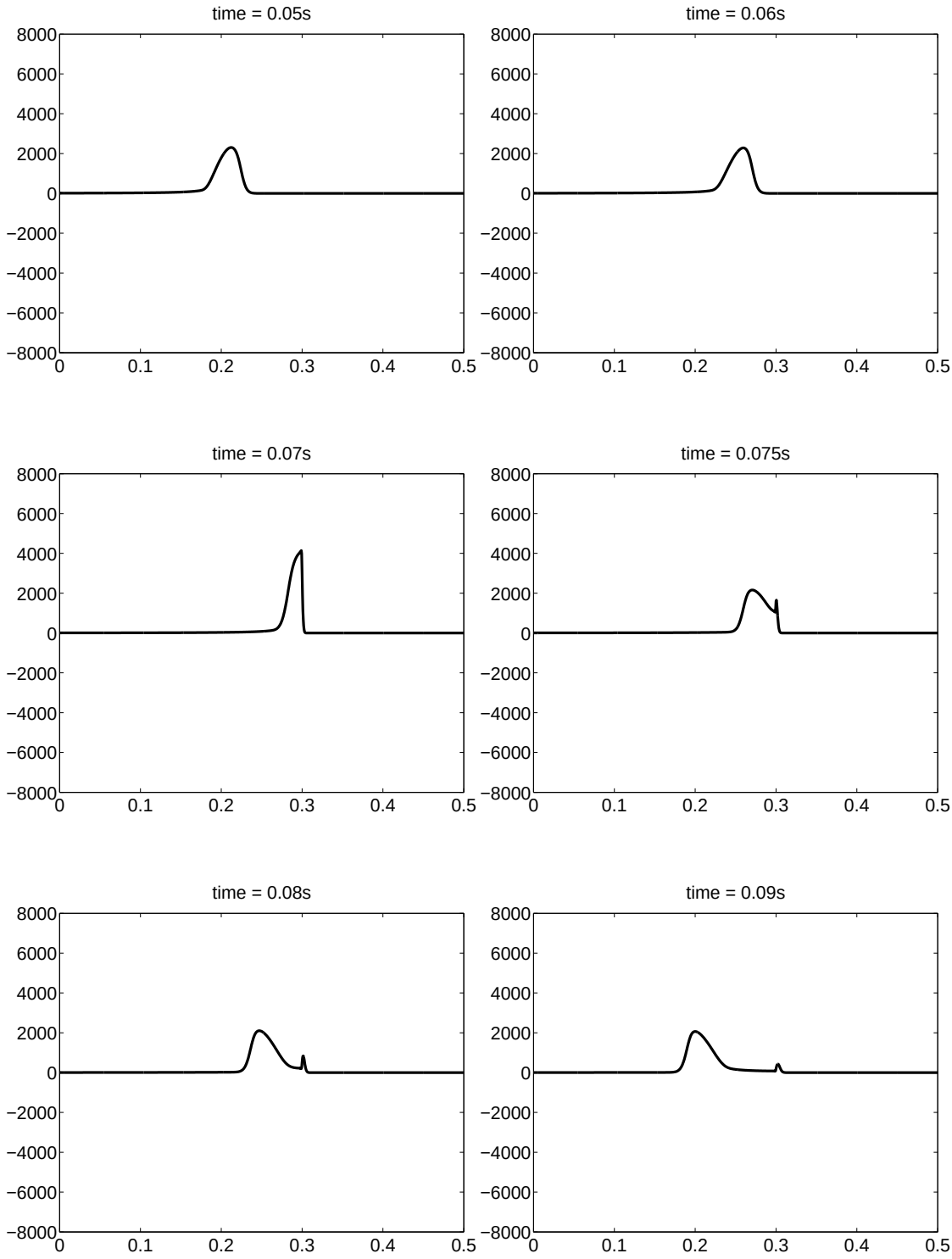

Figure 5.10: Reflection from the blockage (more in appendix D). Pressure difference Δp in every point of mesh.

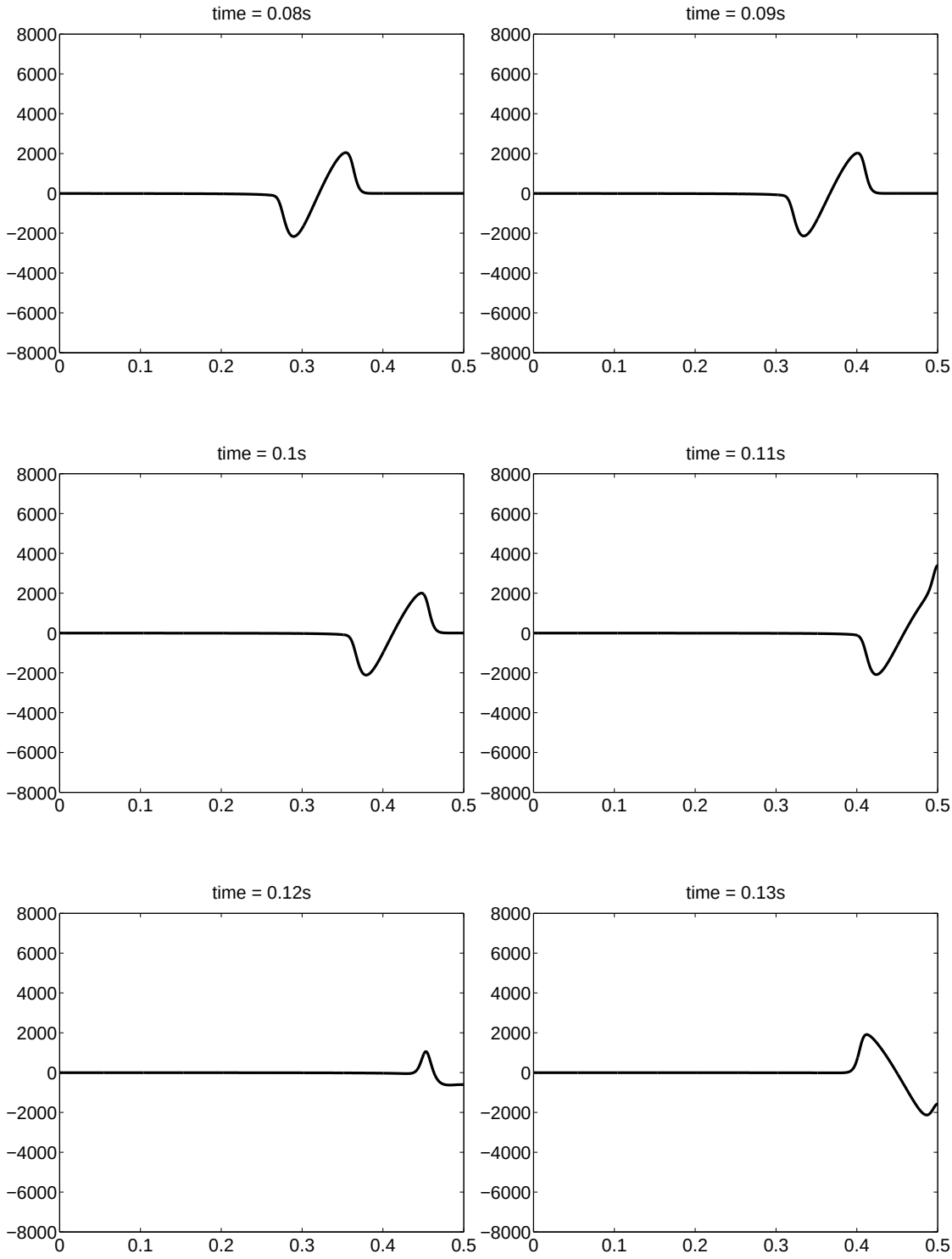

Figure 5.11: One sinusoidal pulse (more in appendix E). Pressure difference Δp in every point of mesh.

Conclusion

We constructed a fluid-filled co-axial elastic tubes model for CSF flow in and around spinal cord, derived governing equations forming a quasi-one-dimensional hyperbolic system of conservational laws describing the model and we demonstrated mechanism for forming big transmural pressure differences in spinal cord. There's a question if they are high enough for actually damaging the spinal cord, but considering the spinal cord could already be weakened, it is still possible for them to cause problems. According to[4], spinal cord should be modelled as porous tube and that the amount of CSF that flow through dura mater and pia mater has dissipative effects on pressure pulse making it too small to actually cause syrinxes. Thus making mechanism of development of syringomyelia due to high transmural pressure differences only improbable. However even small rise in pressure can cause damage in certain points. Most promising seems reflection of pressure pulse from blockage located close to the start of the pulse. For example impact to the head and blockage in the upper regions of spinal cord.

The nonlinear behaviour of the system and various assumptions needed for finding a solution make this an interesting problem that is still being solved.

Bibliography

[1] Berkouk K., Carpenter P.W., Lucey A.D.:*Pressure Wave Propagation in Fluid-Filled Co-Axial Elastic Tubes*, Journal of Biomechanical Engineering, **125**, 2003, 852-863.

[2] Bressan, A., Serre, D., Williams, M., Zumbrun, K. Marcati, Pierangelo (Ed.): *Hyperbolic Systems of Balance Laws*, Springer Berlin / Heidelberg, 2007

[3] Dafermos, Constantine M.:*Hyperbolic Conservation Laws in Continuum Physics*, Springer-Verlag Berlin Heidelberg, 2010

[4] Elliott, Novak Samuel Jon (2009):*Mathematical modelling and analysis of cerebrospinal mechanics: an investigation into the parthogenesis of syringomyelia*. PhD thesis, University of Warwick.

[5] Gurtin, Morton E.:*An introduction to continuum mechanics.* (Mathematics in science and engineering) New York : Academic Press, 1981

[6] Ko H-Y, Park JH, Shin YB, Baek SY:*Gross quantitative measurements of spinal cord segments in human*, Spinal Cord **42**, 2004, 35-40.

[7] LeVeque, Randall J.:*Numerical methods for conservation laws*, Birkhauser-Verlag, Basel, 1992

[8] Maršík F., Dvořák I.: *Biotermodynamika*, Academia, Praha, 1998, 46-48.

[9] Morton K.W., Mayers D.F.:*Numerical Solution of Partial Differential Equations*, Cambridge University Press, 1994, 87-89.

[10] Mysliveček J.: *Základy neurověd*, Triton, Praha, 2003, 38-39.

[11] Otáhal J., Štěpáník Z., Kaczmarská A., Maršík F., Brož Z., Otáhal S.: *Simulation of cerebrospinal fluid transport*, Advances in Engineering Software, Advances in Engineering Software **38**, 2007, 802-809.

[12] Chan, Michael, and Amin-Hanjani, Sepideh(Jan 2010) Cerebrospinal Fluid and its Abnormalities. In: eLS. John Wiley & Sons Ltd, Chichester. http://www.els.net [doi: 10.1002/9780470015902.a0002191.pub2]

[13] James W. Clack, Human Anatomy Website, Indiana University - Purdue University http://iupucbio2.iupui.edu/anatomy/ Copyright 1999-2004

Notation

a	...	$max(\lambda_1, \lambda_2, \lambda_3)$, generalized characteristic speed for analysis of numerical method
A_A	...	cross-sectional area of tube A
A_B	...	cross-sectional area of tube B without A_A
A_T	...	cross-sectional area of tube B, $A_A + A_B$
c, c_0	...	pressure wave speeds, $\sqrt{\frac{\alpha(1-\alpha)}{D\rho}}$, $\sqrt{\frac{\alpha_0(1-\alpha_0)}{D\rho}}$
$C_0^1(\Omega)$	...	continuously differentiable functions of compact support contained in Ω
D	...	distensibility
$F(W)$	...	vector of fluxes
$F'(W)$	...	Jacobian matrix of fluxes
h	...	spatial interval; thickness of wall in section 1.5
Δp	...	transmural pressure difference, $p_B - p_A$
p_A	...	pressure in tube A
p_B	...	pressure in tube B
t	...	time coordinate
u_A	...	flow velocity in tube A
u_B	...	flow velocity in tube B
$\bar{u}$	...	$u_A + u_B$
$\acute{u_0}$	...	$\alpha_0 u_A + (1 - \alpha_0) u_B$
$\acute{u}$	...	$\alpha u_A + (1 - \alpha) u_B$
U_j^n	...	approximation of solution $W(h \cdot j, \tau \cdot n)$
$W(x,t)$	...	vector of variables, solution
x	...	spatial coordinate
α	...	cross-sectional area ratio, $\frac{A_A}{A_T}$
α_0	...	cross-sectional area ratio, $\frac{A_{A_0}}{A_T}$
$\beta(k)$	...	phase error of numerical scheme
γ	...	artificial viscosity coeficient, τQ, where Q is constant
ϵ	...	small parameter, $D\Delta p$
λ, $\lambda(W)$	...	eigenvalues of matrix $F'(W)$, characteristic speeds
$\lambda(hk)$	...	amplification factor of numerical scheme
ν	...	Courant number, $a\frac{\tau}{h}$
$\tilde{\nu}$	...	2ν
ρ	...	density of cerebrospinal fluid
τ	...	time step
$\chi(\lambda)$	...	characteristic polynomial of $F'(W)$
$\overline{\chi(\lambda)}$	...	characteristic polynomial similar to $\chi(\lambda)$

List of abbreviations

CSF	...	cerebrospinal fluid
CNS	...	central nervous system

A. One pulse without artificial viscosity

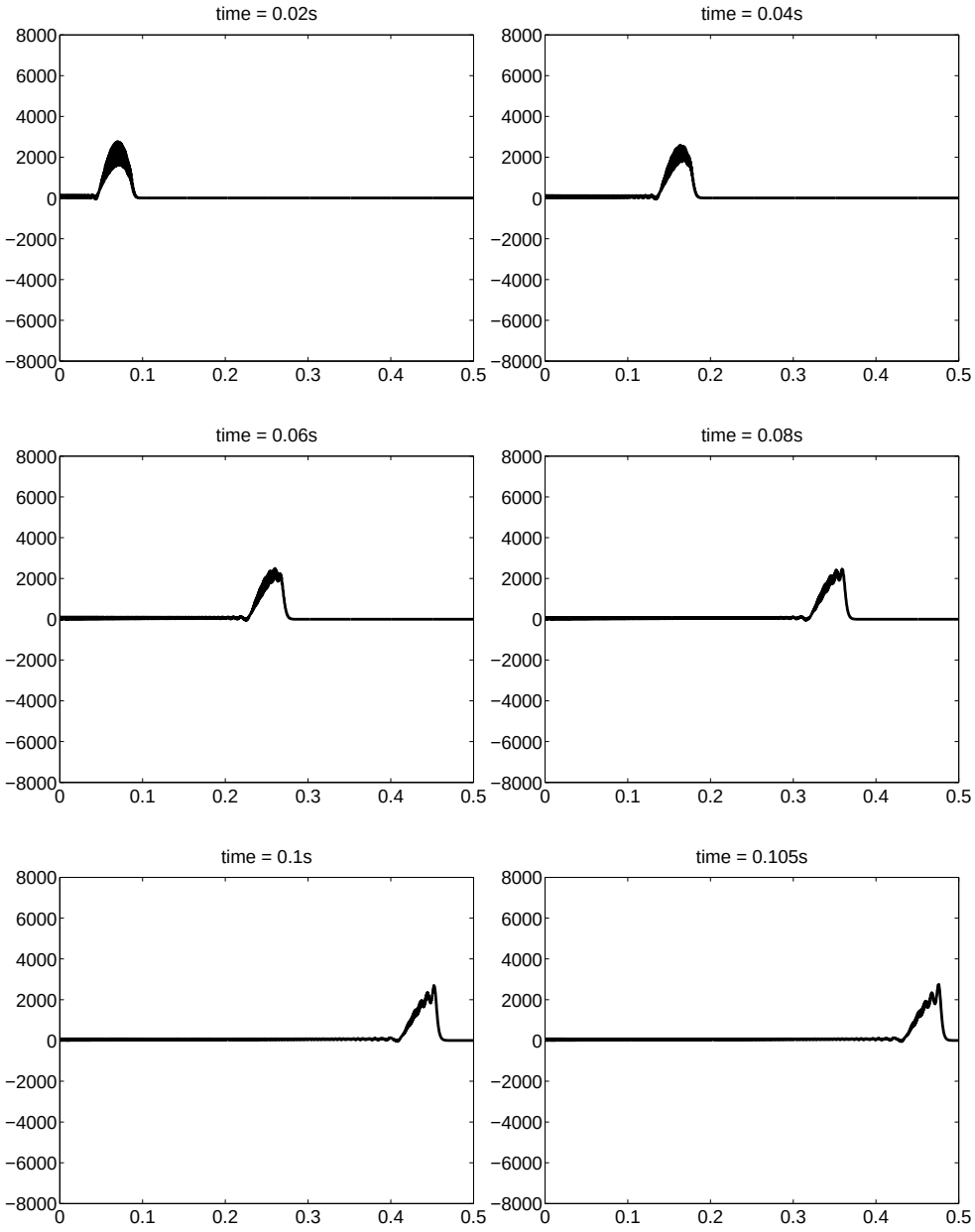

Figure A.1: Δp plotted in every point of mesh

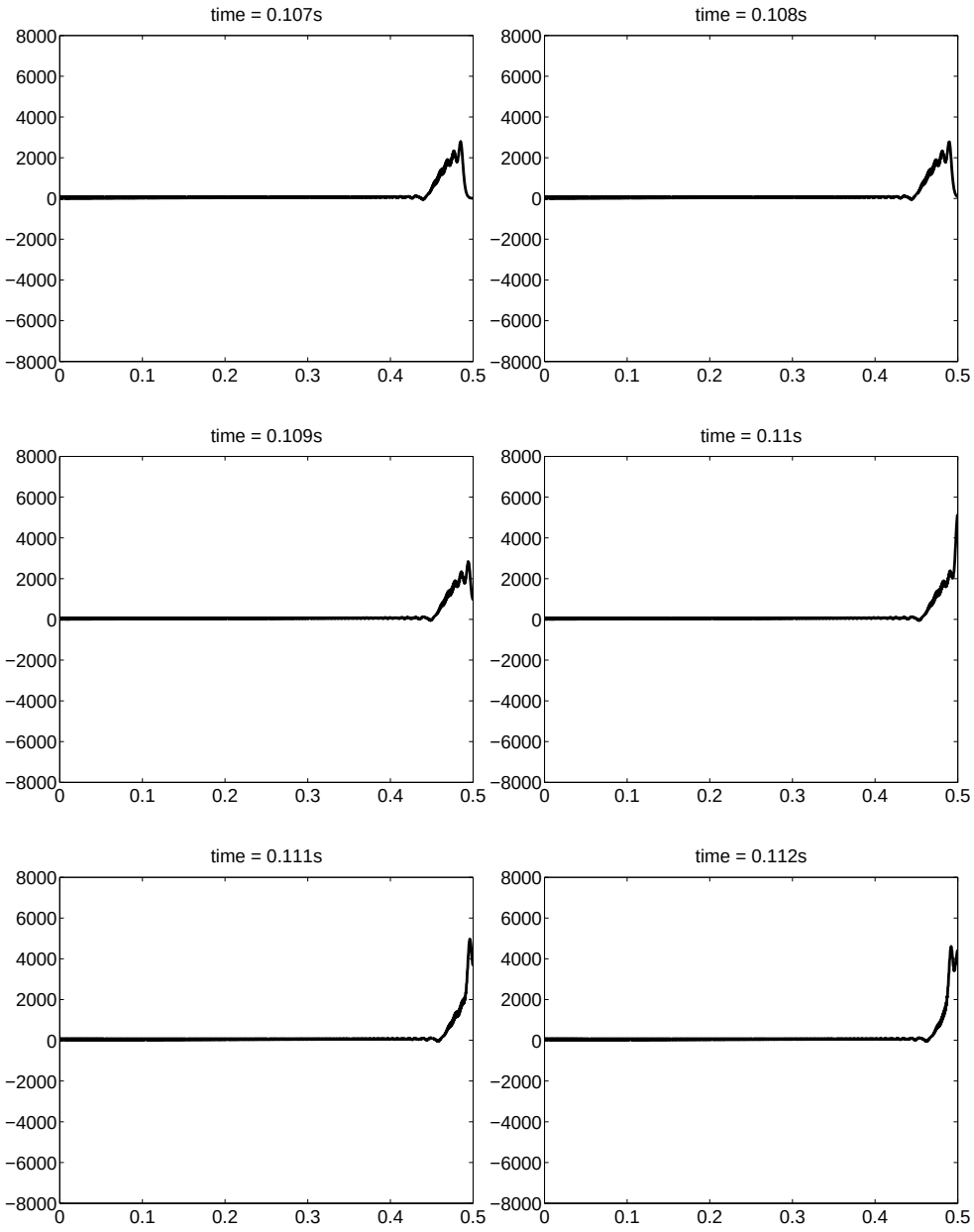

Figure A.2: Δp plotted in every point of mesh

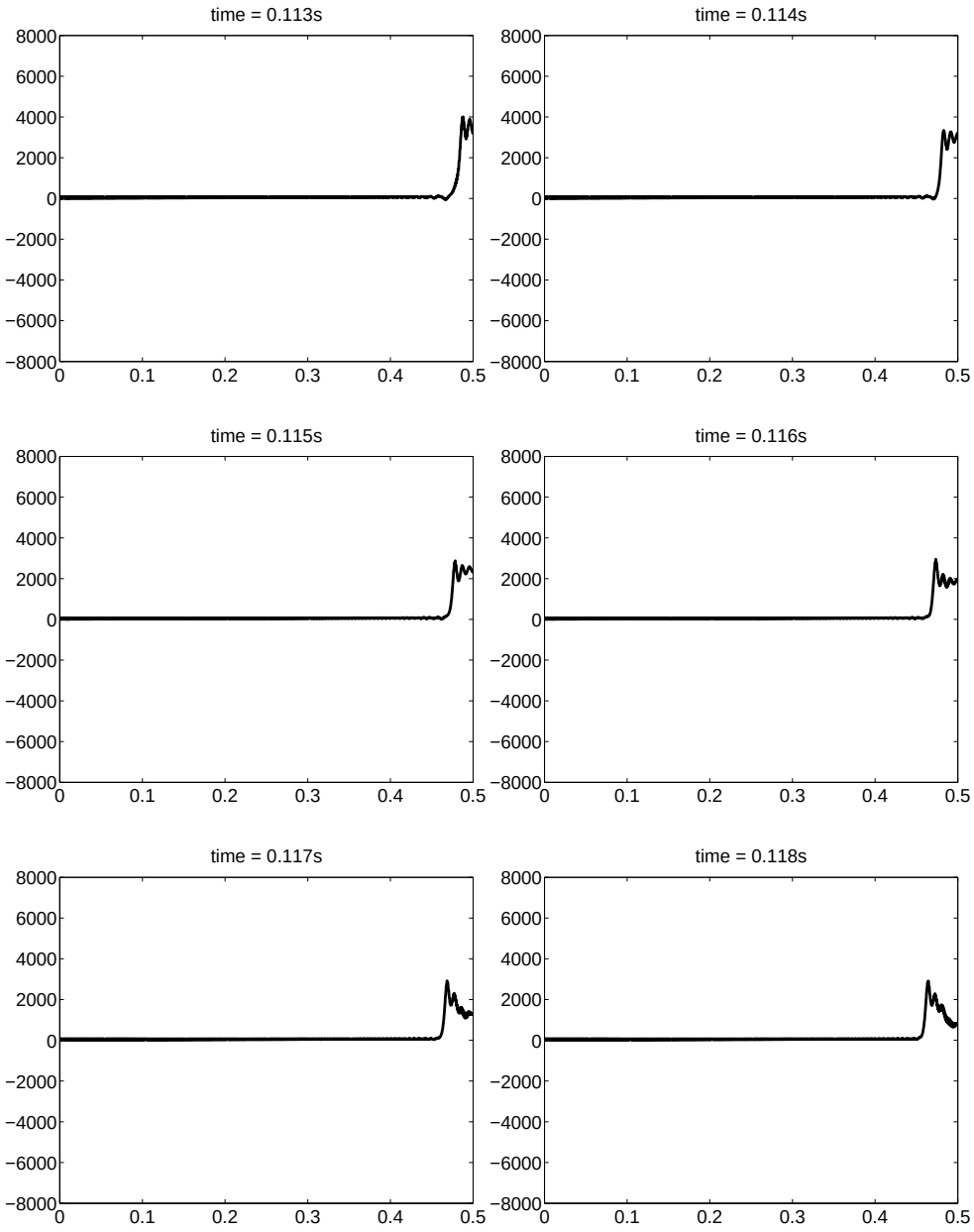

Figure A.3: Δp plotted in every point of mesh

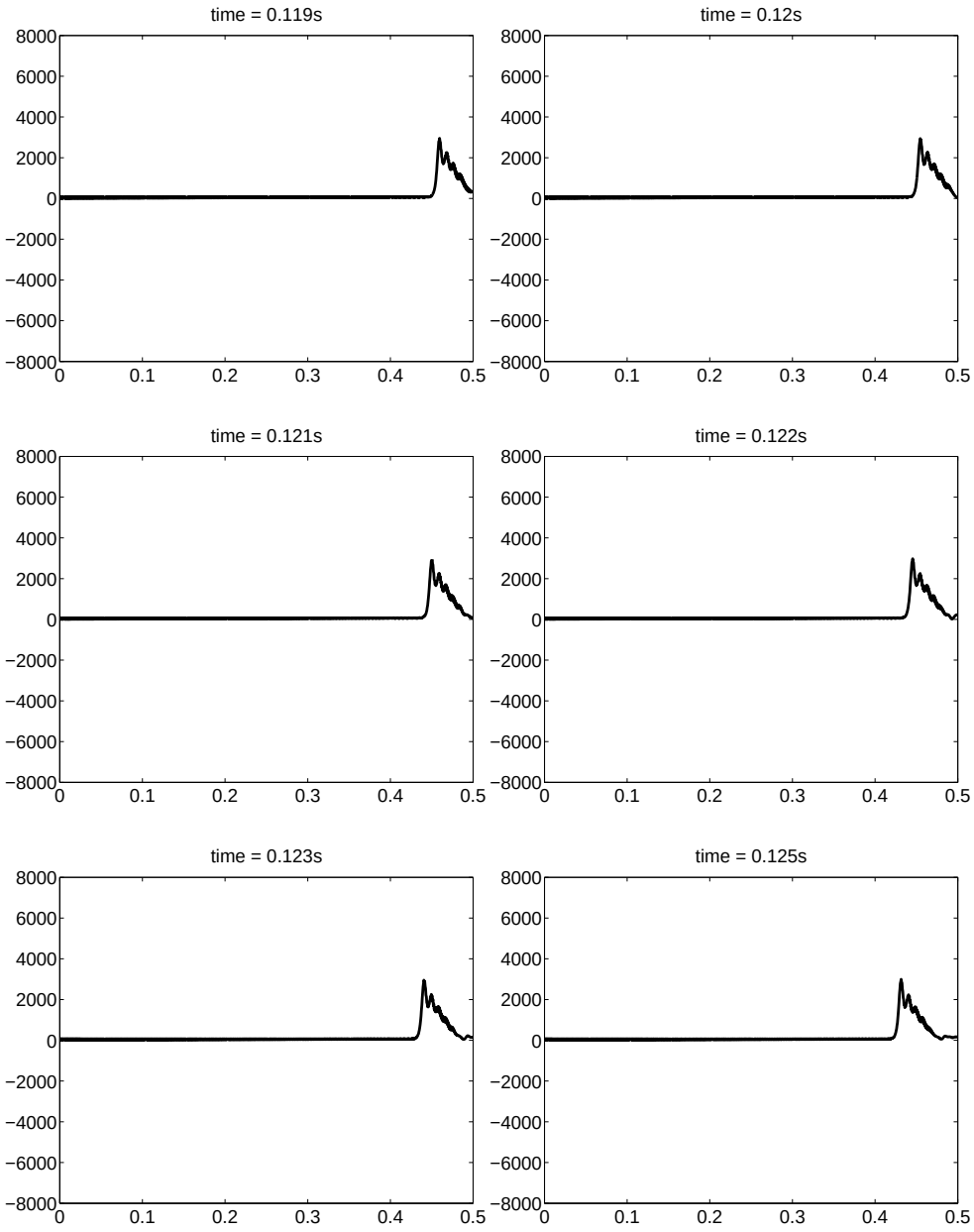

Figure A.4: Δp plotted in every point of mesh

B. One pulse with bigger Courant number ν

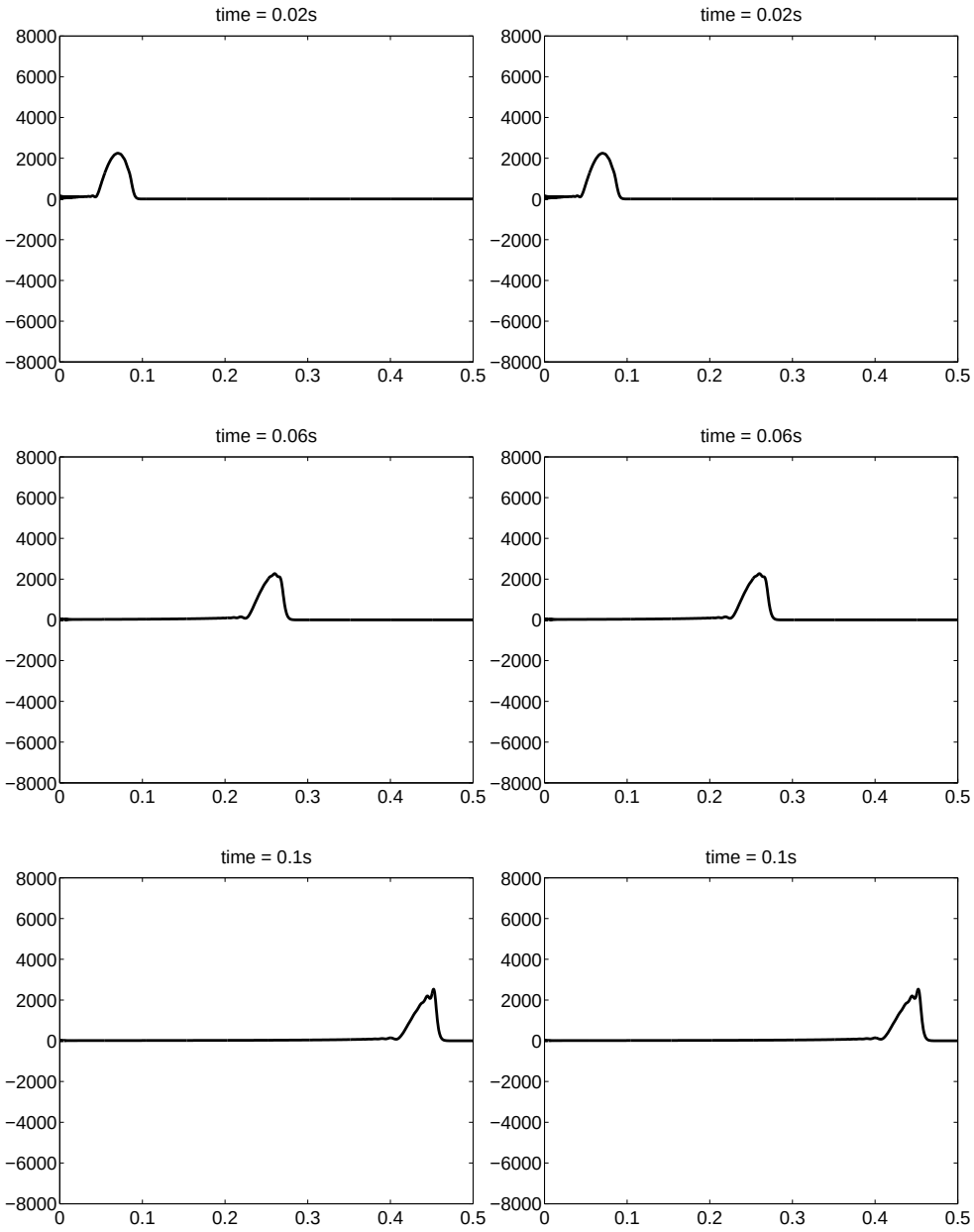

Figure B.1: Δp plotted in every point of mesh for parameters $\tau = 10^{-6}$, $h = 5 \cdot 10^{-5}$, $\nu \approx 10^{-1}$ (left) and for $\tau = 10^{-6}$, $h = 5 \cdot 10^{-4}$, $\nu \approx 10^{-2}$ (right).

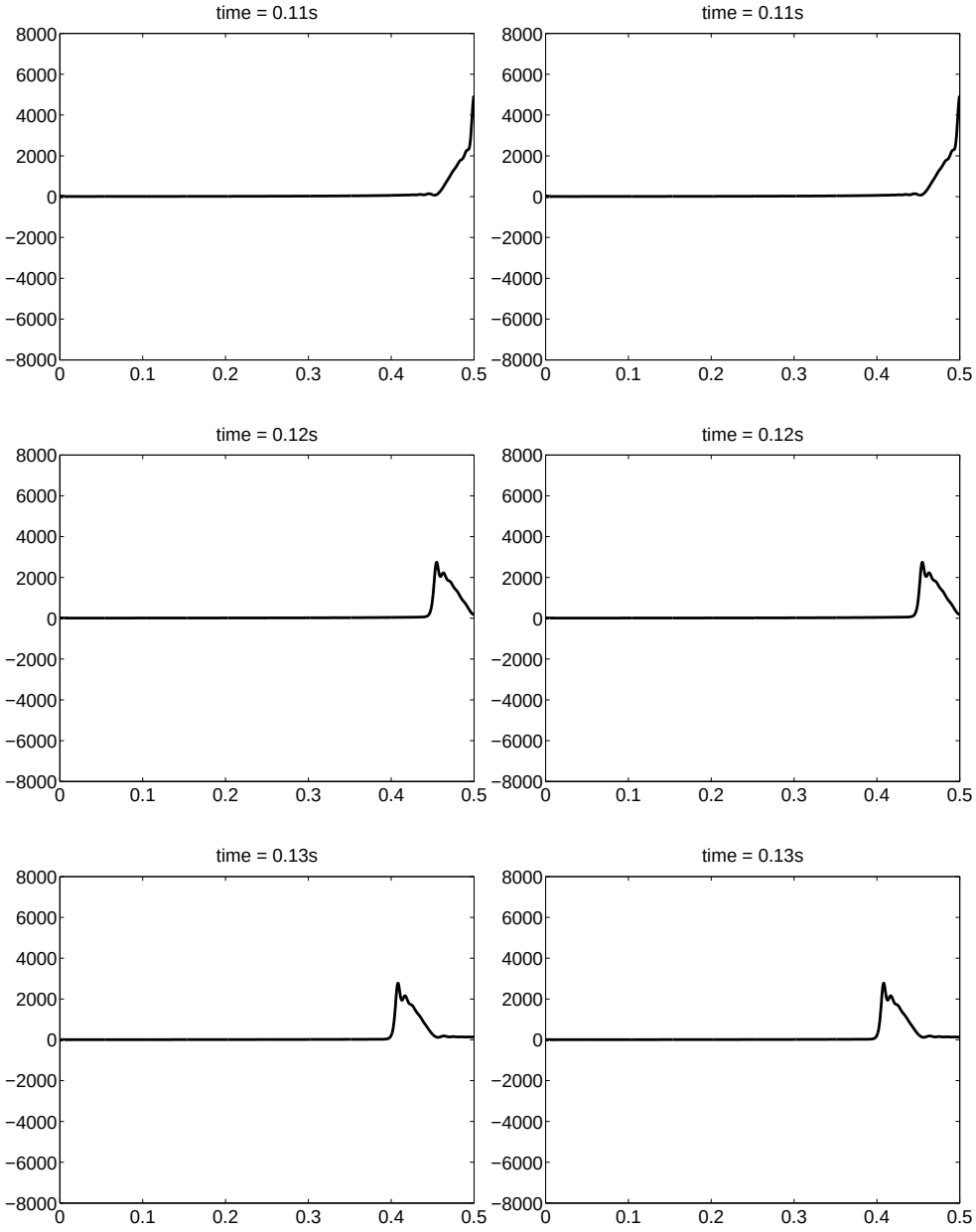

Figure B.2: Δp plotted in every point of mesh for parameters $\tau = 10^{-6}$, $h = 5 \cdot 10^{-5}$, $\nu \approx 10^{-1}$ (left) and for $\tau = 10^{-6}$, $h = 5 \cdot 10^{-4}$, $\nu \approx 10^{-2}$ (right).

C. One pulse

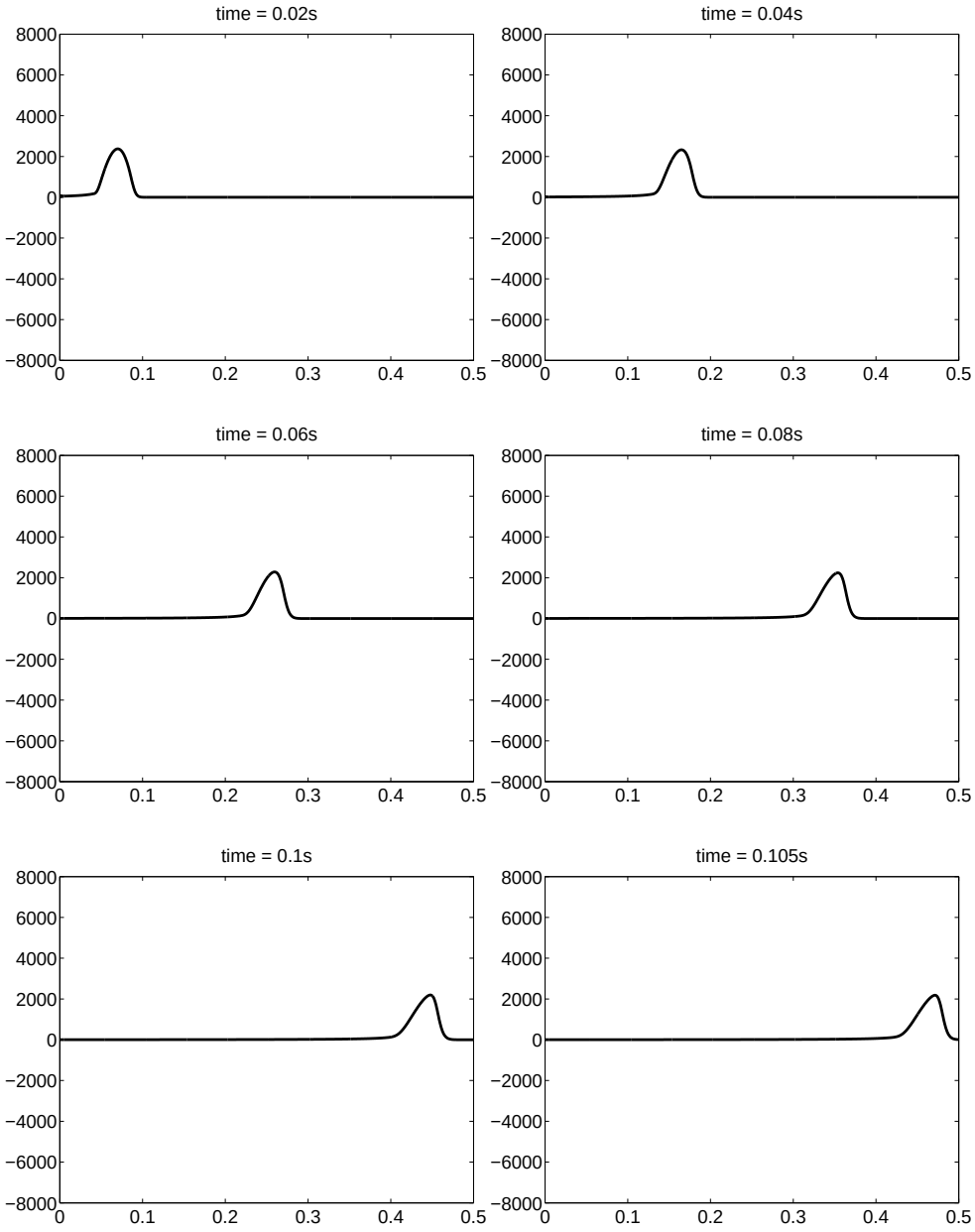

Figure C.1: Δp plotted in every point of mesh

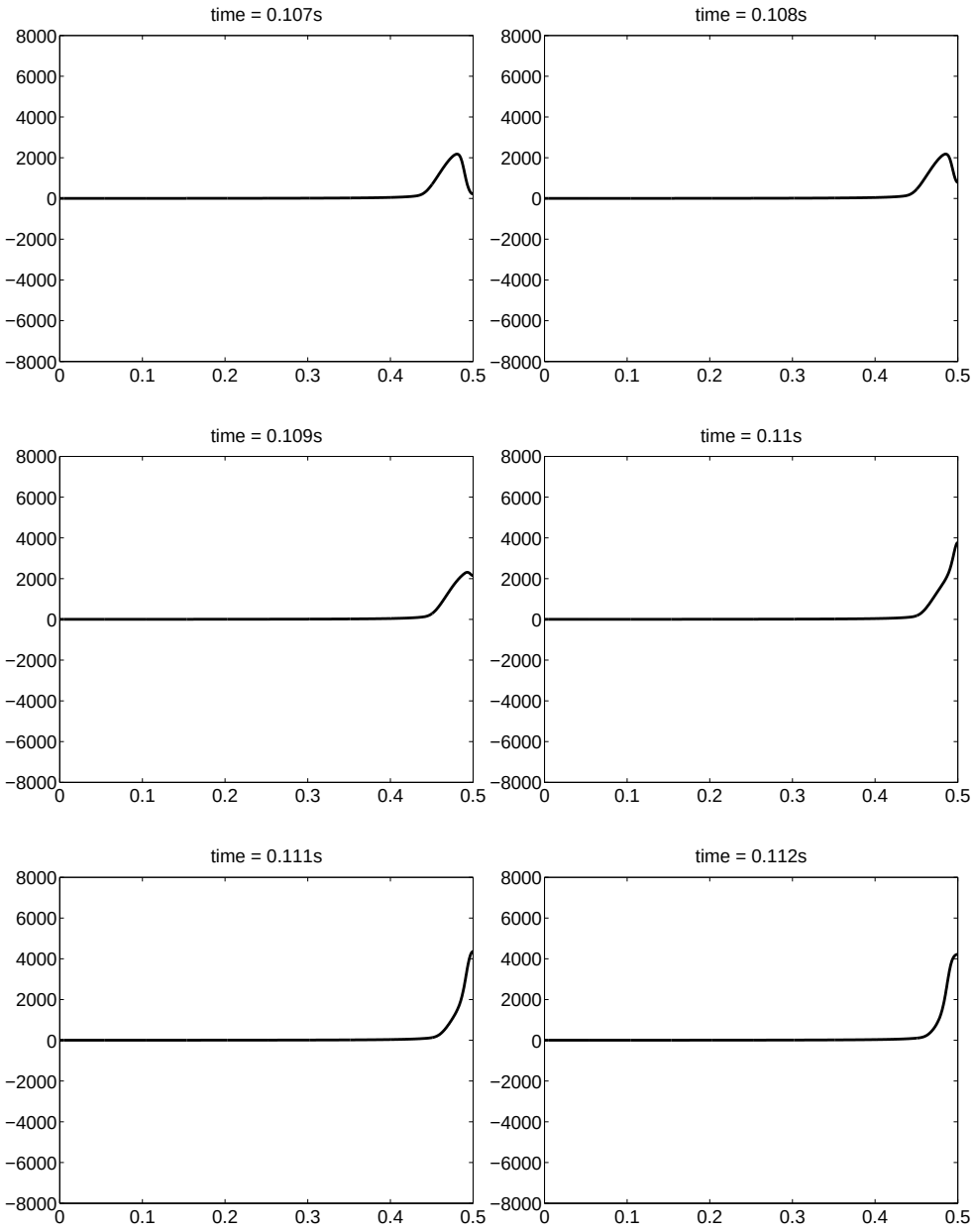

Figure C.2: Δp plotted in every point of mesh

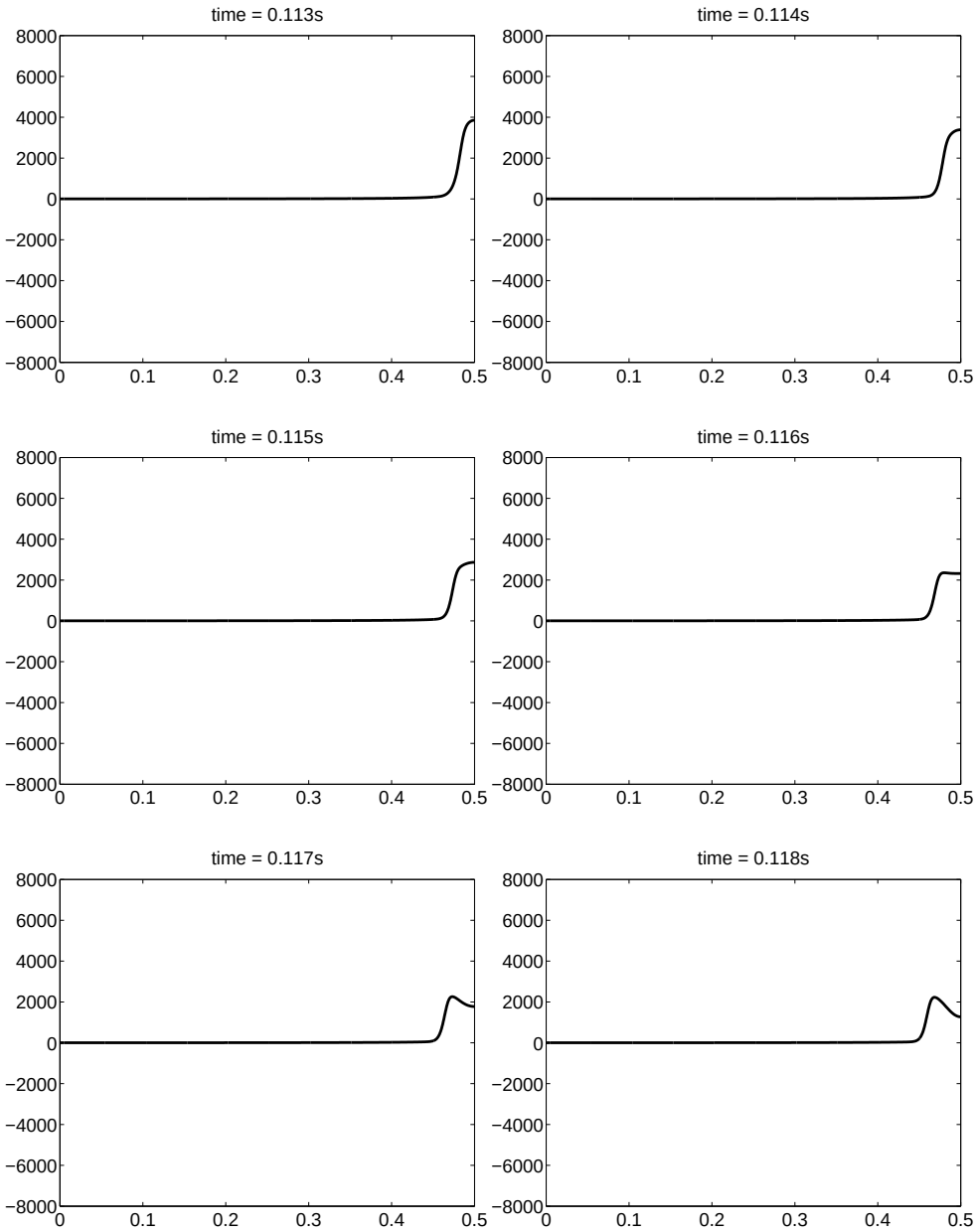

Figure C.3: Δp plotted in every point of mesh

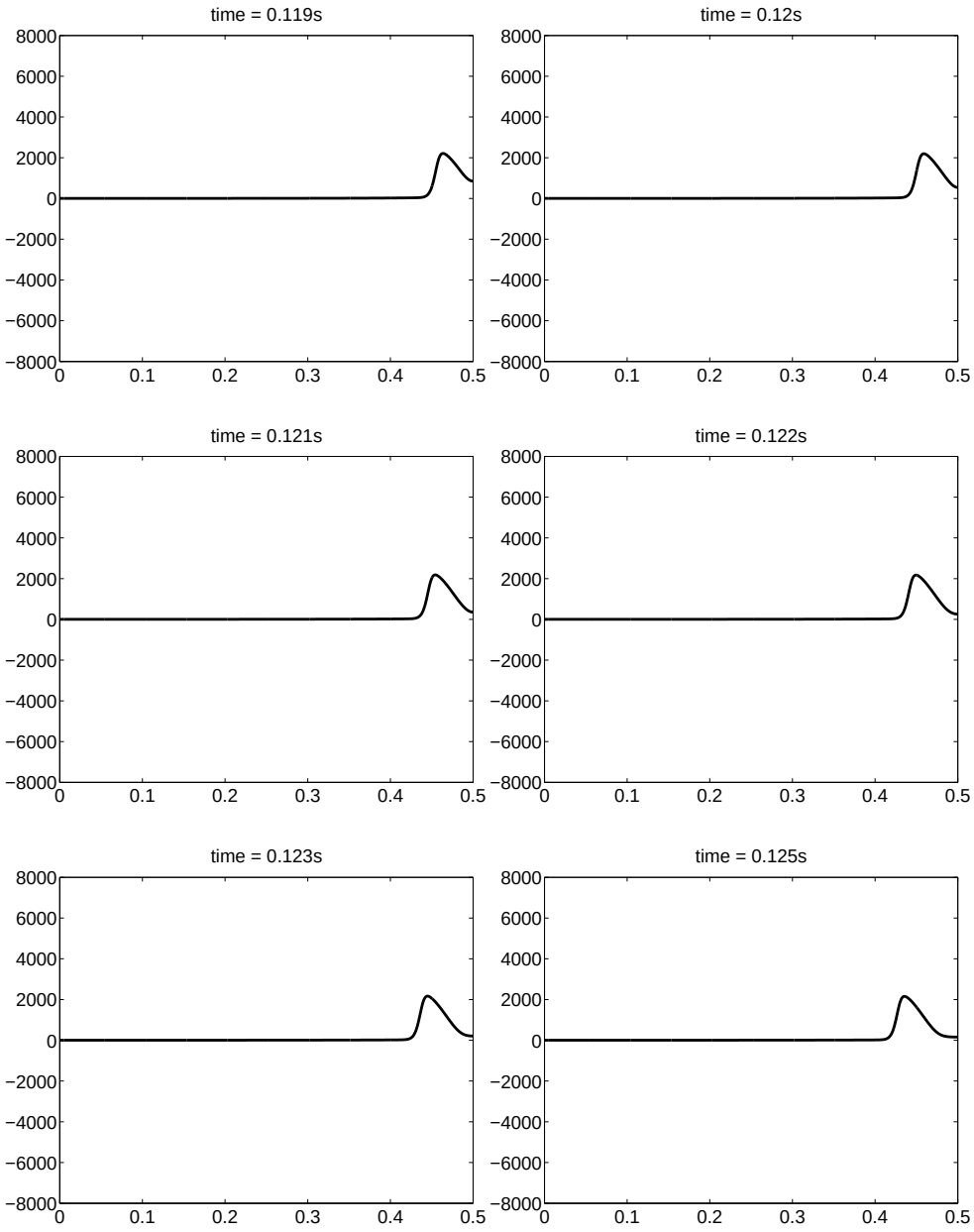

Figure C.4: Δp plotted in every point of mesh

D. Two pulses

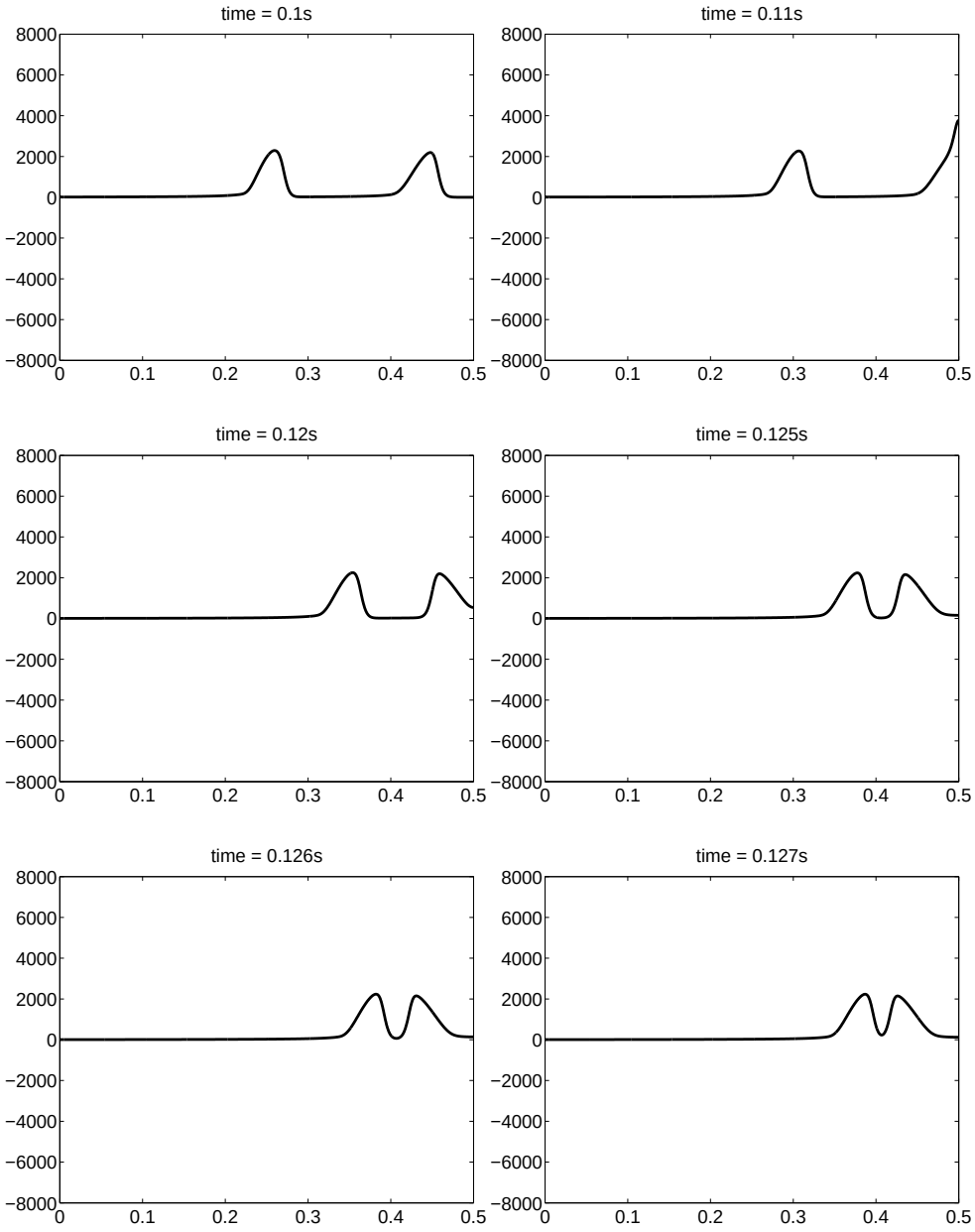

Figure D.1: Δp plotted in every point of mesh

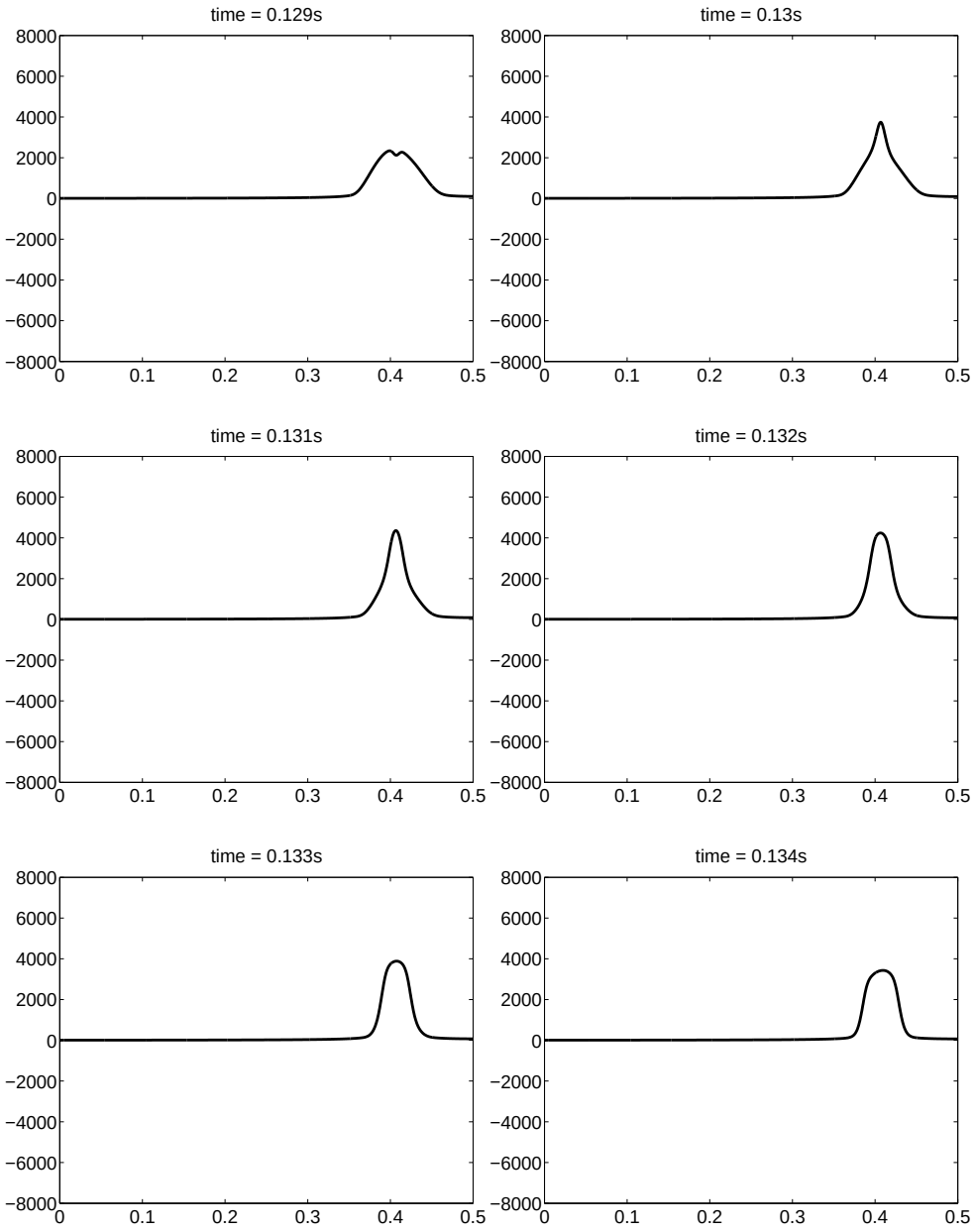

Figure D.2: Δp plotted in every point of mesh

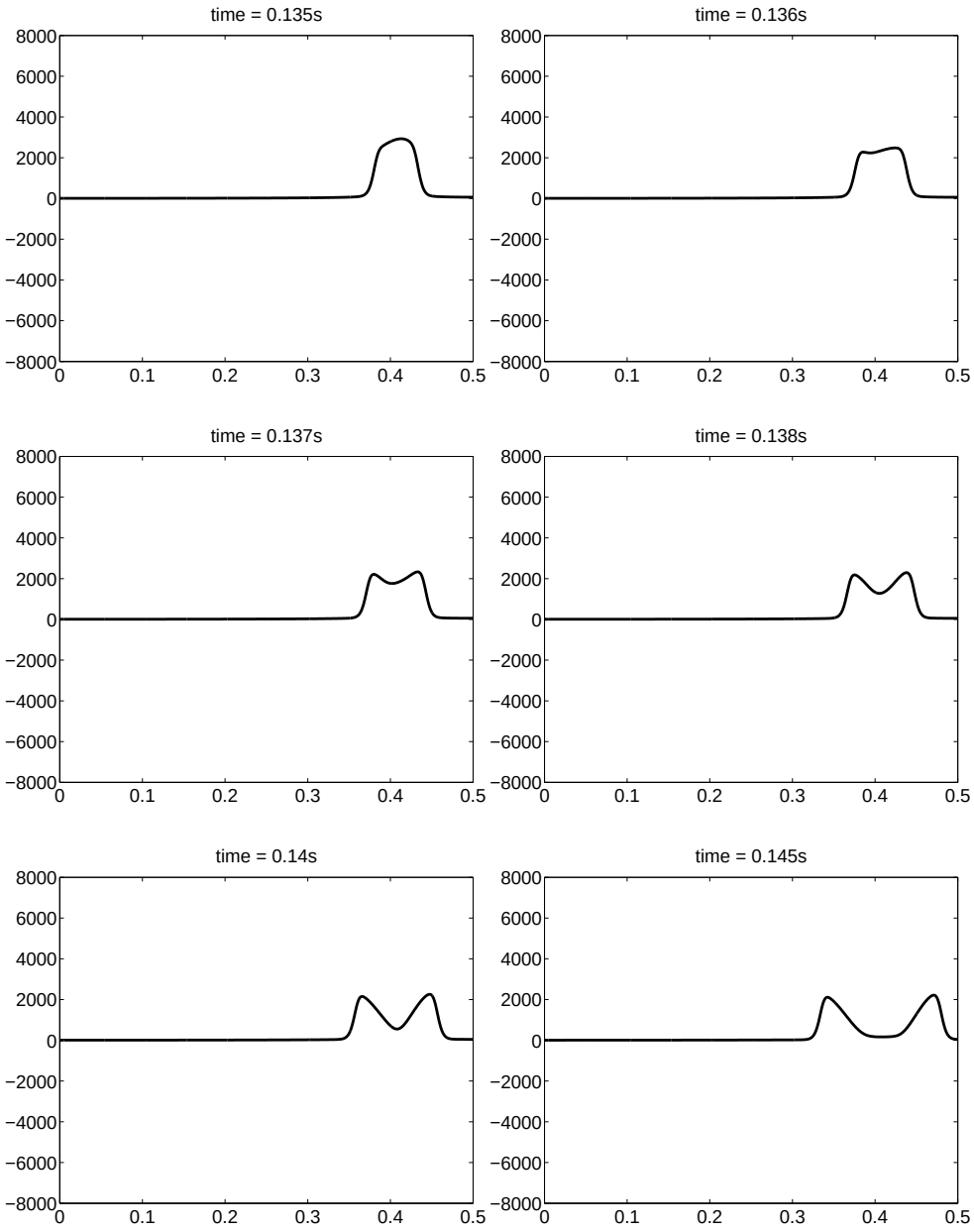

Figure D.3: Δp plotted in every point of mesh

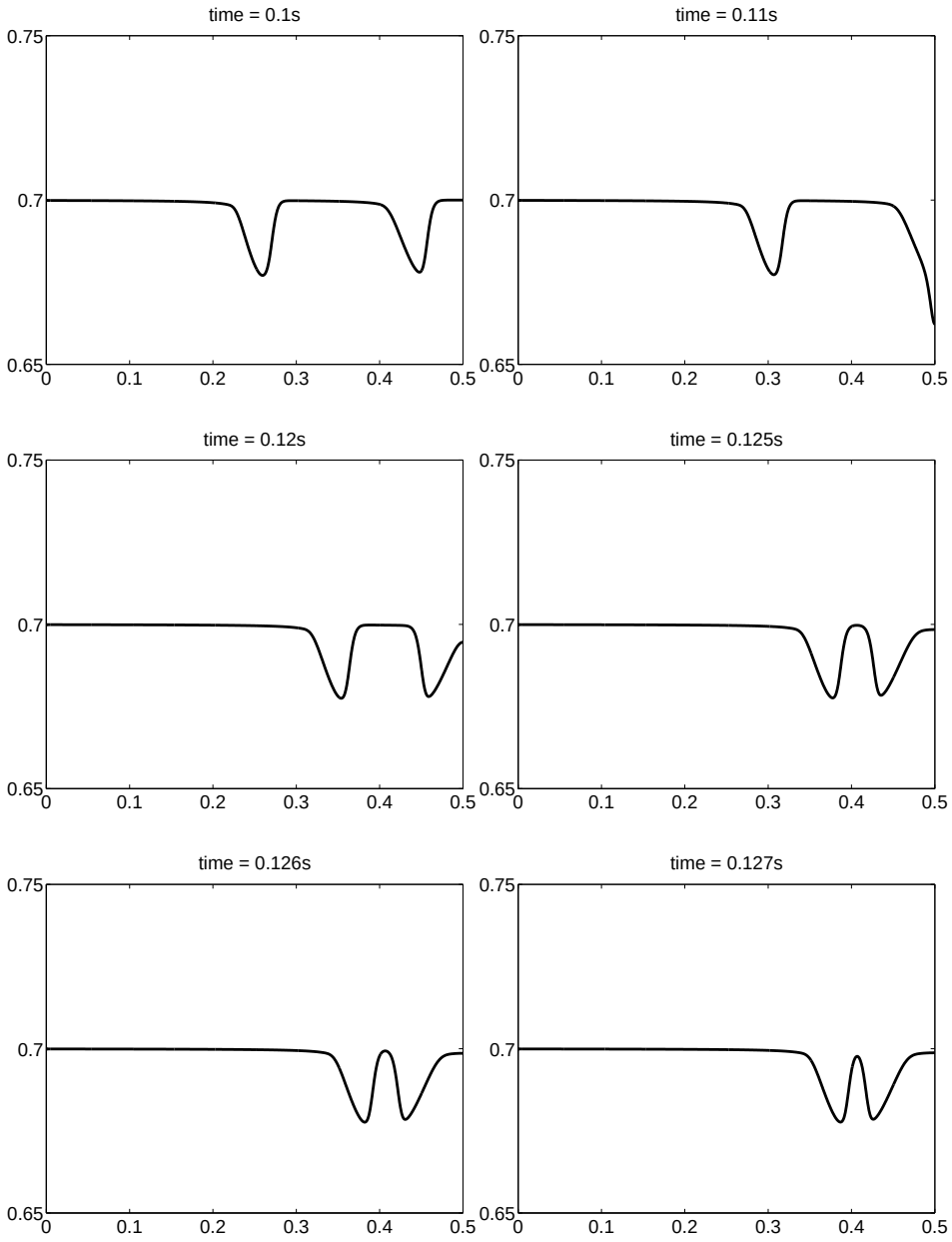

Figure D.4: Cross-sectional area ratio α plotted in every point of mesh

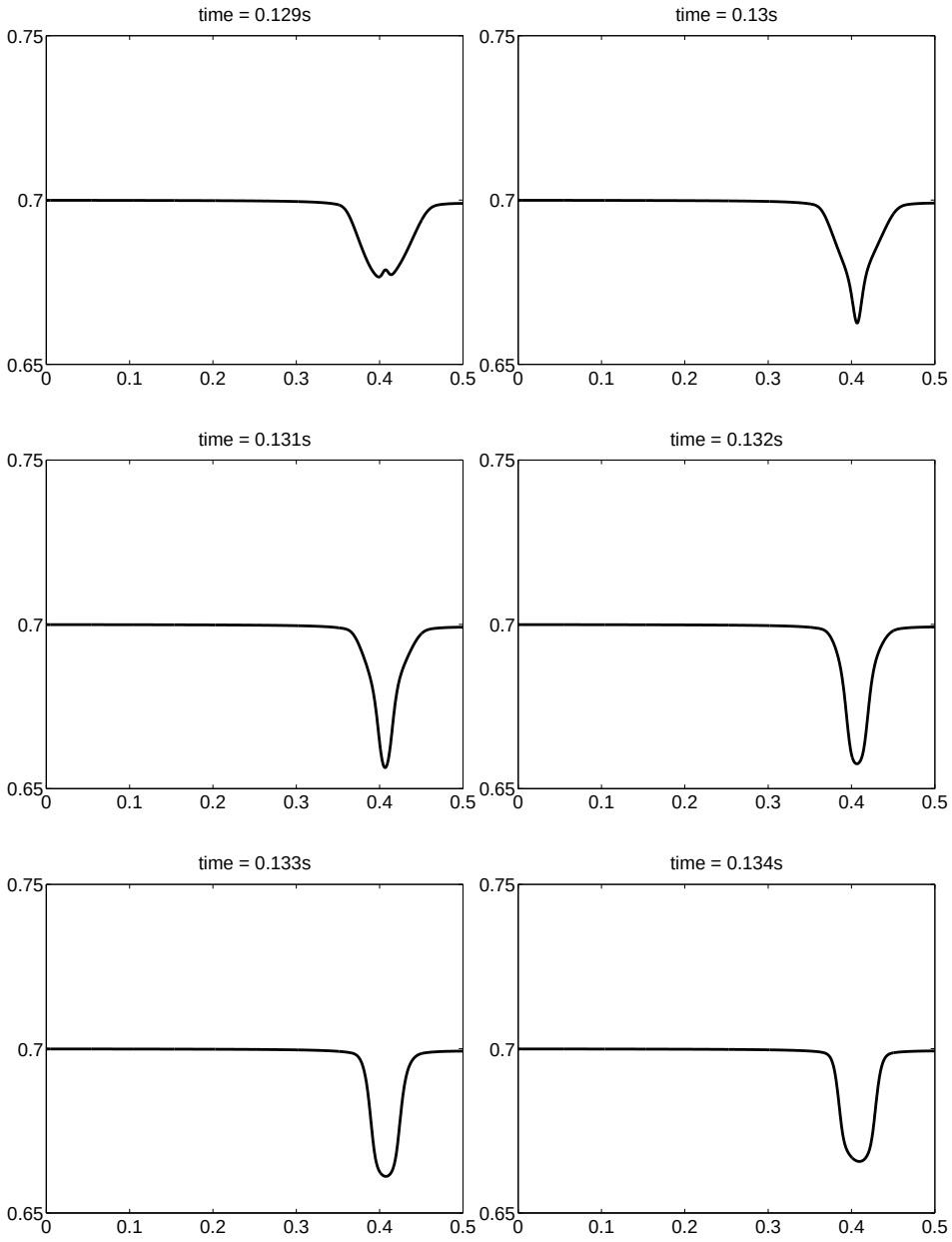

Figure D.5: Cross-sectional area ratio α plotted in every point of mesh

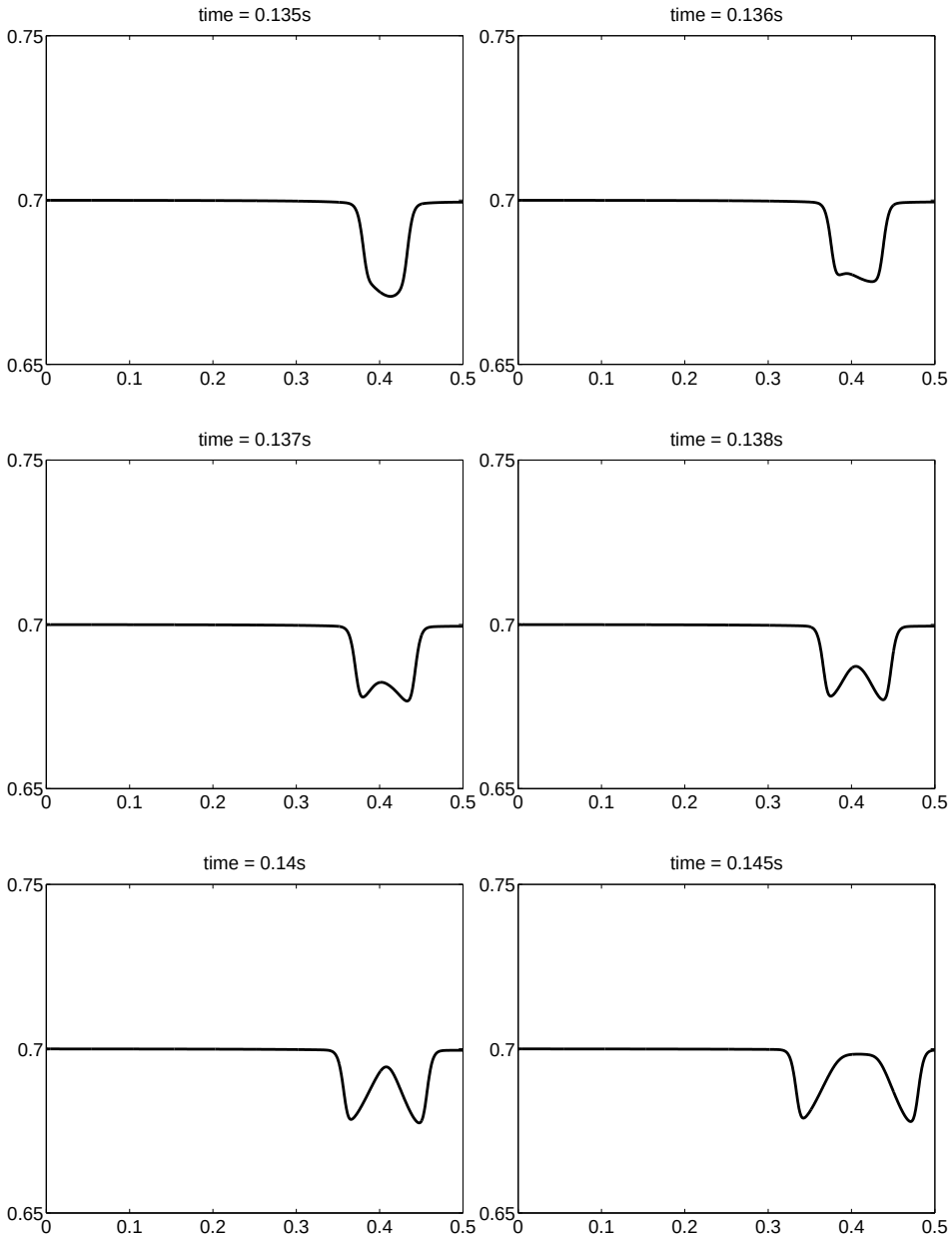

Figure D.6: Cross-sectional area ratio α plotted in every point of mesh

E. Reflection from the blockage

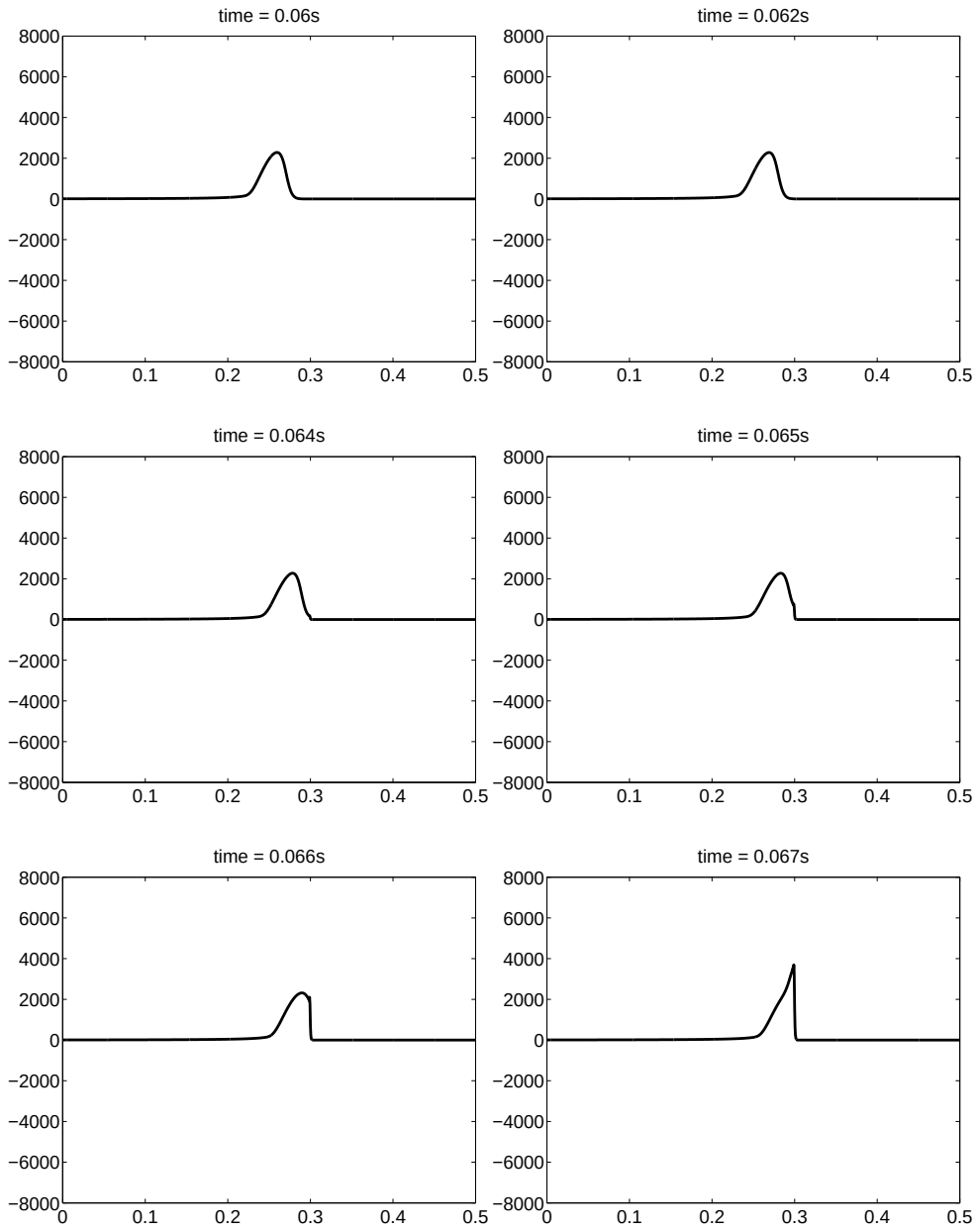

Figure E.1: Δp plotted in every point of mesh, blockage starts at $x = 0.3$

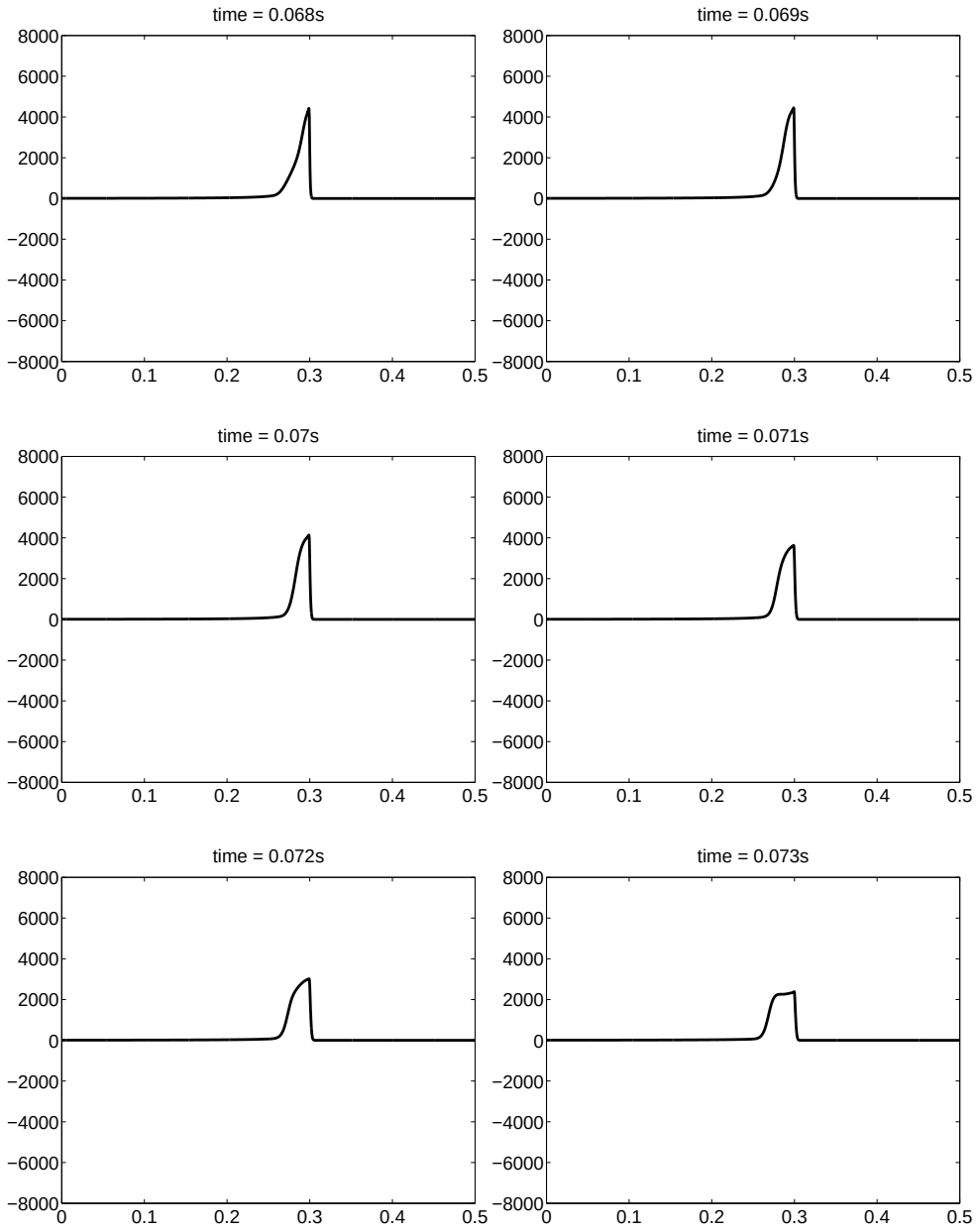

Figure E.2: Δp plotted in every point of mesh, blockage starts at $x = 0.3$

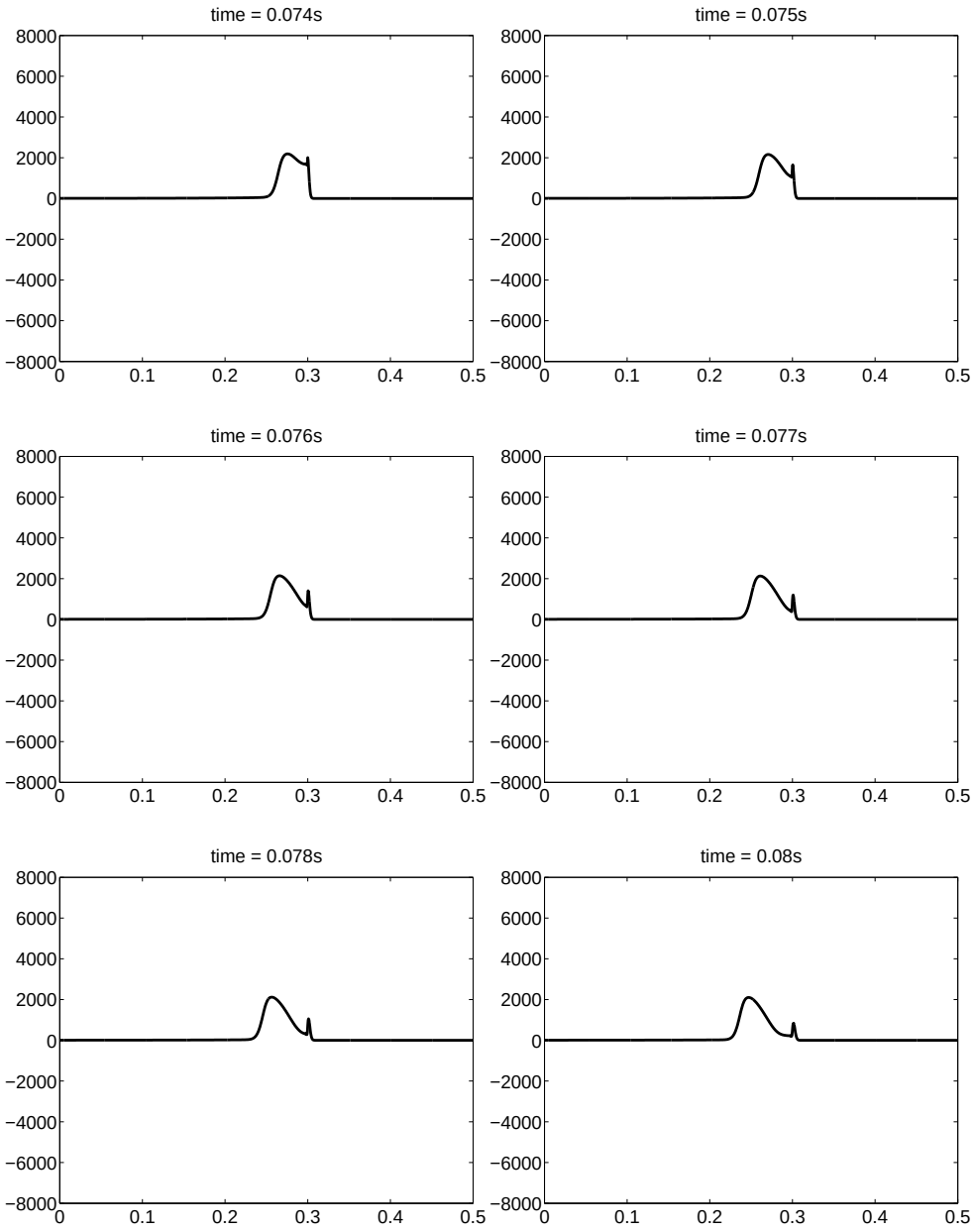

Figure E.3: Δp plotted in every point of mesh, blockage starts at $x = 0.3$

F. Sinusoidal wave

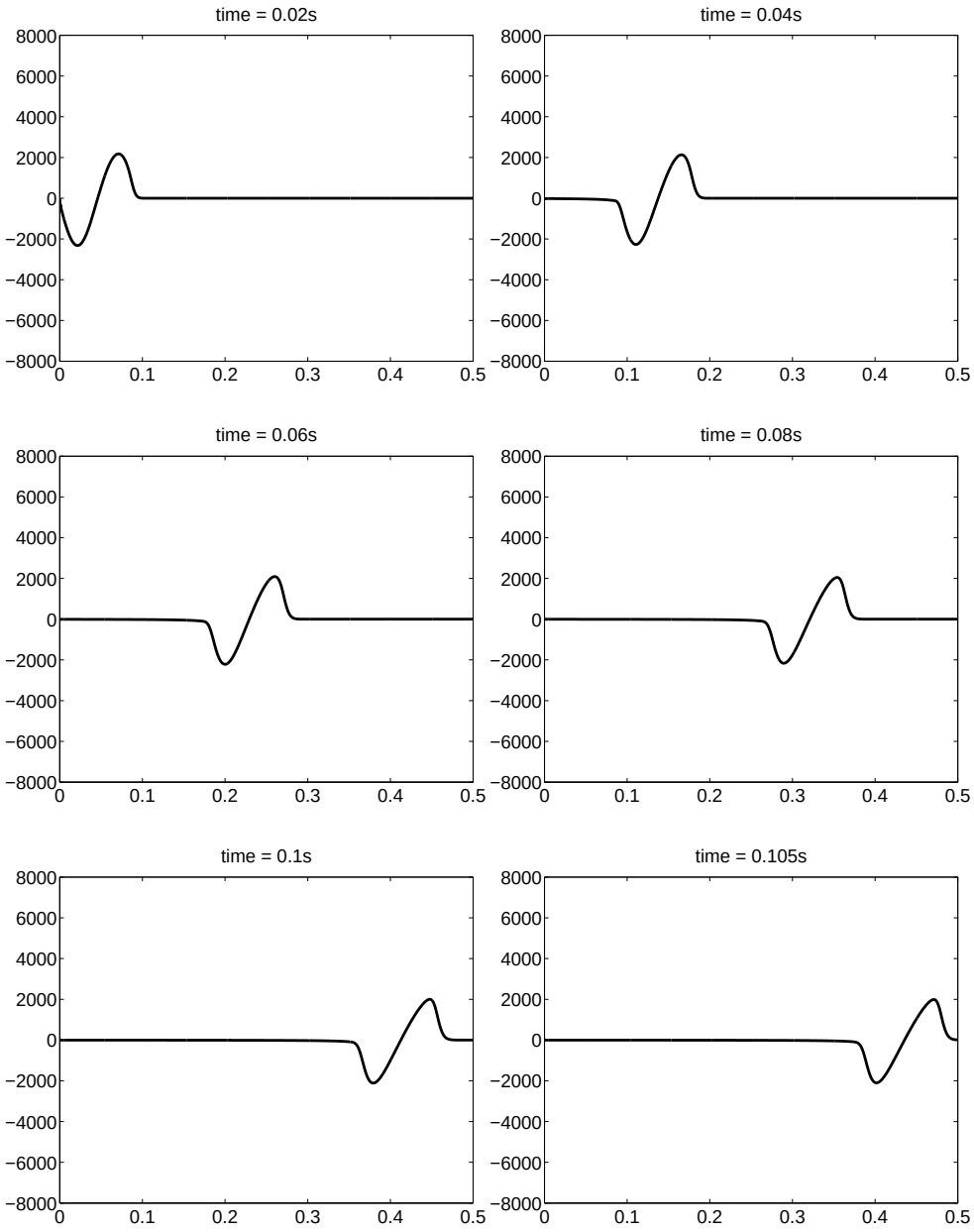

Figure F.1: Δp plotted in every point of mesh

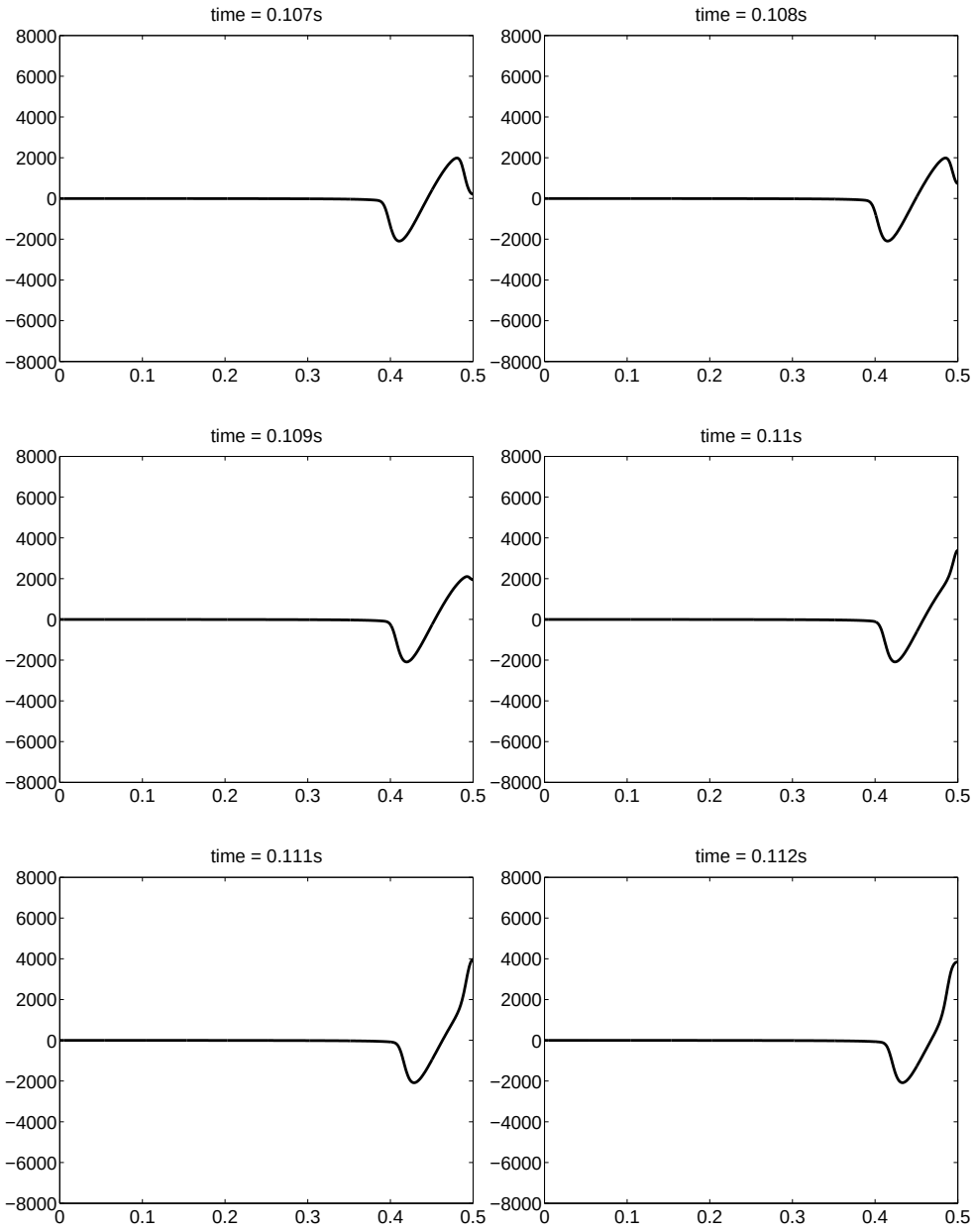

Figure F.2: Δp plotted in every point of mesh

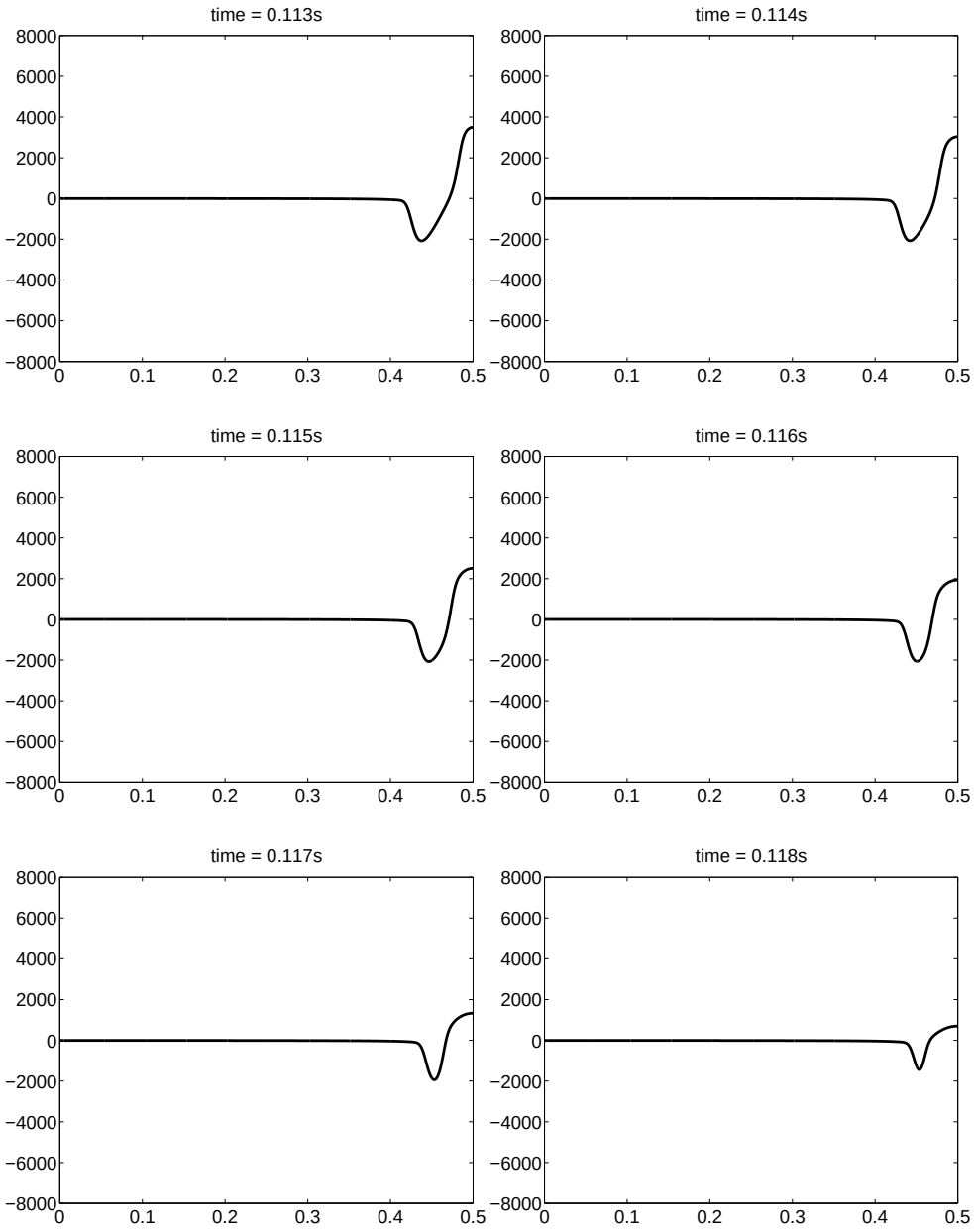

Figure F.3: Δp plotted in every point of mesh

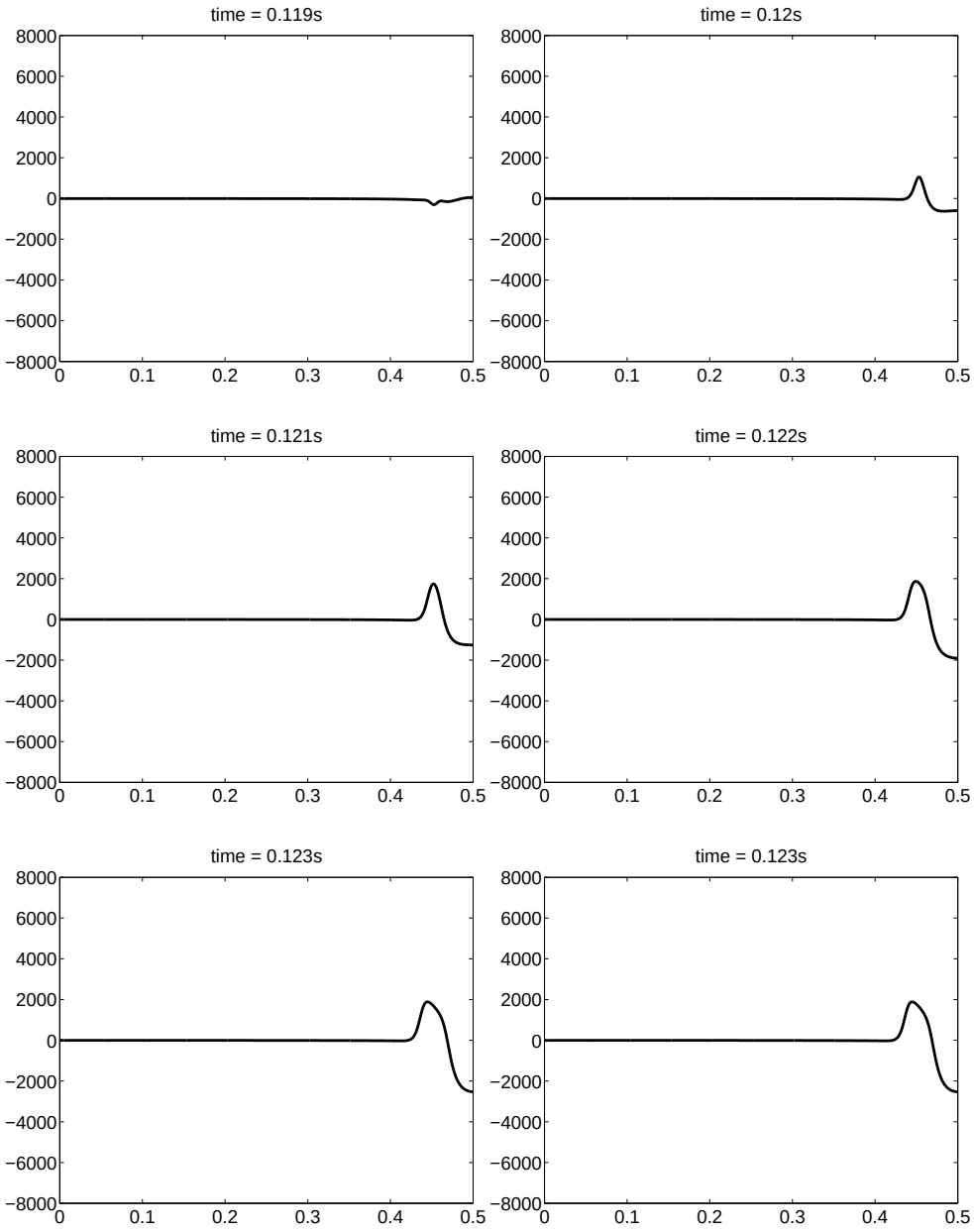

Figure F.4: Δp plotted in every point of mesh

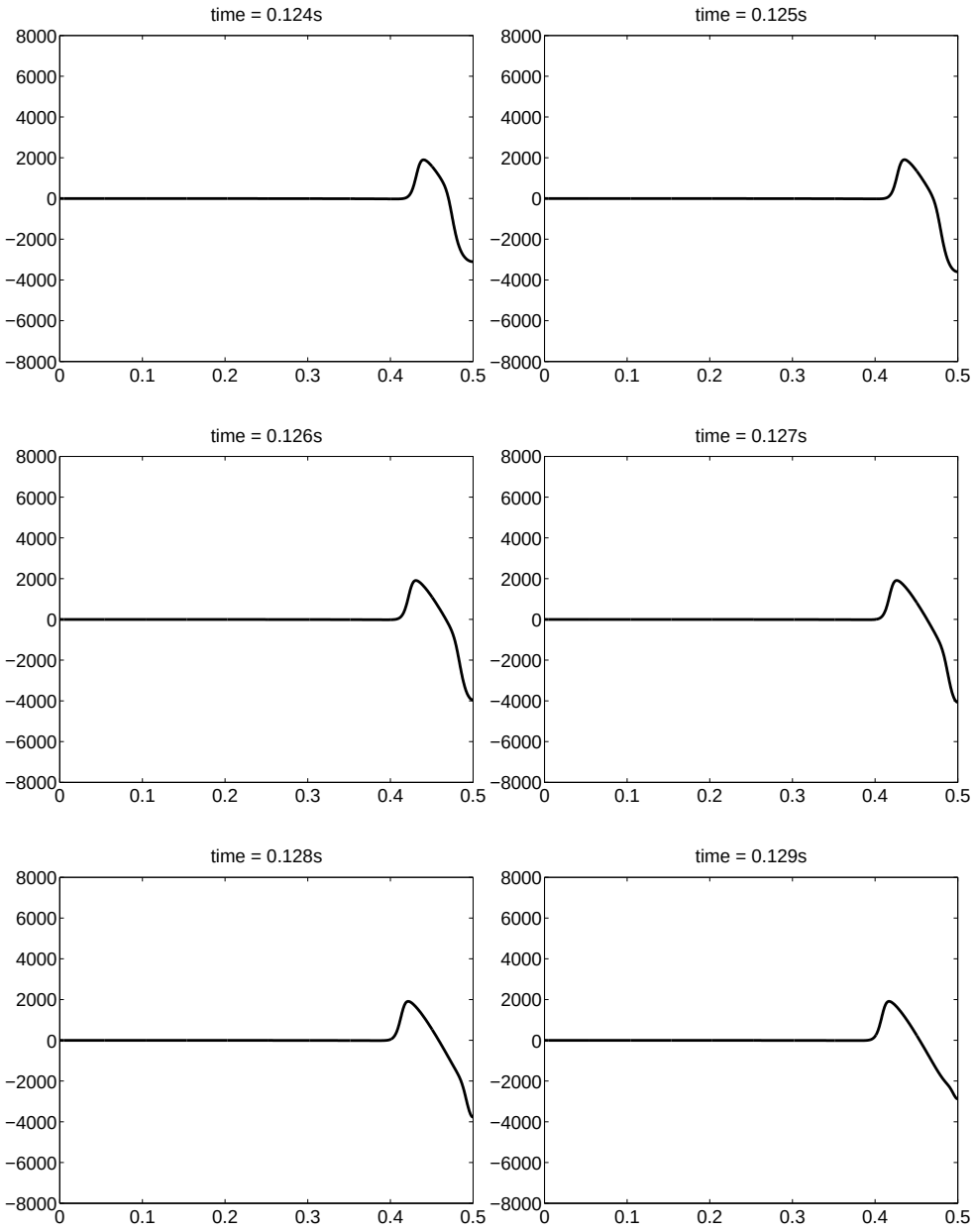

Figure F.5: Δp plotted in every point of mesh

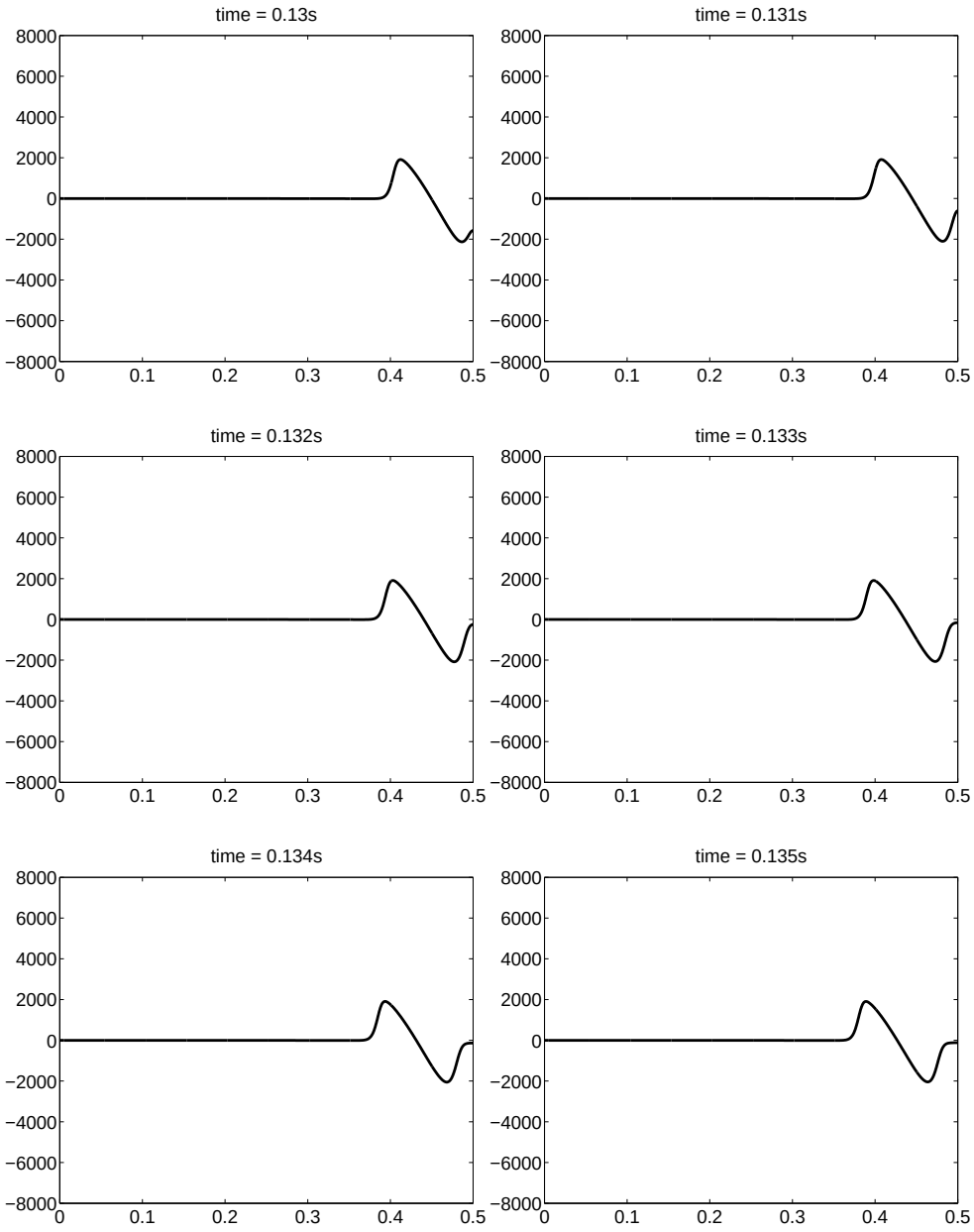

Figure F.6: Δp plotted in every point of mesh

G. Source code for MATLAB (one pulse with artificial viscosity)

```
% CONSTANTS

T = 0.5; % maximum computation time
tau = 0.0000001; % time step
J = 1000; % number of spatial intervals
h = 0.0005; % spatial interval length
AT = 0.00015; % total cross-sectional area
A0 = 0.7; % alpha 0, initial cross-sectional ratio
gamma = 0.0001; % artificial viscosity coeficient
rho = 1000; % CSF density
D = 0.00001; % distensibility
rychlostA = 0; % initial speed in tube A
rychlostB = 0; % initial speed in tube B

% INITIALIZATION

% spatial steps

x = zeros(J+1,1);

for j=1:J+1
    x(j) = (j-1)*h;
end

% initial values of solution in every time step

u01 = zeros(J+1,1); u02 = zeros(J+1,1); u03 = zeros(J+1,1);

% first step of method

u11 = zeros(J,1); u12 = zeros(J,1); u13 = zeros(J,1);

% solution

u1 = zeros(J+1,1); u2 = zeros(J+1,1); u3 = zeros(J+1,1);

% fluxes in first step of method

f01 = zeros(J+1,1); f02 = zeros(J+1,1); f03 = zeros(J+1,1);

% fluxes in second step of method
```

```
f11 = zeros(J,1); f12 = zeros(J,1); f13 = zeros(J,1);

A = zeros(J+1,1); % alpha, cross-sectional ratio

t=0; % time step

% INITIAL CONDITION

for j = 1:J+1
    u1(j) = rychlostA;
    u2(j) = rychlostB;
    u3(j) = 0;
end

% LAX-WENDROFF SCHEME

while (t < T)

% known boundary conditions

u01(J+1) = rychlostA;
u02(1) = rychlostB;
if 100*t < 1
    u03(1) = 3000*sin(100*pi*t);
else u03(1) = 0;
end

% computed boundary conditions

u01(1) = u1(1);
u02(J+1) = u2(J+1);
u03(J+1) = u3(J+1);

% substituting of computed values to initial values of solution

u01(2:J) = u1(2:J);
u02(2:J) = u2(2:J);
u03(2:J) = u3(2:J);

% first step of method

f01(1:J+1) = u01(1:J+1).*u01(1:J+1)/2 - (1-A0)*u03(1:J+1)/rho;
f02(1:J+1) = u02(1:J+1).*u02(1:J+1)/2 + A0*u03(1:J+1)/rho;
f03(1:J+1) = (u01(1:J+1)+u02(1:J+1)).*u03(1:J+1)/2 +
((1-A0)*u02(1:J+1) - A0*u01(1:J+1))/(2*D);

u11(1:J) = ((u01(1:J) + u01(2:J+1)) - (tau/h)*(f01(2:J+1) - f01(1:J)))/2;
```

```
u12(1:J) = ((u02(1:J) + u02(2:J+1)) - (tau/h)*(f02(2:J+1) - f02(1:J)))/2;
u13(1:J) = ((u03(1:J) + u03(2:J+1)) - (tau/h)*(f03(2:J+1) - f03(1:J)))/2;

% second step of method

f11(1:J) = u11(1:J).*u11(1:J)/2 - (1-A0)*u13(1:J)/rho;
f12(1:J) = u12(1:J).*u12(1:J)/2 + A0*u13(1:J)/rho;
f13(1:J) = (u11(1:J)+u12(1:J)).*u13(1:J)/2
+ ((1-A0)*u12(1:J) - A0*u11(1:J))/(2*D);

u1(2:J) = u01(2:J) - (tau/h)*(f11(2:J) - f11(1:J-1))
+ gamma*(u01(3:J+1) - 2*u01(2:J) + u01(1:J-1));
u2(2:J) = u02(2:J) - (tau/h)*(f12(2:J) - f12(1:J-1))
+ gamma*(u02(3:J+1) - 2*u02(2:J) + u02(1:J-1));
u3(2:J) = u03(2:J) - (tau/h)*(f13(2:J) - f13(1:J-1))
+ gamma*(u03(3:J+1) - 2*u03(2:J) + u03(1:J-1));

% boundary conditions

u1(1) = u1(2); u1(J+1) = u01(J+1);
u2(1) = u2(2); u2(J+1) = u02(J+1);
u3(1) = u03(1); u3(J+1) = u3(J);

A(1:J+1) = A0 - D*u3(1:J+1);
t = t + tau;

% possible plotting of main variables u1, u2, u3 and ratio A
end
```